AD-A044 735 HUGHES AIRCRAFT CO CULVER CITY CALIF DISPLAY SYSTEMS LAB F/G 17/2
CONTRAST ENHANCEMENT TECHNIQUES STUDY. PHASE III.(U)
JUL 77 E W OPITTEK N00014-76-C-0563
UNCLASSIFIED HAC-P77-210R ONR-CR213-124-3F NL

1 OF 2
AD A044735

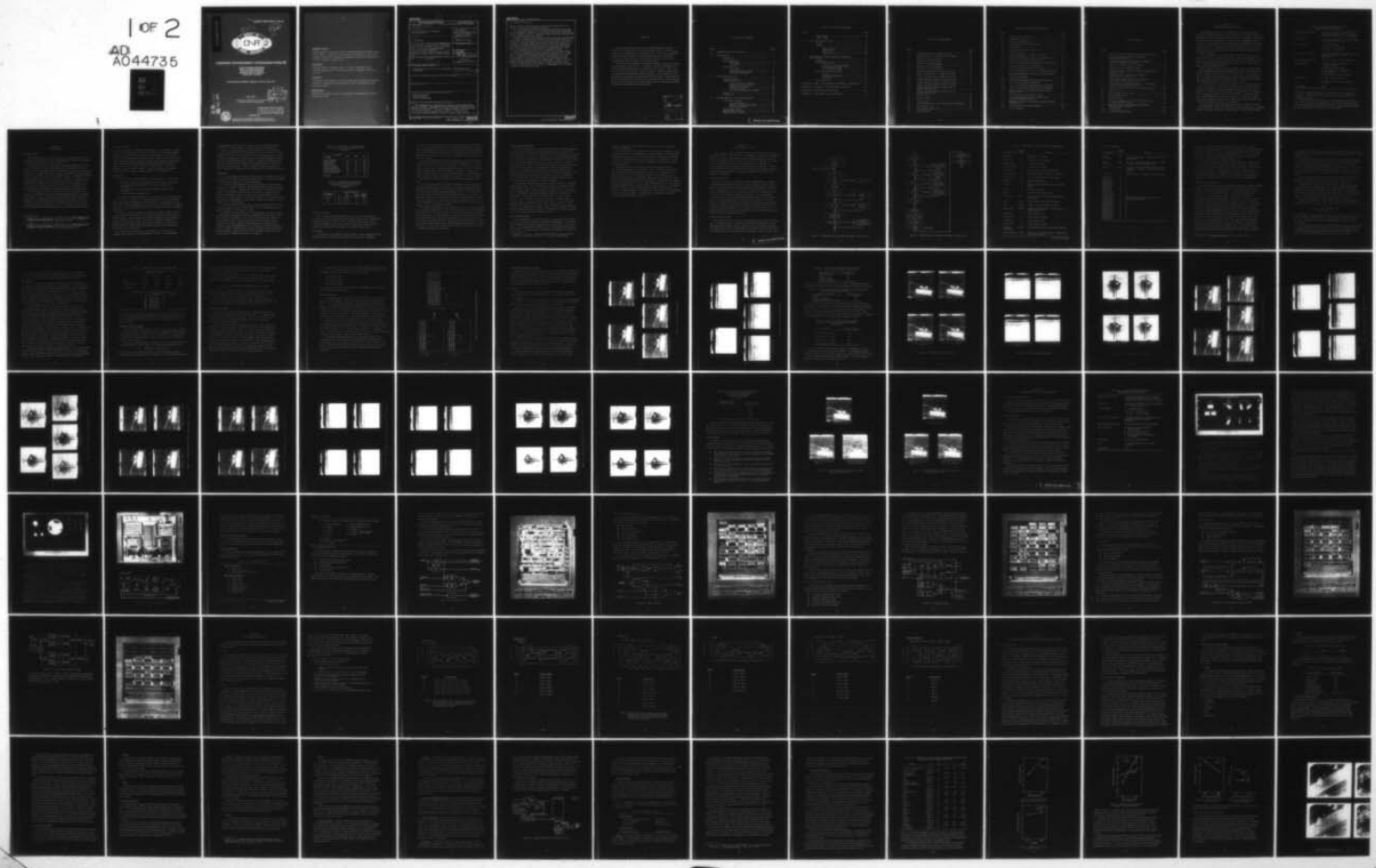

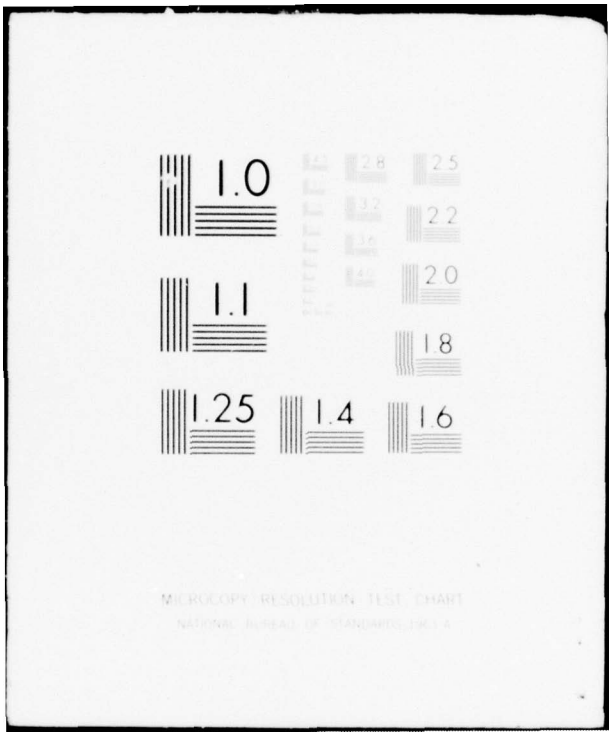
1.0
1.1
1.25
1.4
1.6
2.8
2.5
3.2
2.2
3.6
2.0
4.0
1.8
MICROCOPY RESOLUTION TEST CHART
NATIONAL BUREAU OF STANDARDS 1963 A

REPORT ONR-CR213-124-3F



# CONTRAST ENHANCEMENT TECHNIQUES PHASE III

DISPLAY SYSTEMS DEPARTMENT
DISPLAY SYSTEMS LABORATORY
HUGHES AIRCRAFT COMPANY
CENTINELA AND TEALE STREETS
CULVER CITY, CA 90230

FINAL REPORT FOR PERIOD 1 FEBRUARY 1976 TO 4 MAY 1977



JULY 1977







PREPARED FOR

OFFICE OF NAVAL RESEARCH • DEPARTMENT OF THE NAVY
WILSON BLVD., NORTH QUINCY STREET • ARLINGTON, VA 22217

Change of Address

Organizations receiving reports on the initial distribution list should confirm correct address. This list is located at the end of the report. Any change of address or distribution should be conveyed to the Office of Naval Research, Code 221, Arlington, Virginia 22217.

Disposition

When this report is no longer needed, it may be transmitted to other authorized organizations. Do not return it to the originator or the monitoring office.

Disclaimer

The findings in this report are not to be construed as an official Department of Defense or Military Department position unless so designated by other official documents.

Reproduction

Reproduction in whole or in part is permitted for any purpose of the United States Government.

(9) Final rept. 1 Feb 76 - 4 May 77

UNCLASSIFIED
SECURITY CLASSIFICATION OF THIS PAGE (When Data Entered)

| REPORT DOCUMENTATION PAGE | READ INSTRUCTIONS BEFORE COMPLETING FORM |
|---|---|
| 1. REPORT NUMBER (18) ONR-CR213-124-3F (19) | 2. GOVT ACCESSION NO. |
| 3. RECIPIENT'S CATALOG NUMBER | |
| 4. TITLE (and Subtitle) (4) Contrast Enhancement Techniques Study + Phase III | 5. TYPE OF REPORT & PERIOD COVERED Final Report. Feb 1, 1976 - May 4, 1977 |
| 6. PERFORMING ORG. REPORT NUMBER P77-210R, D7402 | |
| 7. AUTHOR(s) (10) E. W. Opittek | 8. CONTRACT OR GRANT NUMBER(s) (15) N00014-76-C-0563 |
| 9. PERFORMING ORGANIZATION NAME AND ADDRESS Display Systems Department, Display Systems Laboratory, Hughes Aircraft Company, Centinela and Teale Streets, Culver City, California 90230 | 10. PROGRAM ELEMENT, PROJECT, TASK AREA & WORK UNIT NUMBERS |
| 11. CONTROLLING OFFICE NAME AND ADDRESS Department of Navy, Office of Naval Research, Wilson and N. Quency Street Arlington Virginia 22217 | 12. REPORT DATE (11) July 1977 |
| | 13. NUMBER OF PAGES ~~140~~ (12) 143 p. |
| 14. MONITORING AGENCY NAME & ADDRESS (if different from Controlling Office) (14) HAC-P77-210R, HAC-Ref-D7402 | 15. SECURITY CLASS. (of this report) Unclassified |
| | 15a. DECLASSIFICATION/DOWNGRADING SCHEDULE |

16. ~~DISTRIBUTION STATEMENT~~ (of this Report)

Reproduction in whole or in part is permitted for any purpose of the United States.

DISTRIBUTION STATEMENT A
Approved for public release; Distribution Unlimited

17. DISTRIBUTION STATEMENT (of the abstract entered in Block 20, if different from Report)

18. SUPPLEMENTARY NOTES

19. KEY WORDS (Continue on reverse side if necessary and identify by block number)

Image Enhancement
Video Processing
Contrast Enhancement

20. ABSTRACT (Continue on reverse side if necessary and identify by block number)

The development of a real-time TV compatible contrast enhancement unit was conducted. This development was the result of a three phase study program to evolve and evaluate, by computer simulation, alternate contrast enhancement techniques. The three techniques studied were the Local Area Histogram Equalization (LAHE), Local Area Brightness and Gain Control (LABGC), and Haar Transform Filtering (HTF). The

DD FORM 1 JAN 73 1473 EDITION OF 1 NOV 65 IS OBSOLETE

409205

UNCLASSIFIED
SECURITY CLASSIFICATION OF THIS PAGE (When Data Entered)

20. Abstract (Continued) .

LABGC technique was selected for hardware implementation due to its relative simplicity and simulated performance.

The LABGC algorithm basically operates on and adjusts the gain and bias of a single pixel element as a function of the statistics of immediate surrounding pixels. If there is a wide variation in the values (high contrast) no gain is applied; conversely, high gain is applied when the immediate area exhibits small variations (low contrast).

During the first part of this project, a design study was conducted using the computer simulation model to optimize the mechanization parameters. In particular, the pixel area size of 4 x 4 pixels was selected, the video is digitized to 6 bits and multiple gain transfer functions were selected. An all digital mechanization was selected in order to eliminate analog noise and nonlinearity problems. The resulting unit was built to flight safety standards and measures 19 inches wide, 10.5 inches high and 14 inches deep. A future production unit would be substantially smaller.

Initial evaluation of closed circuit TV video, processed through the unit, revealed a significant increase in apparent image contrast. Initial subjective studies showed that performance improvements may result in target recognition due to sharpened target shape definition. It is also possible that scene contrast improvements may provide performance improvement in reconnaissance sensor applications. However, carefully designed laboratory experiments are recommended in order to fully evaluate the applicability of this LABGC unit (and processing technique). It is also recommended that a wide dynamic range sensor (e.g., FLIR) be employed to fully evaluate the unit.

# PREFACE

This final report covers the work accon plished during the period February 1976 through April 1977 under Contract N0014-76-C-0563 entitled Phase III Contrast Enhancement Techniques Study. This work was supported by the Office of Naval Research under the sponsorship of Commanders Don Hanson and Stacy Holmes. Stephen Young of the Air Force Avionics Laboratory provided assistance as a technical advisor.

The work was accomplished by the Display Systems Laboratory at Hughes Aircraft under the direction of E. W. Opittek. Special acknowledgement is given the following individuals who contributed to the project. Roger Lowe conducted and documented the computer simulation. Mike Pruznick directed the unit design and contributed to the final report. Vern Nicklow performed the digital circuit design and contributed to the final report. Roland Andrews performed the analog circuit design. Joe Setto performed the unit mechanical design. Jane Herman and Larry Scanlan performed the equipment evaluations and studies and contributed to the final report.

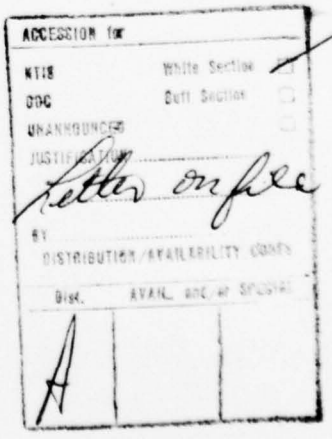

TABLE OF CONTENTS

TABLE OF CONTENTS (Continued)

## LIST OF ILLUSTRATIONS

LIST OF ILLUSTRATIONS (Continued)

LIST OF TABLES

## Section 1.0
## INTRODUCTION AND SUMMARY

Cockpit display systems are used today to provide pilots and sensor operators with radar, infrared, or television information which is used for navigation, intelligence gathering, target detection, recognition, identification, and designation. In many cases, these tasks require high quality imagery for optimum operator performance. Unfortunately, limitations in the display or sensor system, or both, may lead to degraded performance in meeting mission objectives. Techniques for real time enhancement of sensor imagery show promise for improving operator performance with a minimal increase in system complexity.

This final report documents the results of the third phase of Contract N00014-76-C053 to develop a real time image enhancement technique. This three phase program was funded by the Office of Naval Research and the Air Force Avionics Laboratory. Section 2.0 provides a review of the first two phases of this three phase program.

Phase I provided for the development of three enhancement algorithms, Local Area Histogram Equalization (LAHE), Local Area Brightness and Gain Control (LABGC), and Haar Transform Filtering (HTF). A complexity performance tradeoff indicated that LABGC was the most promising algorithm. The second phase was a noise sensitivity study. The noise study concluded that LABGC and LAHE were moderately sensitive to noise.

The third phase of the program, documented herein, resulted in a hardware development of a real time enhancement unit employing the LABGC algorithm. An extensive computer simulation design study, described in Section 3, resulted in an optimum hardware mechanization. The results of this mechanization study are summarized in Table I. A unit description of the LABGC hardware is provided in Section 4.0. Section 5.0 contains an extensive diagnostic test procedure, and Section 6.0 documents all of the performance studies conducted on the equipment.

Four appendices to the final report are included. Appendix A includes a description of the enhancement algorithms. Appendix B provides a reliability and thermal analysis of the unit. The acceptance test and detailed example

TABLE 1. LABGC BRASSBOARD TABLE OF PERFORMANCE PARAMETERS

| | |
|---|---|
| Algorithms Performed: | Local Area Brightness and Gain using Range and Pixel Difference as a measure of contrast and Mean as a measure of level. |
| Window Size: | 4 Horizontal elements x 2 Vertical elements per Field (4 x 4 per Frame) |
| A/D Sampling: | 3 - 6 BITS Selectable<br>9.072 MHz - 525 Line Mode<br>15.0 MHz - 875 Line Mode |
| Gain Transfer Function: | 32 Multiple Selectable (Gain functions are programmed in Prom listed in Appendix D.) |
| Input Video/Output Video: | 525 per EIA RS170; 875 per EIA RS330 |
| Other Features: | • Ability to Accept, Generate, Separate Syncs<br>• BIT and Checkout Modes<br>• Built-in Element Value Selector and Display<br>• Front Panel or Remote Control |
| Input Power: | 178 Watts (60 or 400 Hz AC) |
| Size: | 19" Rack Mounted Unit; 10.5" high x 14" deep |
| Unit Weight: | 40 lb |

calculations to explain the LABGC algorithm are provided in Appendix C. A discussion of the test PROM (Programmable Read Only Memory) is included in Appendix D.

An initial estimate of the parameters of an ultimate production unit was made. Such a unit would be significantly smaller than the brassboard unit. It is estimated that it could be less than 400 $in^3$, weigh less than 10 lbs and dissipate approximately 50 watts, for a 525 line system.

## Section 2.0
## BACKGROUND

### INTRODUCTION

This section provides a summary of the work conducted under Phase I and Phase II of this program. The results of these two phases are thoroughly documented in the two previous final reports.[1, 2]

On the Phase I program, two contrast enhancement techniques, namely, Local Area Histogram Equalization and Local Area Brightness and Gain Control, and one resoluation enhancement technique, namely, Haar Transform Filtering, were studied with regard to relative mechanization complexity and a subjective evaluation of the relative display quality. A technical description of these techniques is provided in Appendix A. Images were digitized, processed through a digital computer and printed on film for evaluation. The results of these studies led to the selection of the LABGC technique as the most promising for further evaluation. The Haar was considered least desirable due to its complexity and apparent degradation of display quality.

Under the Phase II effort the effects of noise on all techniques were evaluated. Both digital (hit miss) and analog (gaussian) noise were included in the computer model. The results indicated that the LABGC continued to provide signal enhancement but also amplifies the noise under high noise conditions. The Haar technique was most sensitive to noise. As a result of the Phase I and Phase II efforts, the LABGC technique was selected for design optimization and development performed as Phase III of this program.

---

1. Ketcham, D. J., Lowe, R. W., and Weber, J. W., Image enhancement techniques for cockpit displays, Tech. Rep. NR 213-124. Arlington, Virginia: Office of Naval Research, December 1974.

2. Ketcham, D. J., Lowe, R. W., and Weber, J. W., Image enhancement techniques for cockpit displays, Final Tech. Rep. NR 213-124-2. Arlington, Virginia: Office of Naval Research, March 1976.

## PHASE I SUMMARY

The major objective of the Phase I Program was to evaluate three image enhancement techniques capable of improving operator performance utilizing sensor display systems. The techniques under evaluation were all judged suitable for implementation and utilization in the cockpit environment. Evaluation was based on subjective analysis of picture quality improvement after the enhancement technique had been applied and on physical data such as complexity and cost. The three techniques evaluated were: Local Area Brightness and Gain Control (LABGC), Local Area Histogram Equalization (LAHE), and Haar Transform Crispening (HTC). (See Appendix A.)

### Methodology

In the performance of this program, four major tasks were performed:

1. Selection, collection, and digitizing of representative sensor data.
2. Development and optimization of the respective enhancement techniques.
3. Processing of the selected images by each of the enhancement processes.
4. Evaluation of the resulting images.

Representative samples of imagery from each of three major sensor types (IR, TV, Radar) were selected. A flying spot scanner was used to digitize the input image data from photographic transparencies. A digital scan converter was used to capture and digitize frames of raw FLIR sensor data from magnetic video tape. Radar image data was collected directly from computer-compatible digital tapes.

Software for the three enhancement techniques (LABGC, LAHE, and HTC) was developed on the Hughes Real Time System Simulation Facility Sigma 5 digital computer. Each technique was refined to produce the best enhancement possible within real-time cockpit environment constraints. Enhancement parameters such as gain, window size, and filter shapes were empirically adjusted until the resultant image showed the most improvement possible in the opinion of the experimenters.

After the images selected for use in this study were processed, the resulting enhancements were photographically recorded. The photographs

(including those of the unprocessed image) were used during the subjective evaluation to determine relative merits of each processing technique.

Subjective evaluation of the processing techniques was accomplished by asking each of ten experienced subjects to rate (on a scale of 1 to 7 with a rating of 4 defined as "normal") the quality of each of the processed images. The rating was applied to a spectrum of operator tasks ranging from vehicle and sensor control through target detection, recognition, and identification. Thus the effectiveness of an enhancement technique could be measured as a function of sensor and task. Further evaluation consisted of designing a tentative hardware mechanization of each technique for estimating complexity.

## Conclusions

Several conclusions were drawn from this study. All techniques produced the expected observable results in the sensor imagery. Contrast was enhanced and edges in FLIR imagery were indeed sharpened.

The effects of the enhancement processes on improved operator performance were most notable with the contrast enhancement processes applied to FLIR and TV imagery. Although noticeable changes were produced in radar imagery by all enhancement techniques, the subjective evaluations did not indicate that significant improvements in operator performance would be achieved. The study results are summarized in Table 2. The evaluation data is inconclusive regarding the effects of these enhancement techniques (LAHE, LABGC, HTC) on radar imagery.

It is estimated that LABGC and HTC would be much (by a factor of about 2:1) less complex to implement than LAHE. The initial mechanization complexity estimates are summarized in Table 3.

In summary, one can conclude from this study that of the three enhancement techniques investigated, local area brightness and gain control offers the potential for significant improvement in performance when applied to electro-optical sensor imagery particularly at mid- and close-ranges. Estimates of hardware complexity suggest that implementation of this technique for use with flight hardware is feasible and well within the state of the art. Further evaluation of this technique through real-time man-in-the-loop simulation or flight test will yield more quantitative data on the cost effectiveness of LABGC in the mission environment.

TABLE 2. SUBJECTIVE EVALUATION OF ALTERNATE CONTRAST ENHANCEMENT TECHNIQUES

| OPERATOR TASK \ TECHNIQUE | LAHE | LABGC | HTC |
|---|---|---|---|
| VEHICLE CONTROL | 4.2 | 4.1 | 3.9 |
| SENSOR CONTROL | 4.2 | 4.2 | 3.8 |
| ORIENTATION | 4.1 | 4.1 | 3.7 |
| TARGET DETECTION | 4.1 | 4.2 | 3.6 |
| TARGET RECOGNITION | 4.4 | 4.2 | 3.6 |
| TARGET IDENTIFICATION | 4.7 | 4.6 | 3.8 |
| TARGET DESIGNATION | 4.6 | 4.3 | 3.9 |
| AVERAGE | 4.3 | 4.2 | 3.8 |

TABLE 3. HARDWARE COMPLEXITY TRADEOFF BETWEEN ALTERNATE CONTRAST ENHANCEMENT TECHNIQUES

| ENHANCEMENT TECHNIQUES | HARDWARE COMPLEXITY | | | |
|---|---|---|---|---|
| | ICs | SIZE, INCHES | WEIGHT, POUNDS | POWER, WATTS |
| LABGC | 330 | 6 x 8 x 8.6 | 5 | 66 |
| LAHE | 770 | 6 x 8 x 17.4 | 11.5 | 154 |
| HTC | 384 | 6 x 8 x 9.7 | 5.8 | 77 |

## PHASE II SUMMARY

Three somewhat independent tasks were performed under the Phase II Program and only the first of these tasks applied to the LABGC mechanization. These three tasks were a noise study, a filtering technique study, and a restoration technique study. These tasks are summarized below and more detailed information can be obtained from the Phase II final report.

### Noise Study

An evaluation of the techniques studied in Phase I showed that they offered significant improvement in selected images under noise-free conditions.

Since the real world is seldom noise-free, a thorough study of the effects of noise on the enhancement processes was undertaken in the Phase II effort. Analog and digital noise models were developed to generate images that had controlled, but realistic levels of noise. The enhancement processes were then applied to the "noisy" images and the results compared with enhanced noise-free images.

The noise sensitivity study utilized a digital noise model that randomly changed the state of individual bits in the image as though it were a serial bit stream. Three error rates were selected: 0.01, 0.05 and 0.1 error per bit on the average. Images containing these noise levels were enhanced with the LABGC, LAHE and HTC techniques. Subjective evaluation of enhanced noisy images revealed that the LAHE technique was least sensitive to noise while the LABGC was slightly more sensitive. The HTC technique was most sensitive to noise and produced a degraded image at high error rates.

Analog noise was injected into images by adding a normally (gaussian) distributed random number to each picture element (pixel). The standard deviation of the random number was chosen to produce a selected signal-to-noise (S/N) ratio. Images containing analog type noise were produced that represented three typical S/N ratios of analog-type noise: 30, 10 and 5. Subjective evaluation of enhanced noisy images revealed that both the LABGC and LAHE techniques were moderately sensitive to analog type noise. As with the digital noise, the HTC was quite sensitive, and at low S/N ratios the enhancement was worse than the original.

When images containing noise are enhanced, the noise is equally enhanced. If the enhancement process were able to discriminate between noise and image data, so that only image information were enhanced, then improved results could be possible. A small side task was undertaken to develop some simple noise suppression logic in the LABGC technique. This logic produced very good results, suggesting that future enhancement work can effectively combine image enhancement and noise suppression techniques simultaneously. A more thorough discussion of this study, including illustration of the effect of noise, is included in the Phase II final report.

## Filtering Techniques Study

The application of filtering techniques that utilize non-linear manipulation of transform domain coefficients and of those that utilize logarithmic and exponential processes before filtering has shown dramatic image improvement. The most notable work in this area has been done by Thomas Stockham at the University of Utah. Most of these approaches have utilized the Fourier transform, which is unsuitable for real-time (e.g., TV rates) use. The non-linear filtering developed here uses the Haar transform, which was expected to produce similar results. This approach was taken because the Haar transform is a mathematical transformation using only addition and subtraction which is much easier to mechanize for real-time applications. Two non-linear enhancement techniques were studied. One was to apply non-linearly the HTC filter previously developed. The other utilized a filter derived from that successfully developed by Stockham.

The non-linear Haar transform study evaluated two filters; a crispening and a Stockham type. The crispening filter was developed in the previous contract while the other was derived from Stockham's work.[3] The non-linear crispening filter produced enhancements that were different from the linear crispening type but judged not significantly better than its linear counterpart. The Stockham type non-linear filter showed a slight decrease in the improvement over the non-linear crispening filter for TV type images. An improvement was noted, however, for FLIR images enhanced by the Stockham type filter. The most dramatic improvement resulted in the enhancement of radar imagery with the non-linear Stockham type filter applied in the Haar domain. This enhancement technique appears to have significant potential for radar type imagery.

## Blur Restoration Study

Image degradation by motion blur can have an important effect on pilot effectiveness in target detection, recognition and designation. Furthermore, sensor stabilization systems designed to prevent this problem can be quite costly. Since significant work has been done in restoring images degraded by motion blur, an attempt was made to apply such techniques to real-time,

3. Stockham, T. G., Jr., "Image Processing in the Context of a Visual Model", Proc. IEEE, Vol. 60, No. 7, July 1972, pp. 828-842.

airborne applications. This would, in turn, lead to reduced investment in sensor stabilization.

Most of the prior work has utilized Fourier transform techniques. Since the Haar transform has a straightforward real-time hardware mechanization, an attempt was made to derive a Haar domain filter suitable for motion blur restoration. This filter proved to be too complex for real-time use. This led to the development of a direct blur restoration technique not involving the Haar transform.

Restoration of blurry images was restricted to the class of space invariant and constant linear motion blur. The derivation of a Haar domain blur restoration filter proved impractical. However, a spatial domain operator was derived to restore blurred images, but residual terms are produced in the process. An algorithm was developed to estimate the magnitude of these terms to produce a full restoration. Application of the spatial domain operator and the error term estimating algorithm proved quite successful and significantly easier to implement in real-time hardware. A functional hardware design was performed to estimate the chip count for such a real-time blur restoration system. Horizontal blur restoration is mechanizationally simple, requiring 162 chips. Vertical and two-dimensional restoration required 556 and 718 chips, respectively.

## Section 3.0
## LABGC DESIGN STUDY

Based upon the results of the Phase I and II work discussed in Section 2.0, the LABGC technique was selected for mechanization. Therefore, the Phase III effort was directed at optimizing the LABGC algorithm hardware design and the actual implementation of a brassboard system. The optimization criterion used was a subjective evaluation of pictures generated using different mechanization parameters which appreciably affected complexity. A digital mechanization for the brassboard unit was selected over an analog mechanization due to the inherent nature of the process and the desire for maximum reliability and stability.

### DESIGN SIMULATION

In order to evaluate various LABGC design configurations, a detailed computer hardware simulation was developed. This non-real time computer program was designed to simulate the hardware at every stage of the mechanization. Additionally, sufficient flexibility was included in the simulation to vary major design parameters. These parameters are; 1) technique for the measure of local contrast; 2) technique for measure of local brightness; 3) window size; 4) number of input gray shade bits, and 5) various truncation points in the flow of operations. A flowchart of this program is shown in Figure 1. The specific hardware configuration is selected by setting values to the NAME LIST variables listed in Table 4. The variables were initialized to select the standard deviation as the contrast measure, select a 4 x 4 noninterlaced window, and select 6 bit input video. Different programs were utilized to vary the brightness measure.

### DESIGN OPTIMIZATION

There are many ways to minimize the complexity of the LABGC hardware unit. As initially conceived, the LABGC algorithm computes the mean and standard deviation within a sliding window to measure intensity and contrast (see Appendix A). These computations involve squares, divisions and a square root which contribute greatly to hardware complexity. Therefore, alternative

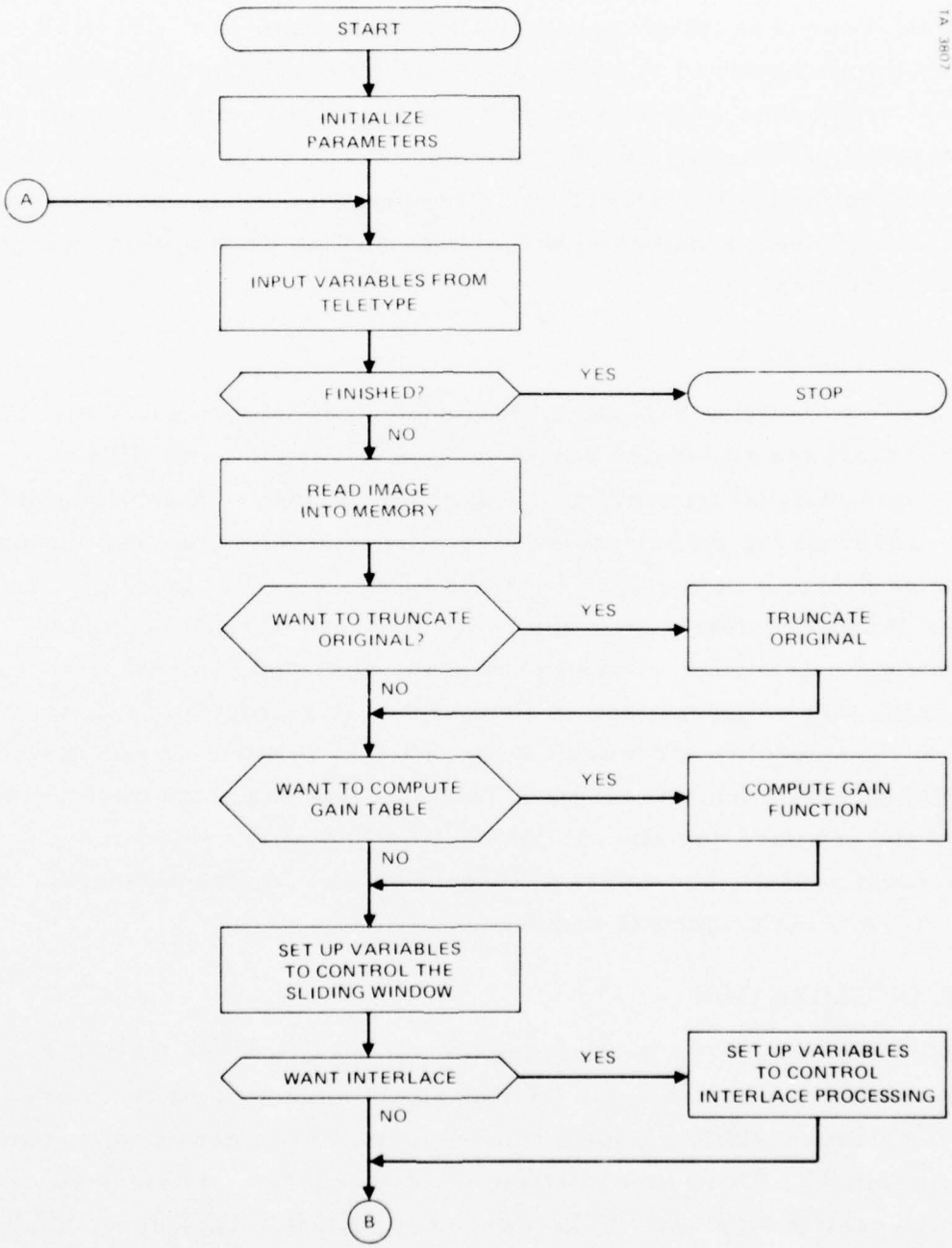


Figure 1. LABGC hardware simulation flowchart. (Sheet 1 of 2)

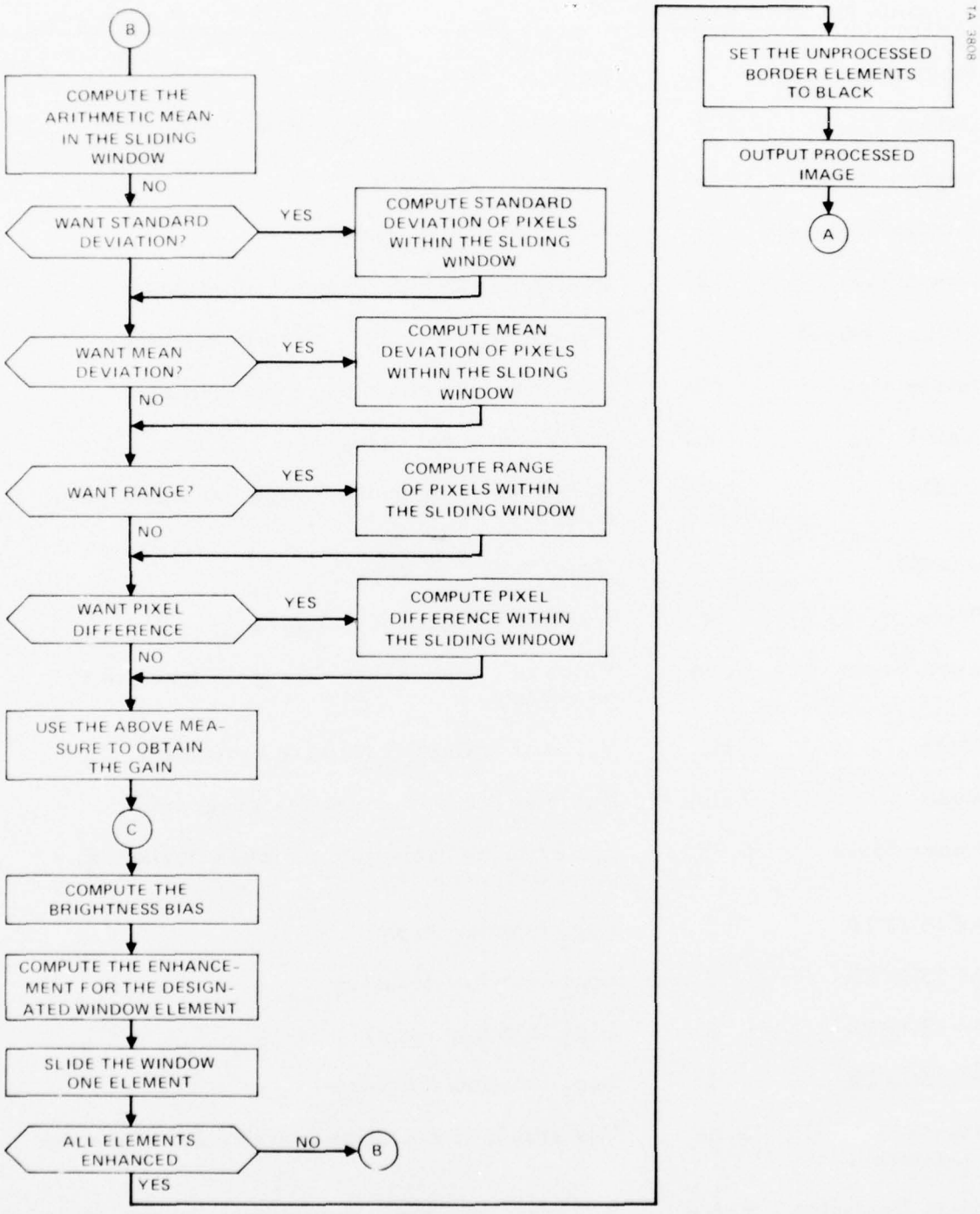


Figure 1. LABGC hardware simulation flowchart. (Sheet 2 of 2)

TABLE 4. "HARDWARE" LABGC PROGRAM VARIABLES

| Variable Name | Preset Value | Function |
|---|---|---|
| Input File | 1 | Logical file # of image |
| Output File | 2 | Logical unit # of output file |
| Window Rows | 4 | # of rows in window |
| Window Columns | 4 | # of columns in window |
| Row Offset | 2 | Row in window of "center" element-1 |
| Column Offset | 2 | Column in window of "center" element-1 |
| Image Size | 256 | # of rows and columns of input image |
| Max Value | 63 | Maximum pixel value |
| GLIM1 | 16 | Value of "standard deviation" at which gain equals 1 |
| GLIM2 | 4 | Upper bound of gain |
| Scale | 4 | # of bits of accuracy of gain |
| Burn Prom | True | Value of "true" causes the gain function to be computed |
| More | True | Value of "false" terminates program |
| Done | False | Value of "true" terminates program |
| Range Scale | 0.283 | Scalar to multiply range, mean deviation, or pixel difference by |
| AC1SHFTR | 2 | $\text{Log}_2$ (window rows) |
| AC2SHFTR | 2 | $\text{Log}_2$ (window columns) |
| AV1SHFTR | 2 | $\text{Log}_2$ (window rows) |
| AV2SHFTR | 2 | $\text{Log}_2$ (window columns) |
| Standard Deviation | True | Use standard deviation to drive gain function |
| Mean Deviation | False | If "true", use mean deviation * "range scale" to drive gain function |

(Continued next page)

(Table 4, concluded)

| Variable Name | Preset Value | Function |
|---|---|---|
| Range Deviation | False | If "true", use range * "range scale" to drive gain function |
| Pixel Deviation | False | If "true", use (center pixel - mean) * "range scale" to drive the gain function |
| Interlace | False | If "true", process odd lines then even lines (interlace). If "false", process all lines in window |
| INPSHFTR | 0 | Number of bits to truncate from input image |
| AC1SHFTL | 0 | Performs internal hardware truncations - see listing for usage. |
| AC2SHFTL | 0 | |
| AC3SHFTL | 0 | |
| AD1SHFTR,L | 0 | |
| AD2SHFTR,L | 0 | |
| AD3SHFTR,L | 0 | |
| AV1SHFTL | 0 | |
| AV2SHFTL | 0 | |
| INPSHFTL | 0 | |
| ML1SHFTR,L | 0 | |
| ML2SHFTR,L | 0 | |
| ML3SHFTR,L | 0 | |
| MX1SHFTR,L | 0 | |
| MX2SHFTR,L | 0 | |
| OUTSHFTR,L | 0 | |
| SB1SHFTR,L | 0 | |
| SB2SHFTR,L | 0 | |
| SB3SHFTR,L | 0 | |
| SB4SHFTR,L | 0 | |
| SB5SHFTR,L | 0 | |
| SQ1SHFTR,L | 0 | |
| SQ2SHFTR,L | 0 | |
| SQ3SHFTR,L | 0 | |
| SR1SHFTR,L | 0 | |
| SM1SHFTR,L | 0 | |

measures of intensity and contrast within the sliding window result in significant reductions in hardware complexity. Another hardware optimization is achieved if the number of elements in the sliding window is held to a binary power of 2. Then, the division in the algorithm could be replaced by binary shifts. Also, the smaller the sliding window, the simpler the hardware because fewer elements are computationally involved.

Great hardware savings result if the LABGC algorithm is applied to the odd and even fields of a frame separately instead of jointly. If the odd and even fields are processed together, large storage buffers are needed to store an entire field. However, no such storage is required if the fields are processed independently. Further hardware savings result if the number of bits of input gray-shades is minimized. Each of these mechanization considerations was analyzed and are discussed in the following paragraphs.

Contrast Measure Tradeoff

Since the standard deviation calculation involves sums of squares, squares of sums, divisions, and a square root which are complex to implement in hardware, alternate contrast measures were considered fruitful areas of evaluation. It has been shown[4] that for normal distributions the statistical range (maximum-minimum) can be used to estimate the standard deviation of the population. Furthermore, it can be corrected by applying a performance scale factor. Therefore, an alternate to the standard deviation is the range of values within the window, properly scaled. To determine the proper scale factor a computer program was written to compute the range and standard deviation for discrete windows within an image. The ratios of standard deviation to range were printed out and their arithmetic means computed for five TV images and various window sizes. An average ratio for each image was obtained for each window size. The average ratio for each window size over all scenes was then computed to provide a scene independent scale factor. The standard deviation of the average was also computed for each window size. The average plus one standard deviation was used as the optimum range scale factor. In most cases this insures that the estimated standard deviation is greater than the

4. Snedecor, G., Statistical Methods, 1946, Collegiate Press.

actual standard deviation. This further guarantees that the gain factor applied to the center pixel is less than or equal to that which is derived from the actual standard deviation.

To check the above procedure the computer was used to generate random numbers from a normal distribution. A computer program was then written to compute the ratios of range to standard deviation for various window sizes. An average ratio was computed for each window size. These average ratios were identical to those published in Snedecor.[4] Hence, it was concluded that the procedure for computing the optimum range scale factor was valid.

Based largely on Snedecor's work, the scaled range has a confidence factor of 97%. That is, 68% of the time, the scaled range is within 3% of the actual standard deviation and 99% of the time it is within 10%.

The hardware savings that result from using the range in place of the standard deviation are considerable. The complex multiplies and high bit precision required by the standard deviation algorithm are replaced by a peak detection algorithm to determine the maximum and minimum intensities. The net result is that the range algorithm requires from 34% to 40% fewer ICs than does the standard deviation, depending upon window size.

Another known statistical measure that is used to estimate the standard deviation is the mean deviation. The formula for the mean deviation is

$$MD = \frac{1}{n^2} \sum_{i=1}^{n} \sum_{j=1}^{n} \left| \overline{X} - X_{ij} \right|$$

where $\overline{X}$ is the average intensity within an n element by n line window and $X_{ij}$ is the i-$j^{th}$ entry within the window. Simply stated, the mean deviation is the average difference between each intensity and the average intensity in the window.

The computer program was modified to compute the ratio of mean deviation to standard deviation in local windows of an image. This program was then used in the same manner as outlined earlier to compute the optimum scale factor to estimate the standard deviation from the mean deviation.

The scaled mean deviation has a confidence factor of 98%. That is, 68% of the time the scaled mean deviation is within 2% of the standard deviation. Hence, it can be used to approximate the standard deviation very accurately.

The mean deviation implementation requires less hardware than does the standard deviation but somewhat more than the range. The mean deviation algorithm can be accomplished with additions instead of complex multiplies. The net result is that the mean deviation requires from 27% to 35% fewer ICs than does the standard deviation and from 5% to 7% more than does the range, depending upon window size. The hardware savings would be greater if it were possible to mechanize the calculation of the correct mean for the sliding window. As it is mechanized, a complicated mean correcting circuit is required to obtain an accurate mean for the window.

A third alternative contrast measure can be termed pixel difference. It is simply the absolute value of the difference between the center pixel and the average of all pixels in the sliding window. It is designed to exploit the LABGC algorithm rather than approximate the standard deviation. The principle behind the LABGC algorithm is that the difference between the center pixel and the average of all pixels in a local window is multiplied by a gain factor to increase local contrast. Historically, the gain factor is a function of the standard deviation of the pixels within the window. In the pixel difference algorithm, the gain factor is a function rather of the difference to which it is to be applied, i.e., the difference between the center pixel and the pixel average. In this way, the LABGC algorithm is more sensitive to the intensity of the center pixel. If the center pixel's intensity is near the average intensity in the window, a high gain is applied. Conversely, if the intensity of the center pixel is not close to the average intensity, a small gain is applied. The scaling factors as a function of window size for all three alternate measures of contrast are presented in Table 5.

The hardware required to implement pixel difference is extremely simple. Only an additional 4 ICs are needed regardless of window size. This small number of ICs results since the basic hardware needed for its implementation already exists in the system. Since a reasonable amount of flexibility is

TABLE 5. "HARDWARE" LABGC PROGRAM NOTES

"Range Scale" Values

| | 8 x 8 | 8 x 4 | 4 x 4 | 4 x 2 |
|---|---|---|---|---|
| Range | 0.304 | 0.328 | 0.359 | 0.402 |
| Mean Deviation | 1.486 | 1.446 | 1.395 | 1.354 |
| Pixel Diff. | 1.7 | 1.7 | 1.7 | 1.7 |

Input Values for Full Precision Standard Deviation
(4 x 2 Interlace)

- AC1SHFTR = 0
- AV1SHFTR = 0
- SQ2SHFTR = 6
- SM1SHFTR = 3
- INTERLACE = T
- AC2SHFTR = 0
- AV2SHFTR = 4

desirable in an evaluation brassboard and the pixel difference technique is so easily implemented, it was decided to incorporate this technique. There are also indications that it provides better performance under moderate noise conditions.

Intensity Measure Tradeoff

The LABGC algorithm uses the mean or average of intensities within the local sliding window as a brightness measure. Although the mean algorithm is not costly in terms of number of ICs, a small hardware savings results if an alternate measure is utilized. Therefore, two alternate brightness measures were examined.

The first, average variation, is simply the average of the maximum and minimum intensities in the window. It is expressed in equation form as

$$A.V. = (MAXIMUM + MINIMUM)/2$$

Since the average variation uses only two pixels in the sliding window, a significant hardware savings would be expected. For a window with 32 pixels

the average variation algorithm can be implemented with 68% fewer ICs than the mean. For a window with 8 pixels, however, the average variation requires only 20% fewer ICs.

The second alternate intensity measure examined is the average variation with memory. This algorithm uses the average variations from previous windows to estimate the mean for the current window. Its formula is given by

$$A.V.M.(K) = \frac{A.V.(K-3)+A.V.(K-2)+A.V.(K-1)+A.V.(K)}{4}$$

where A.V.(X) = (MAXIMUM + MINIMUM)/2 and K is the window index. In general, the average variation with memory algorithm approximates the mean better than the average variation algorithm without memory.

In terms of hardware complexity, the average variation with memory requires 35% fewer ICs than the mean for a window containing 32 pixels. For fewer pixels in the window, it requires 7% more ICs than the mean.

Window Size Tradeoff

The physical size of the sliding window has a significant effect on the complexity of certain portions of the LABGC hardware. For instance, when the window size is doubled, the input buffer must be enlarged by a factor of three, whereas the contrast and brightness algorithm complexities increase linearly with window size.

Another factor to be considered is the total number of pixels within the window. The mean, or average, within the window involves a division operation which is costly in hardware. However, if the total number of pixels within the window was a power of 2, the divide operation would be equivalent to a right shift. Therefore, all window sizes that were considered contain a power of two number of pixels. One disadvantage to this is that there is now no center pixel in the window. (Recall that the LABGC algorithm alters only the center pixel in each discrete window.) In the absence of a central pixel an arbitrary choice between the four centroid pixels must be made. Since the window is no longer symmetric about the chosen pixel, directional artifacts may possibly be introduced by the LABGC algorithm.

As originally studied in Phase I, the LABGC algorithm operated within a 9 line by 9 element sliding window. In view of the above mechanization considerations, the following window sizes are examined:

8 elements by 8 lines
8 elements by 4 lines
4 elements by 4 lines
4 elements by 2 lines

The nonsquare windows are examined for use in interlace processing which will be discussed in detail later.

Interlace Tradeoff

As originally designed, the LABGC process operates on the odd and even lines of an image together. That is to say that in any given sliding window there are an equal number of odd and even lines from the original image. However, TV displays are composed of odd and even fields. The odd field consists of only the odd lines of the image while the even field is composed of the even lines. For the LABGC hardware unit to process odd and even lines together, it would be necessary to store an entire frame. This storage requirement is unnecessary if the image is processed in an interlace fashion, i.e., odd and even fields are processed alternately and independently.

The window size must be modified to process in an interlace fashion. As originally designed, the sliding window was chosen to be square to minimize directional effects in the processed image. For interlace processing, however, the window is chosen to be a rectangle whose length is twice as long as its width. When the fields are combined for display, these two windows essentially combine to form a square window as illustrated in Figure 2.

A potential disadvantage of interlace processing is that the window contains only half of the information content that it does in noninterlace processing. For a 4 x 2 window, for example, the "center" element in the window is modified based upon information extracted from its own row and from two rows away. This may result in directional sensitivity of the algorithm.

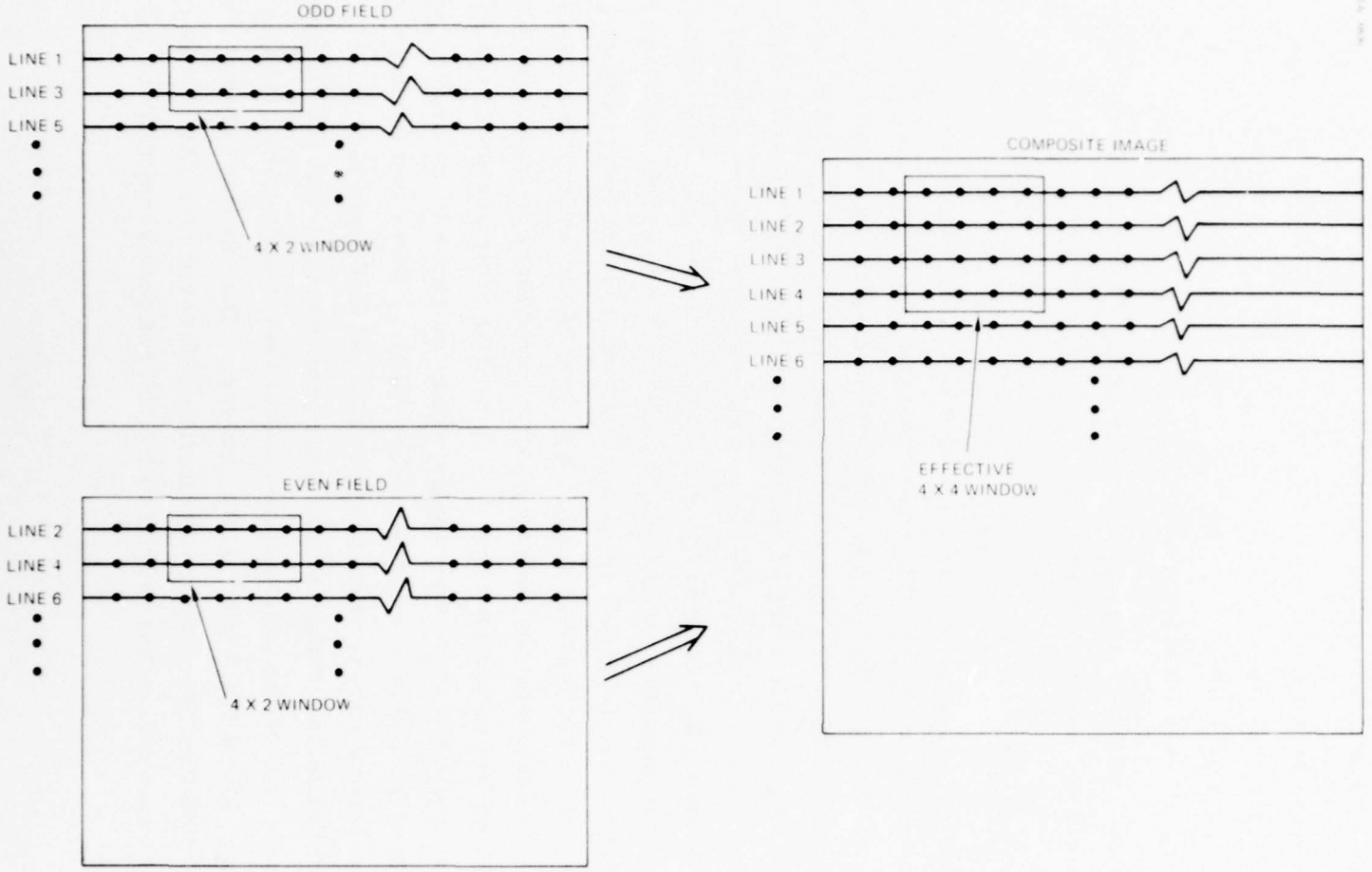


Figure 2. LABGC window size for interlace processing.

## Gray-shade Quantization Tradeoff

Further hardware savings result if the number of display gray-shades is minimized. The tradeoff is that the fewer the gray-shades, the less dynamic range resolution on the display. However, the fewer the gray-shades, the fewer ICs are required to implement the LABGC algorithm. Reducing from 6 to 5 bits of quantization results in a total savings of 15%, while reducing to 3 bits results in a 25% hardware savings.

## RESULTS

This section describes the results of the LABGC hardware tradeoffs in terms of hardware complexity and subjective evaluation of enhancement effectiveness.

The hardware complexity evaluation was performed by making a functional block diagram of each hardware configuration. An estimate was made of the number of integrated circuits required for each configuration.

The subjective evaluation of enhancement effectiveness of a particular configuration was performed by comparing the resulting pictures to those produced by the original LABGC algorithm. Four separate TV images, both noiseless and with gaussian analog noise added, were utilized in the evaluation. The LABGC computer simulation program was used to simulate the results that can be expected from each design configuration. In all the images presented here, the following parameters are applicable unless otherwise noted. The contrast measure is the standard deviation. The brightness measure is the arithmetic mean of intensities within the sliding window, which is 8 elements by 8 rows. The square window indicates that nominally the processing is performed in a noninterlace fashion. Finally the gray-shade quantization is 6 bits.

Figures 3 and 4 contain images processed by the four candidate contrast measures. These images were processed on an interlace basis using a four element by two line sliding window (4 x 4 area in total frame). The corresponding hardware complexity of each of the contrast measures in terms of ICs is shown in Table 6 (for that portion of the mechanization affected).

Images processed by the three brightness measures are contained in Figure 5 through 7. The contrast measure utilized in the range and the


a. Original


b. Standard deviation




c. Mean deviation


d. Range


e. Pixel difference

Figure 3. Measures of local contrast.

a. Original

b. Standard deviation



c. Mean deviation

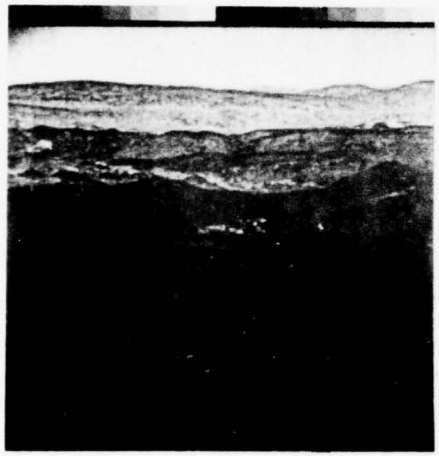

d. Range

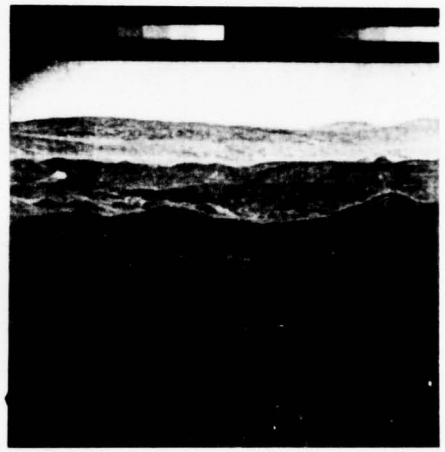

e. Pixel difference

Figure 4. Measures of local contrast.

TABLE 6. CONTRAST MEASURE COMPLEXITY OF LABGC CONFIGURATIONS IN FIGURES 3 AND 4

| Contrast Measure | Number of ICs |
|---|---|
| Pixel Difference | 4 |
| Range | 49 |
| Mean Deviation | 53 |
| Standard Deviation | 82 |

window size is four elements by four rows. The corresponding hardware complexity of each brightness measure configuration is presented in Table 7.

TABLE 7. BRIGHTNESS MEASURE HARDWARE COMPLEXITY OF CONFIGURATIONS IN FIGURES 5 - 7

| Brightness Measure | Number of ICs |
|---|---|
| Mean | 28 |
| Average Deviation | 4 |
| Average Deviation with Memory | 30 |

The window size/interlace tradeoff pictures are presented in Figures 8 through 10. The square windows were processed in a noninterlaced fashion while the nonsquare windows were processed in an interlaced manner. The measure of local contrast applied to these images was the range, scaled properly for each window size. The total LABGC system hardware complexity corresponding to these four window sizes is tabulated in Table 8.

TABLE 8. TOTAL LABGC SYSTEM HARDWARE COMPLEXITY FOR VARIOUS WINDOW SIZES (EXCEPT A/D)

| Window Size | Number of ICs |
|---|---|
| 8 Elements by 8 Lines | 750 |
| 8 Elements by 4 Lines | 350 |
| 4 Elements by 4 Lines | 650 |
| 4 Elements by 2 Lines | 250 |

Figures 11 through 13 contain images that were quantized to 6, 5, 4, and 3 bits and processed by the LABGC technique. This LABGC algorithm utilized the range as local contrast measure and operated within a four element by two element sliding window on an interlace basis. The corresponding hardware complexities are included in Table 9.

a. Original

b. Mean

c. Average deviation with memory

d. Average deviation

Figure 5. Measures of local brightness.

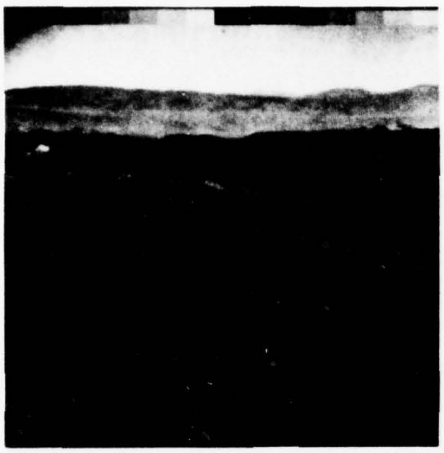

a. Original

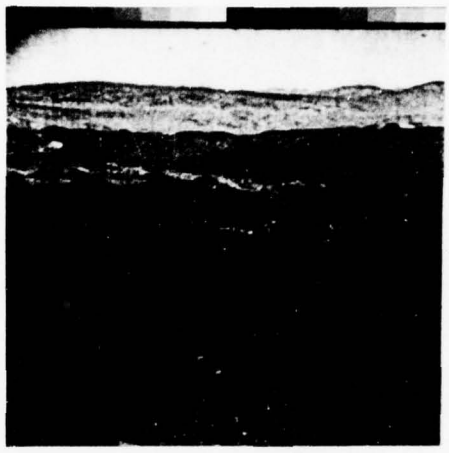

b. Mean

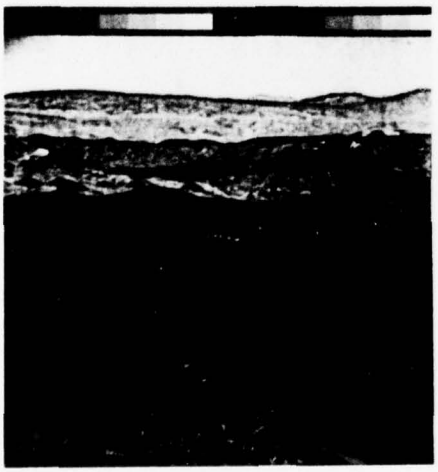

c. Average deviation with memory

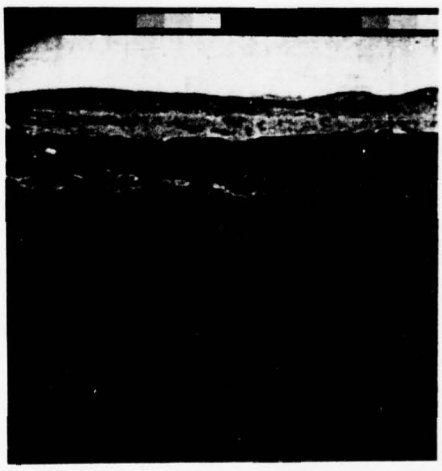

d. Average deviation

Figure 6. Measures of local brightness.

a. Original

b. Mean

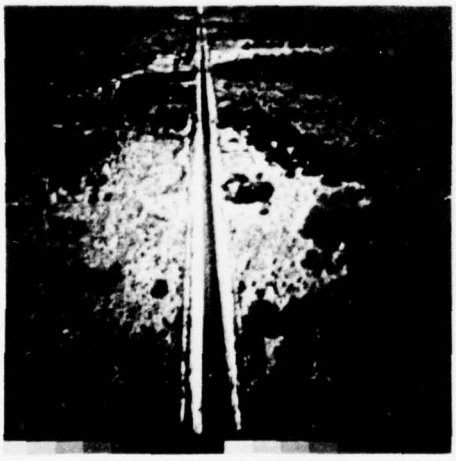

c. Average variation with memory

d. Average variatio

Figure 7. Measures of local brightness.

a. Original

b. 8 elements x 8 lines - non-interlace

c. 8 elements x 4 lines - interlace

d. 4 elements x 4 lines - non-interface

e. 4 elements x 2 lines - interlace

Figure 8. Effect of window size on LABGC processing.

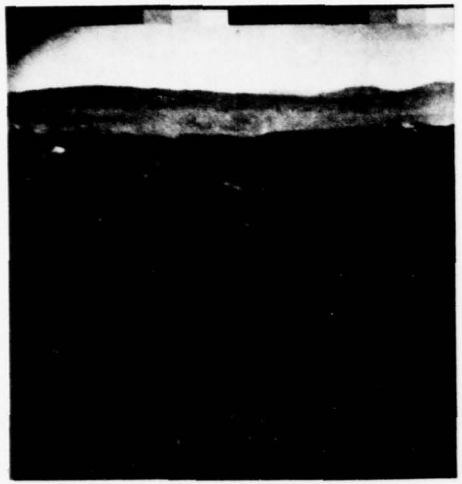

a. Original

b. 8 elements x 8 lines - non-interlace

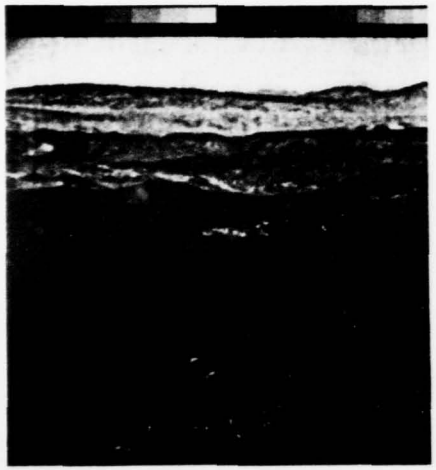

c. 8 elements x 4 lines - interlace

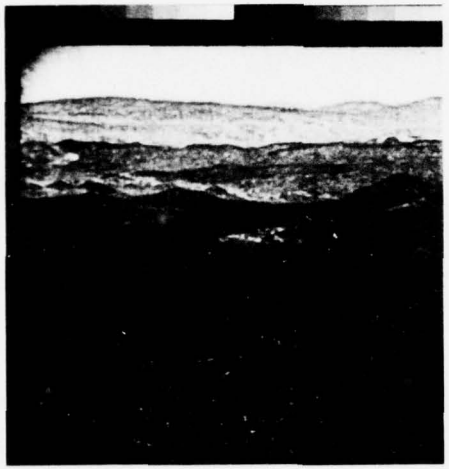

d. 4 elements x 4 lines - non-interlace

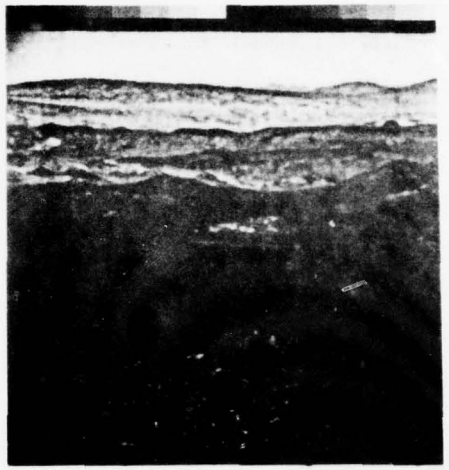

e. 4 elements x 2 lines - interlace

Figure 9. Effect of window size on LABGC processing.

a. Original

b. 8 elements x 8 lines non-interlace

c. 8 elements x 4 lines - interlace

d. 4 elements x 4 lines non-interlace

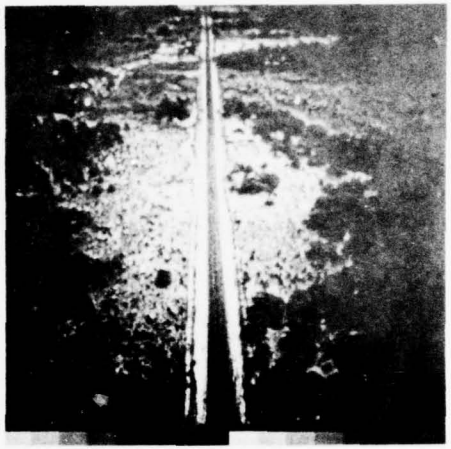

e. 4 elements x 2 lines - interlace

Figure 10. Effect of window size on LABGC processing.


a. Original - 6 bits


b. LABGC processed - 6 bits


c. Original - 5 bits


d. LABGC processed - 5 bits

Figure 11. LABGC algorithm applied to quantized image. (Sheet 1 of 2)


e. Original - 4 bits


f. LABGC processed - 4 bits


g. Original - 3 bits


h. LABGC processed - 3 bits

Figure 11. LABGC algorithm applied to quantized image. (Sheet 2 of 2)

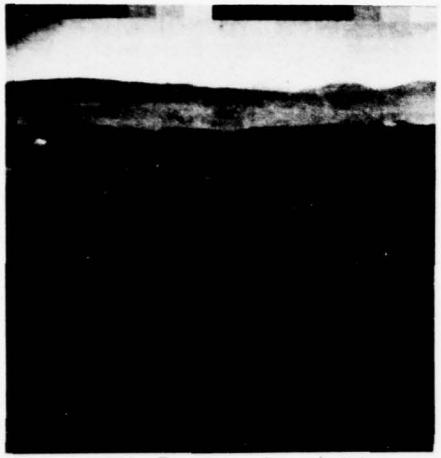

a. Original - 6 bits

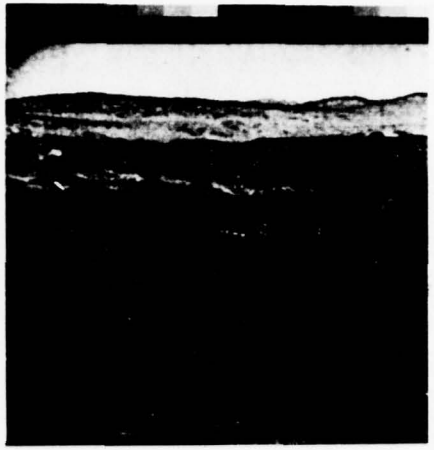

b. LABGC processed - 6 bits

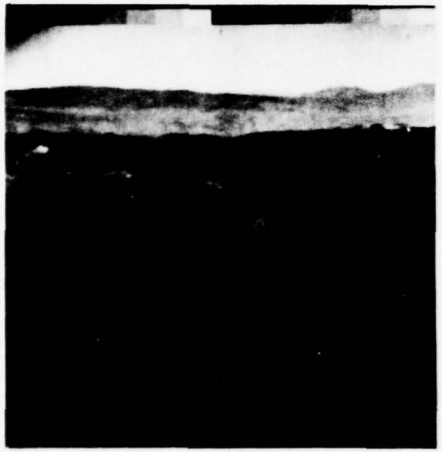

c. Original - 5 bits

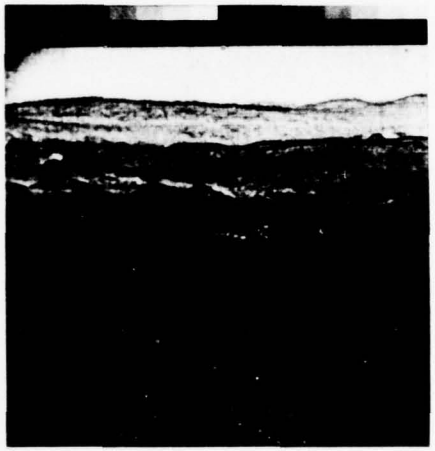

d. LABGC processed - 5 bits

Figure 12. LABGC algorithm applied to quantized image. (Sheet 1 of 2)

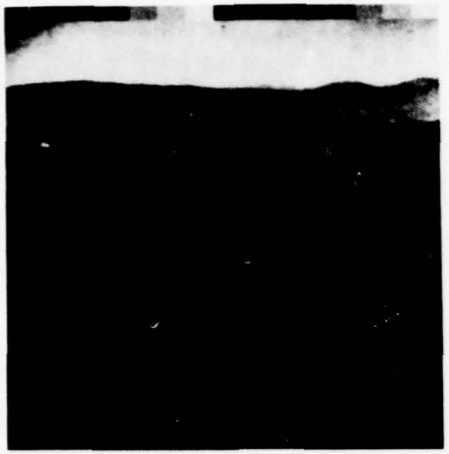

e. Original - 4 bits

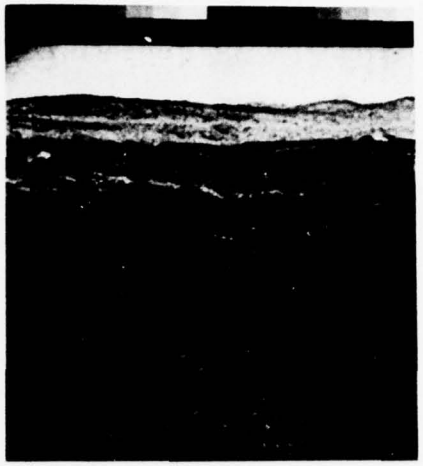

f. LABGC processed - 4 bits

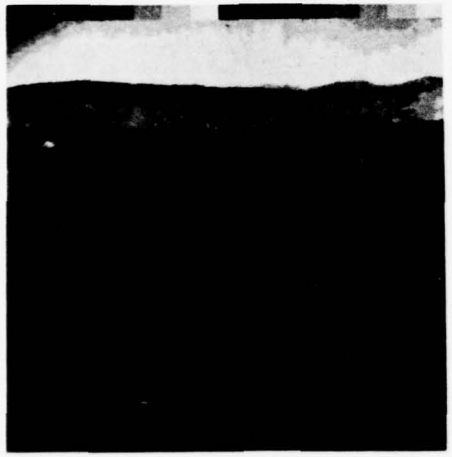

g. Original - 3 bits

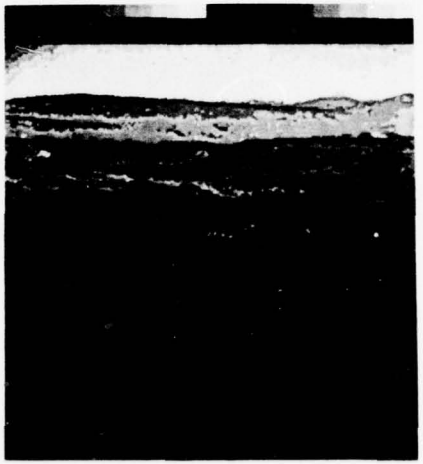

h. LABGC processed - 3 bits

Figure 12. LABGC algorithm applied to quantized image. (Sheet 2 of 2)

a. Original - 6 bits

b. LABGC processed - 6 bits

c. Original - 5 bits

d. LABGC processed - 5 bits

Figure 13. LABGC algorithm applied to quantized image. (Sheet 1 of 2)

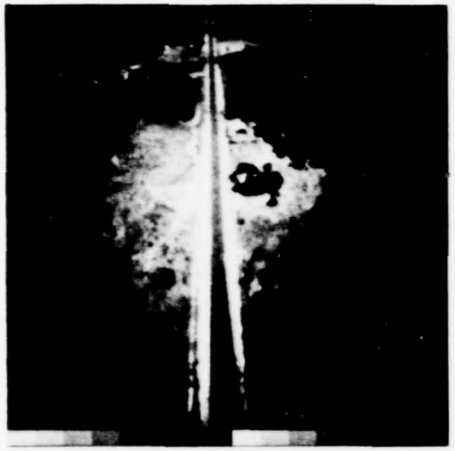

e. Original - 4 bits

f. LABGC processed - 4 bits

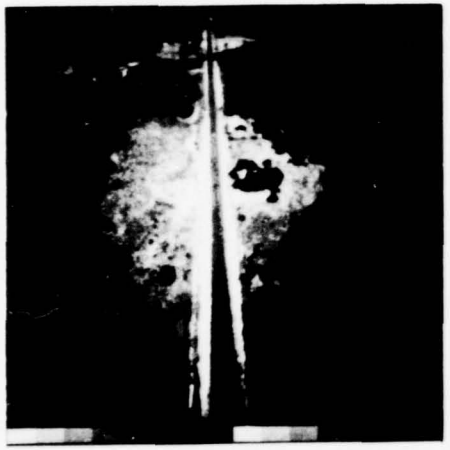

g. Original - 3 bits

h. LABGC processed - 3 bits

Figure 13. LABGC algorithm applied to quantized image. (Sheet 2 of 2)

TABLE 9. TOTAL HARDWARE COMPLEXITY OF LABGC UNIT OPERATING ON QUANTIZED IMAGES (EXCLUDING A/D)

| Number of Bits In Original Image | Number of ICs |
|---|---|
| 6 | 250 |
| 5 | 210 |
| 4 | 180 |
| 3 | 160 |

Finally, the LABGC algorithm was applied to images degraded by various levels of analog noise. These images are presented in Figures 14 and 15. The levels of noise in the images are characterized by a 10:1 signal-to-noise ratio and a 5:1 signal-to-noise ratio, respectively. The LABGC algorithm operated on an interlace basis within a four element by two line window.

## CONCLUSIONS

The objective of this study was to optimize the LABGC algorithm for hardware design and fabrication. The criteria used were estimated hardware complexity and evaluation of the simulated enhancement picture. The results of this study to select the optimum LABGC algorithm are summarized below:

- The measure of local contrast for low noise situations (less than 20:1 S/N) is the range (based on minimum complexity and essentially equal subjective performance).
- The measure of local contrast for high noise situations (10:1 S/N and greater) is the pixel difference (negligible hardware impact to add this capability).
- The measure of local brightness is the mean (subjectively preferred to other techniques).
- The algorithm employs a four element by two line window (based on minimum complexity and no subjective performance degradation).
- The algorithm operates on an interlace basis, based on a substantial complexity increase if entire field is stored and on essentially equal subjective performance.
- The input video is quantized to either 6, 5, or 4 bits (5 bits may be acceptable but commercial A/D converter is available with 6 bits).


a. Original with noise


b. LABGC processed with range as measure of contrast.

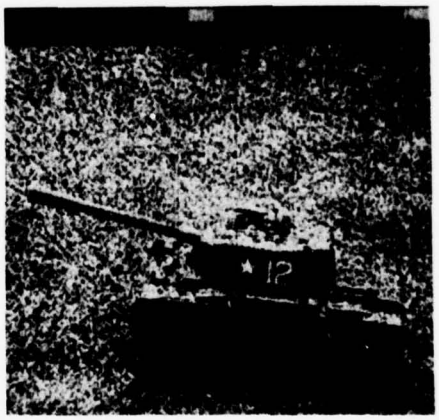


c. LABGC processed with pixel difference as measure of contrast.

Figure 14. LABGC algorithm applied to image with 10:1 signal-to-noise ratio.

a. Original with noise

b. LABGC processed with *range as measure of* contrast.

c. LABGC processed with *pixel difference as* measure of contrast.

Figure 15. LABGC algorithm applied to image with 5:1 signal-to-noise ratio.

## Section 4.0
## DESCRIPTION OF LABGC BRASSBOARD

### FUNCTIONAL DESCRIPTION

The LABGC system accepts and synchronizes to an external video source, performs the enhancement algorithm, and reconstructs the enhanced composite video waveform for transfer to the display. The mechanization parameters as described in Section III of this report are summarized in Table 10. The unit and front panel controls are shown in Figure 16.

#### Control Functions

The power switch connects the 110V AC power (60 Hz or 400 Hz) to the -5V, +5V, +15V, and -15V power supplies. The mode control switch selects either Ext, Range, Bypass, Pixel Difference, Bit 1 and Bit 2 Modes.

The Range mode employs the enhancement algorithm which applies a gain to the video based on the range of the intensity variation within the window. The range is computed as the difference between the maximum and minimum intensity value within the window, multiplied by a predetermined constant. The range closely approximates the standard deviation. The Range algorithm is used in low noise conditions.

The Bypass Mode allows the observer to view the unprocessed original image. The only function performed in this mode is that the video is passed through the AGC (Automatic Gain Control) loop to provide a uniform voltage output. This provides an effective comparison of the three modes.

The third mode is the Pixel Difference Mode. In this mode the gain applied to the center element of the window is inversely proportioned to the difference of the center element and the average value of the window. Indications are that this mode is most effective in relatively high noise conditions.

In both the Range and Pixel Difference Modes, the average value is subtracted from the center element in the window. The 4 x 2 element window starts in the upper left of the display and slides horizontally and vertically with the TV raster.

TABLE 10. LABGC BRASSBOARD TABLE OF PERFORMANCE PARAMETERS

| | |
|---|---|
| Algorithms Performed: | Local Area Brightness and Gain using Range and Pixel Difference as a measure of contrast and Mean as a measure of level. |
| Window Size: | 4 Horizontal elements x 2 Vertical elements per Field (4 x 4 per Frame) |
| A/D Sampling: | 4 - 6 BITS Selectable<br>9.072 MHz - 525 Line Mode<br>15.0 MHz - 875 Line Mode |
| Gain Transfer Function: | 32 Multiple Selectable (Gain functions are programmed in Prom listed in Appendix D.) |
| Input Video/Output Video: | 525 per EIA RS170; 875 per EIA RS330 |
| Other Features: | • Ability to Accept, Generate, Separate Syncs<br>• BIT and Checkout Modes<br>• Built-in Element Value Selector and Display |
| Input Power: | 178 Watts (60 or 400 Hz AC) |
| Size: | 19" Rack Mounted Unit; 10.5" high x 14" deep |
| Unit Weight: | 40 lb |

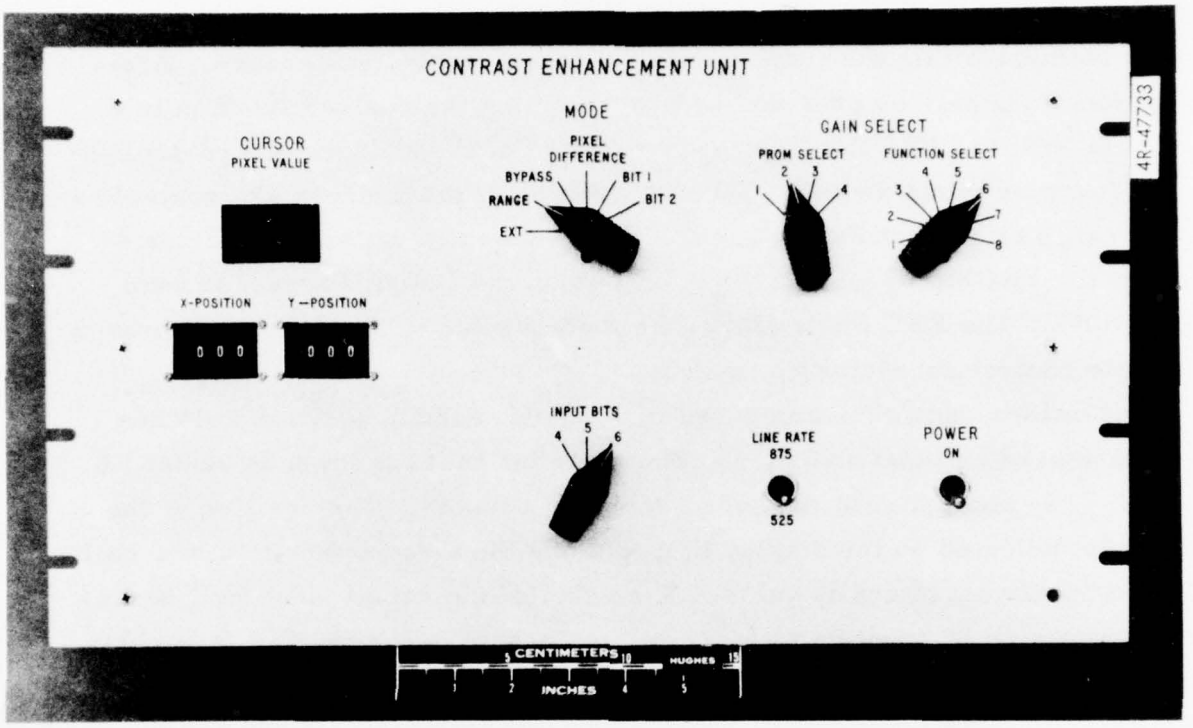


Figure 16. Unit front panel.

The Bit 1 Mode is the analog test mode. In this mode, the input video is analog to digital (A/D) converted and then digital to analog (D/A) converted, completely bypassing the enhancement algorithm. This mode tests all of the analog circuits.

The Bit 2 Mode is the digital test mode. A stored simulated video input is generated and applied to the enhancement circuits. The cursor controlled by the front panel switches can then be positioned at the test location and the intensity value can be read on the light emitting diode (LED), display, and compared with the known correct intensity value.

The 875/525 line switch provides a selection for either RS170, 525 line standard or an RS343A, 875 line standard. The display resolution for the 525 line mode is 480 x 480 pixels. The resolution in the 875 line mode is 512 x 809 pixels.

There are two Gain select switches. The PROM Select enables one of four Programmable Read Only Memories (PROMs). The Function Select addresses three address bits of the PROMs which provides eight selectable

functions. This allows the selection of 32 preprogrammed gain functions. The Gain Function controls the relationship of the video gain applied to the center element within the window with the range or pixel difference. Additional functions may be provided by programming the desired function in a Signetics N82S131 PROM. The three "MSB's" of the address are controlled by the function select switch. The six "LSB's" of the address are controlled by the range or pixel difference. The PROM select position 1, 2, 3, or 4 enables the PROMs U31, U32, U41, or U42 on the Output Processor card, location A3. The EXT Mode allows the mode switch to be controlled through a remote control connector.

The cursor control is composed of X position and Y position switches which are used as octal switches. The three bit codes from each switch, 0 through 7, is compared to the sync generator counter. The position of the cursor is indicated on the display by replacing the video intensity of the cell with the maximum intensity value. The value of the actual video cell is displayed on the front panel on the pixel value readout. The display is in octal with 77 as the maximum intensity.

The rear panel is shown in Figure 17. The test connector on the rear panel allows the bypassing of some of the front panel controls for remote operation. The function select and mode control switches are the only switches bypassed. The Mode switch must be in the EXT position and the function select must be in the "1" position. The rear panel connector signal list identifies each remote bypass control signal.

The power connector provides the unit with 110 VAC 60 or 400 Hz input power.

There are nine coaxial connectors provided on the rear panel. The video input is connected directly to the video output for daisy chaining or for the video termination. The enhanced video and the horizontal and vertical syncs are also provided on coaxial connectors. The enhanced video is buffered to drive 75 ohm cable. The cursor sync is also provided on coaxial connector as an oscilloscope sync. An external horizontal sync input is also provided. The switch mounted on the Sync Stripper module selects either the external horizontal sync or the sync stripper horizontal sync output. There are also two spare connectors provided.

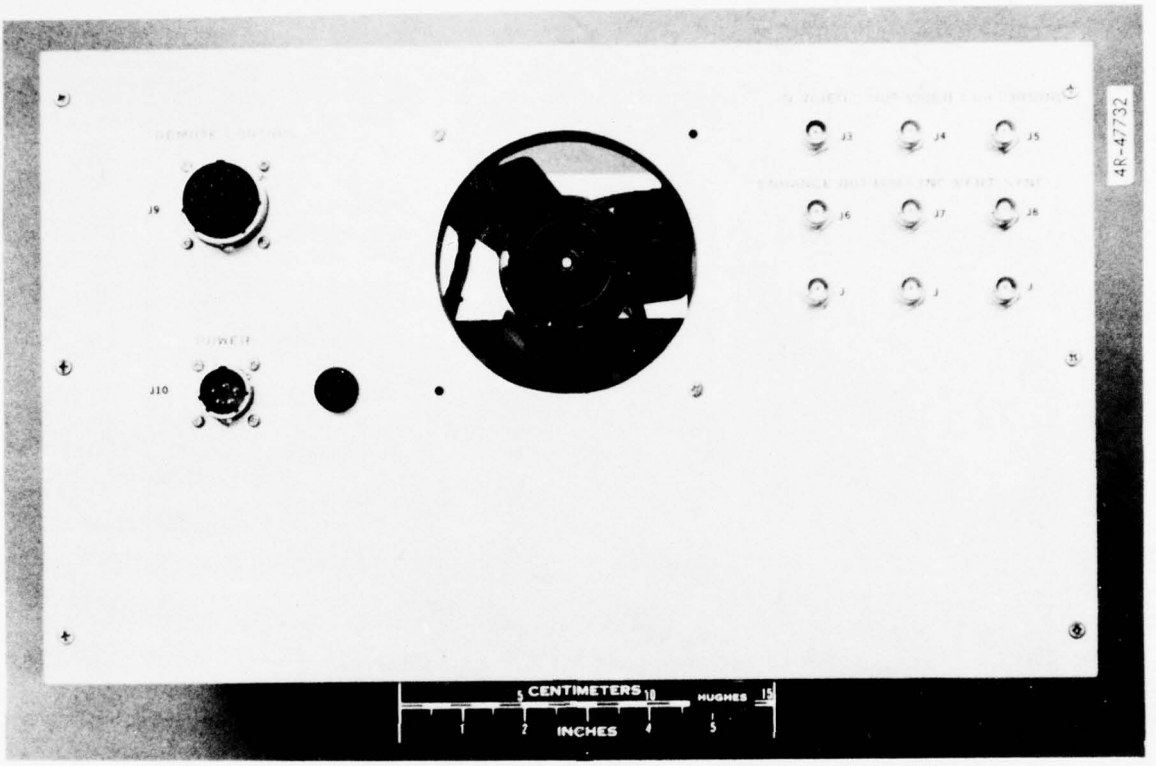


Figure 17. Unit rear panel.

There are two card cages in the LABGC system as shown in Figure 18. One card cage contains the analog to digital converter, the Data Devices Corporation VADC-8/17. The other card cage contains five circuit cards.

These cards are referred to as the Sync Stripper, Input Processor, Output Processor, Mean and Range boards. They are referred to in the system schematic as A5, A6, A7, A8, and A9 respectively. A functional block diagram of the unit is shown in Figure 19.

All input and output analog video processing is performed in the Sync Stripper Module, A5, vertical and horizontal syncs are stripped, the video is AGC processed to take full use of the A/D converter and the post processed digital video is converted back to analog video for display. The A/D converter, A1 - A4, is a purchased assembly and converts the video at real time to 6 bit digital words. The digitized video is transferred to the Input Processor (A6) which stores enough video to allow 2 dimensional real time processing. Syncs are generated, master clocking, and cursor generation are also performed on this module. The video range value

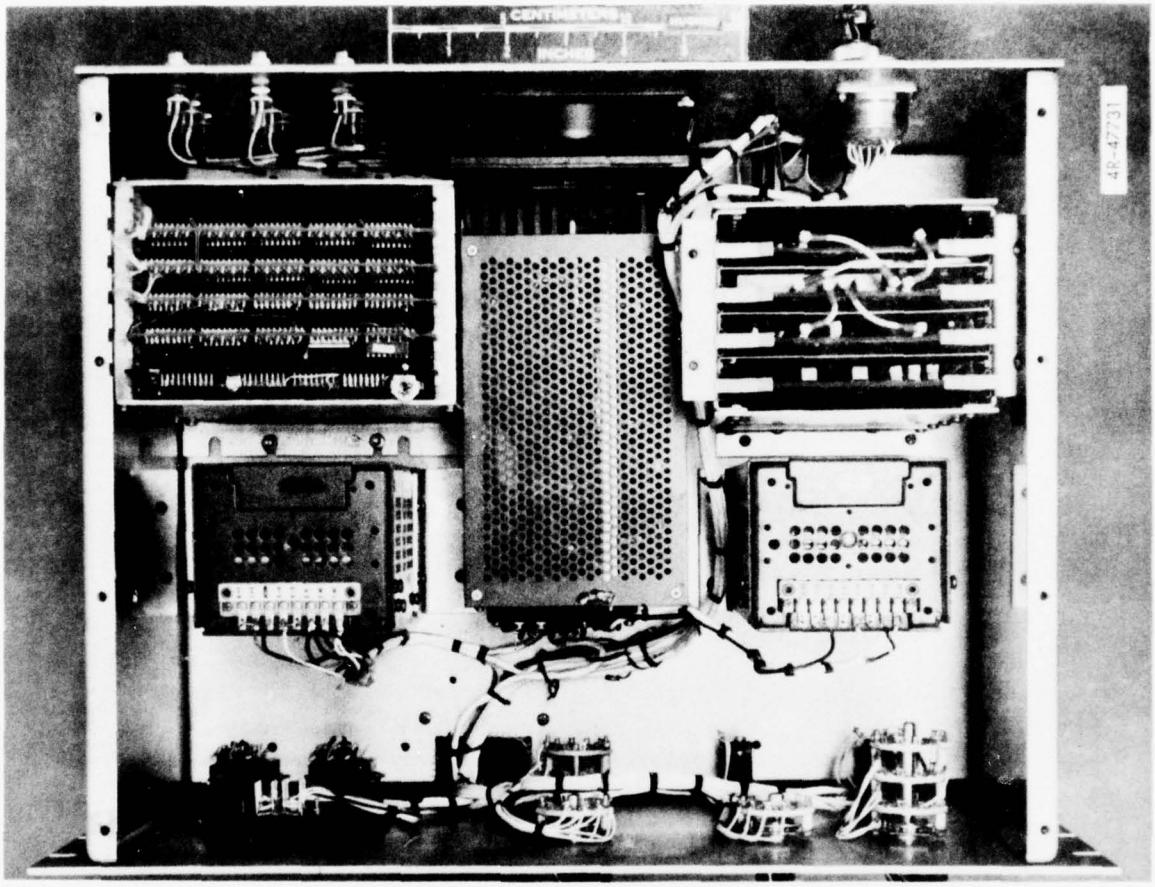


Figure 18. Unit top view.

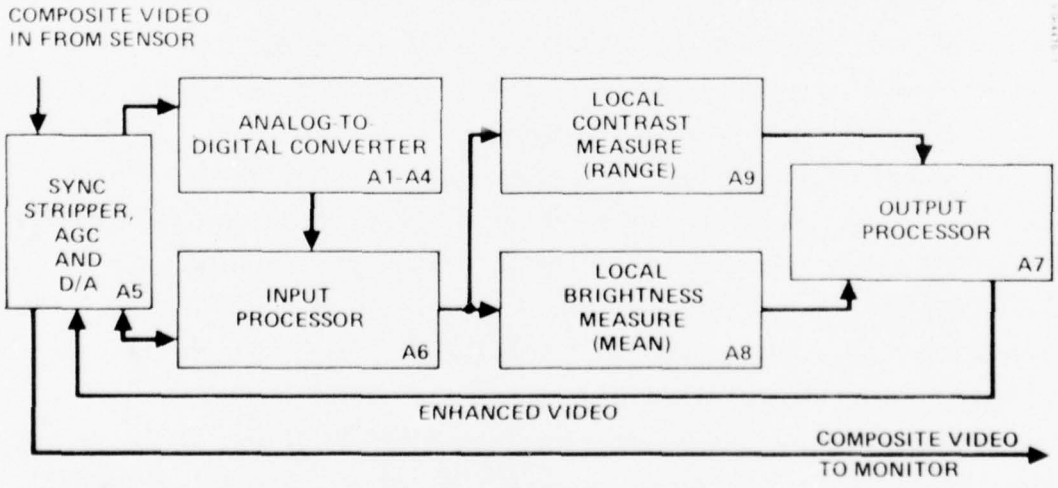


Figure 19. Contrast enhancement unit.

within the window is computed digitally in real time on the A9 module and the mean in the same window is simultaneously generated on A8. These two statistical values are transferred to the Output Processor Module (A7) where the actual gain and bias is applied to the single pixel elements. Variable gain transfer functions are stored in PROMs on this module providing significant flexibility. The output digital processed video is returned to the sync stripper module for D/A conversion to analog video for display.

External Cooling Requirements

The Image Enhancement Unit does not require any external cooling source. It is required that the airflow to the unit not be restricted and the local air temperature does not exceed 30°C at sea level (see appendix B).

Electrical Interface

The electrical interface connectors and signals are documented on the Interface Connector Wire List. The system signal names, and definitions are listed in Table 11.

TABLE 11. CONNECTOR LIST

Internal Connectors

J1 - Input Video to A/D

J2 - Output and Control from A/D

Rear Panel Connectors

J3 - Input Video

J4 - Output Video

J5 - Cursor Sync

J6 - Enhance Video Out

J7 - Horizontal Sync

J8 - Vertical Sync

(Continued next page)

(Table 11, concluded)

J9 - Remote Control (+5V Logic)(Active Low unless otherwise noted)

| | | |
|---|---|---|
| A - 875(+5V)/525(0 V) | F - BIT SL2 Input Bit 2SB | |
| B - Bypass | G - BIT SL1 Input Bit LSB | |
| C - PIXDIF | H - FCMSB | Function Select (Active High) |
| D - BIT 1 | J - FC2SB | |
| E - BIT 2 | K - FCLSB | |

J10 - Power

J11 - External Horizontal Sync

JXX, JXY - Spare

SYNC STRIPPER MODULE

The Sync Stripper Module is functionally shown in the block diagram in Figure 20 and a photograph of the card is shown in Figure 21. The functions performed on this module are as follows:

- Video Automatic Gain Control (AGC)
- External Clock Synchronization
- Sync Stripping
- Digital to Analog Conversion (D/A)
- Video Switching

The video AGC provides a constant ±2.5V input to the A/D, analog to digital converter, for up to a three to one variation of the input voltage. This allows the encoding of the video input to the full dynamic range of the A/D.

The sync signals are removed from the video in the AGC loop to provide AGC on the video only. Furthermore, the video applied to the A/D does not contain the sync pulses.

The sync stripper detects the horizontal and vertical syncs as well as the even or odd field data from the video input. The sync pulses are used to inhibit the AGC loop during this time.

The horizontal sync controls the phase lock loop (PLL). The PLL generates a master oscillator clock of 18 MHz for 525 line operation synchronized with the horizontal sync. This master oscillator is counted down and used as the reference input to the PLL.

The D/A converts the binary weighted enhanced output in the normal modes to analog composite video. The A/D digital output is reconverted to analog for testing in the BIT 1 mode. In this mode, the proper operation of the analog circuitry is verified.

The video output of the AGC loop is summed with the internally generated sync signals. The composite video waveform is multiplexed to the Enhanced Video output in the BYPASS Mode.

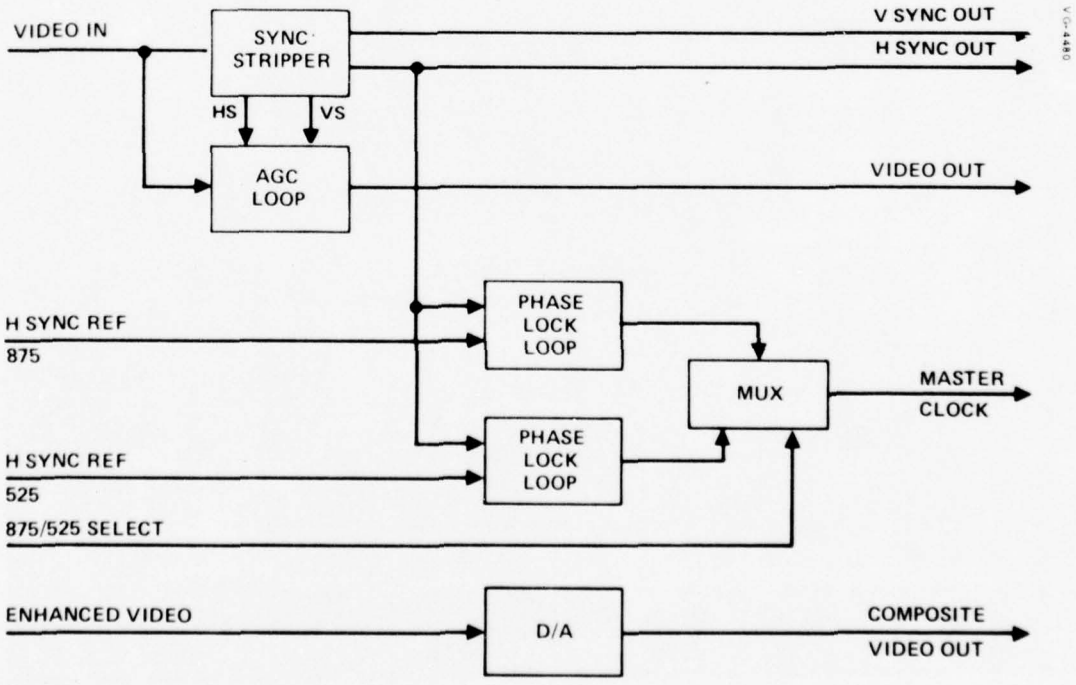


Figure 20. Sync Stripper (A5).

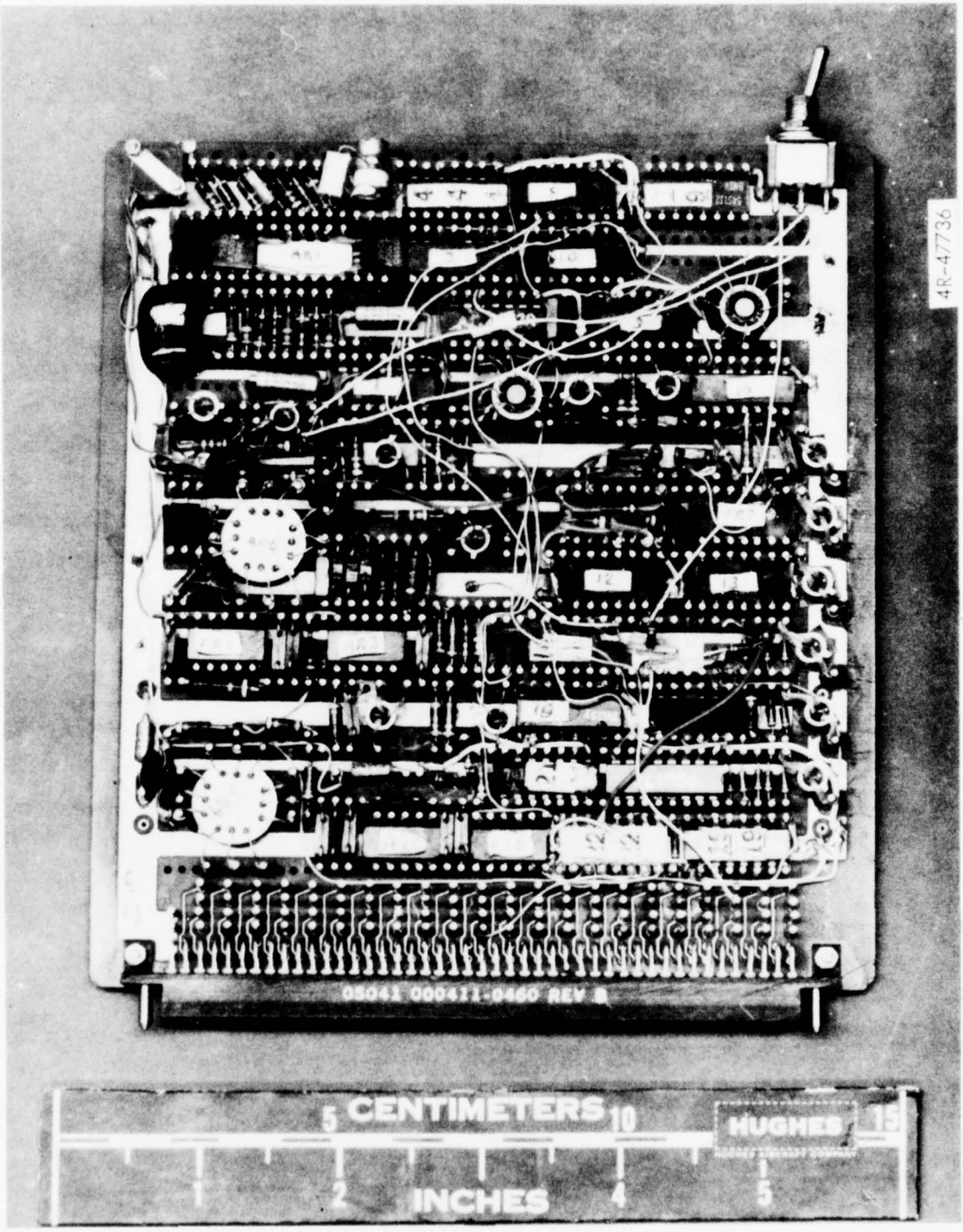


Figure 21. Sync stripper module (A5).

INPUT PROCESSOR MODULE

The functional block diagram of the input processor is as shown in Figure 22 and a photograph of the card is shown in Figure 23. The functions provided by this module are as follows:

- Input Buffer
- Sync Generation
- Test Pattern Generation
- Cursor Generation
- Input Bit Selection
- Timing and Control

The input buffer provides the one line delayed video. The delayed TV line from the buffer and the current TV line are used to form the two line window. The buffer is 512 elements in length and contains six bits in intensity storage. The data intensity storage can be truncated to five or four bits as well as the normal six bits by the Input Bit switch.

The sync generator provides all blanking and sync pulses to regenerate the composite video output in sync with the external TV input.

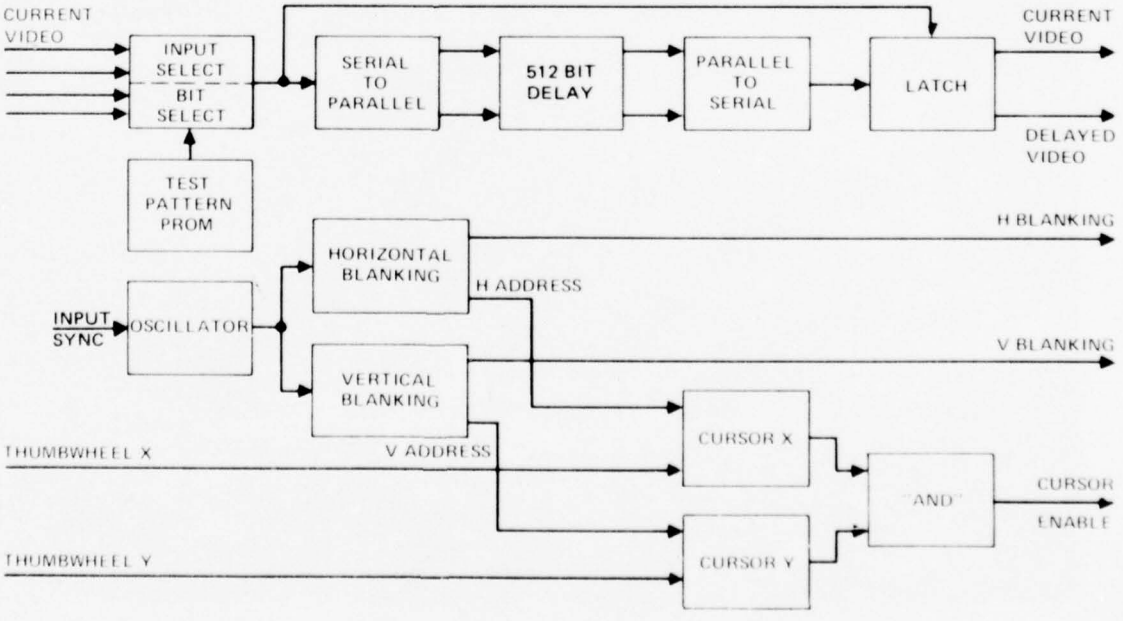


Figure 22. Input processor.

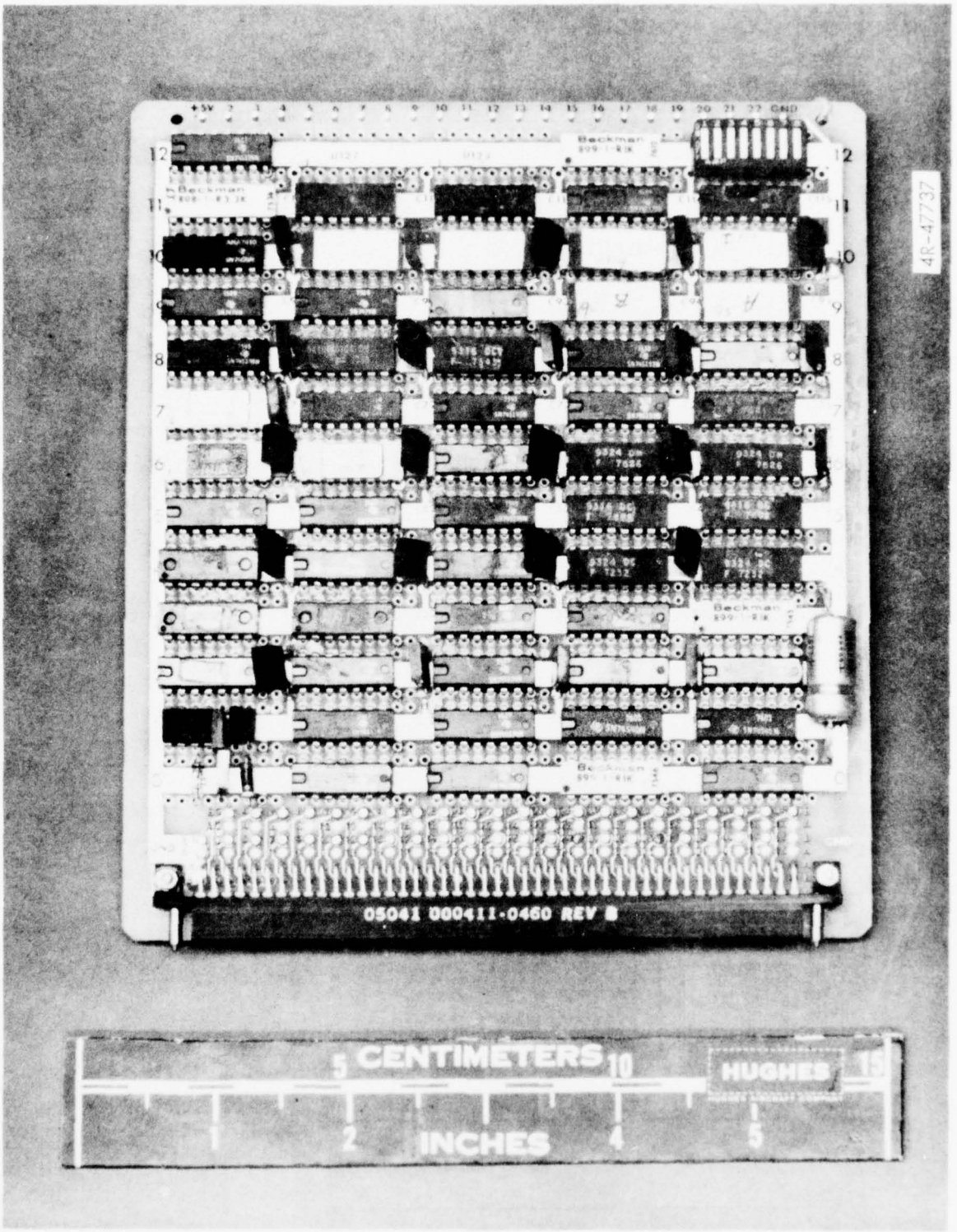


Figure 23. Input processor module (A6).

The sync generator also decodes the 10 to 90 percent of the active time horizontally and vertically to enable the AGC loop. A horizontal enable is also provided for the ROM, Read Only Memory, for the test pattern generator. Two other gating pulses are provided to inhibit the equalizing pulses and to detect the even or odd field. When the horizontal element counter has reached the maximum count, a hold pulse is decoded to hold the counter until the next horizontal sync is detected.

The test pattern generator provides input data in the BIT 2 mode. The test pattern, stored in a ROM, is read out supplying 16 pixel values on each line for all active lines in each field. The ROM is enabled near the horizontal center of the display. There are four selectable test patterns controlled by a dip switch mounted on the input processor module. The operation of the test PROMs is described in detail in the test PROM data selection in Appendix D.

The cursor generator compares the horizontal and vertical addresses of the sync generator with the X position and Y position switches on the front panel. The output strobe of the comparator is sent to the output processor to latch the selected pixel for display in the Pixel Value display. The actual pixel value is replaced by the maximum intensity to indicate the cursor position on the display. The pixel value is displayed in OCTAL on the front panel display.

The timing and control provides 512 clocks to the shift register each TV line to insure registration between the current and delayed TV lines. The clock enable is also synchronized with the horizontal blanking. The master clock buffering for each card is also provided on the module.

## OUTPUT PROCESSOR MODULE

The functional block diagram of the Output Processor Module is as shown in Figure 24 and a photograph of the card is shown in Figure 25. The functions performed on this module are as follows:

- Computes Range Enhanced Video
- Computes Pixel Difference Video
- Computes Brightness Logic
- Provides Gain Function Selection
- Stores Video Cursor Intensity

The output processor module multiplexes either the pixel difference or range input to the Gain Function PROM. The pixel difference is computed on the Mean Module as the center video window element minus the mean of the corresponding window. Since the pixel difference input is symmetrical with respect to the calculation, only the magnitude is processed and the sign bit is inserted at a later point in the computation. The pixel difference value is used in the range enhancement computation as well as the range value. In the range process, the value of the range determines the gain applied to the video minus the mean. Whereas in the pixel difference calculation, the gain applied to the video minus the mean is inversely proportioned to the pixel difference value. Therefore, in the pixel difference mode the gain is based on the difference of the center video element of the window and the mean value of the window.

After the gain is applied to the video minus the mean, the mean value is added back. The brightness logic applies a bias to the enhanced video if the output level is amplified beyond the six bit output. The bias is based on

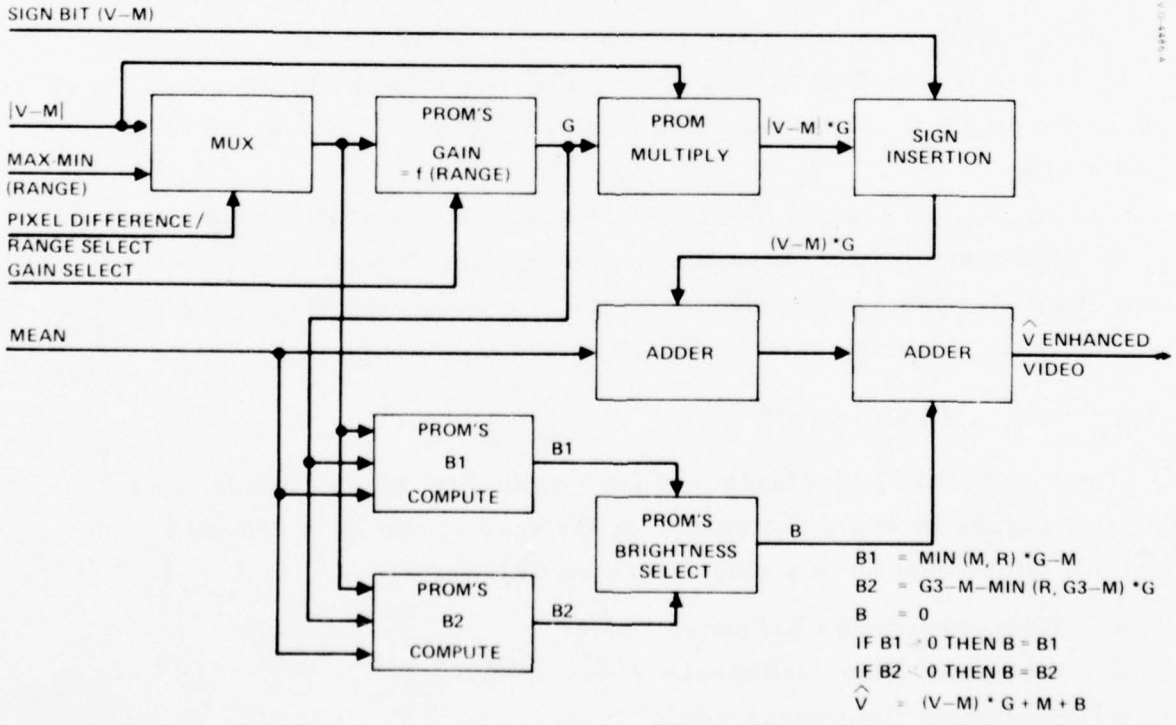


Figure 24. Output processor.

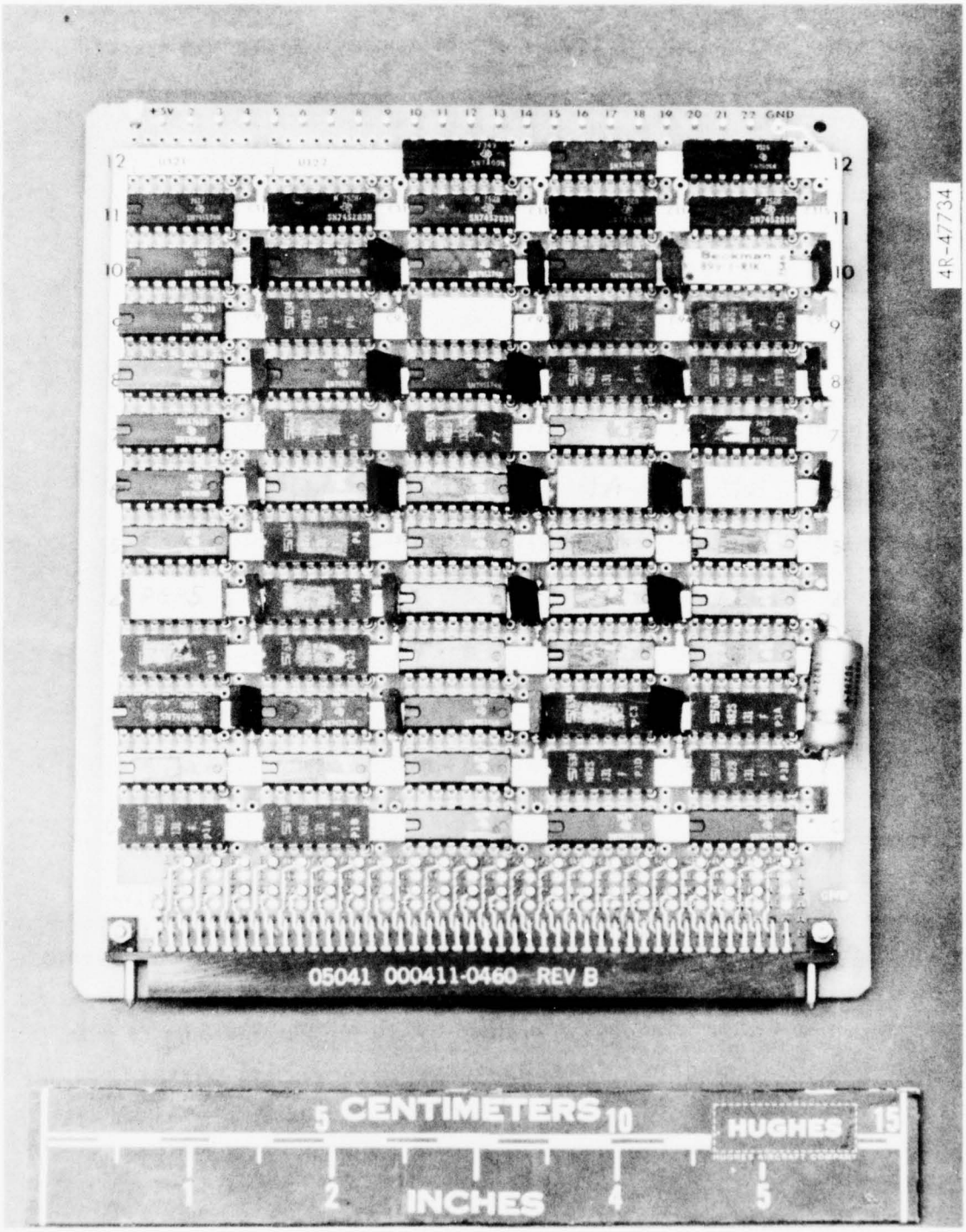


Figure 25. Output processor module (A7).

the mean, gain function, and the range. The equations are stored in PROMs as table lookups. The equations are described in detail in Appendix C of the Technical Description.

The gain functions and multiplies are also performed by PROM table lookups. In order to provide flexibility, 32 separate gain functions are provided via the PROMs. Eight functions are stored in each PROM and four separate PROMs can be selected via front panel controls.

In addition to the brightness compensation circuitry, an overflow/underflow correction circuit is incorporated. Any video level above 63 is forced to a 63 and any video level below 0 is forced to a zero.

MEAN MODULE

The functional block diagram of the Mean Module is as shown in Figure 26 and a photograph of the card is shown in Figure 27. The functions provided by this module are as follows:

- Running Accumulation
- Element Averaging
- Line Averaging

The Mean Module computes the average intensity value of the sliding window. This is performed by accumulating the difference between the video and the video delayed by four elements. This is done for both the current and delayed video line. Each line accumulator contains the sum of four video elements.

When the window is shifted horizontally, the oldest element is subtracted and the newest element is added to each line accumulator. This accumulated sum is then divided by performing a 3 bit binary shift.

The sum of the entire window is obtained by adding the contents of both the current video line and delay video line accumulators. The average or mean of the eight cell window is then computed by dividing the total window accumulator value by eight, which is in actuality a right binary shift of three bits.

The mean is then subtracted from the center video element. This quantity, the Video Minus the Mean (V-M) is separated into sign and magnitude. This was done to reduce the number of ICs required to implement the

enhancement algorithm. The sign of the (V-M) and the V-M is then sent to the Output Processor Module which performs the actual video enhancement.

RANGE MODULE

The functional block diagram of the Range Module is as shown in Figure 28 and a photograph of the board is shown in Figure 29. The functions provided by this module are as follows:

- Video Serial to Parallel Conversion
- Video Intensity Sorting
- Range Calculation

The Range Module computes the intensity difference between the maximum and minimum video pixels within the window. The current video and delayed video is compared and sorted into a maximum and minimum video stream. Each stream is serial to parallel converted to achieve access to four video elements simultaneously. The four parallel elements which form the window

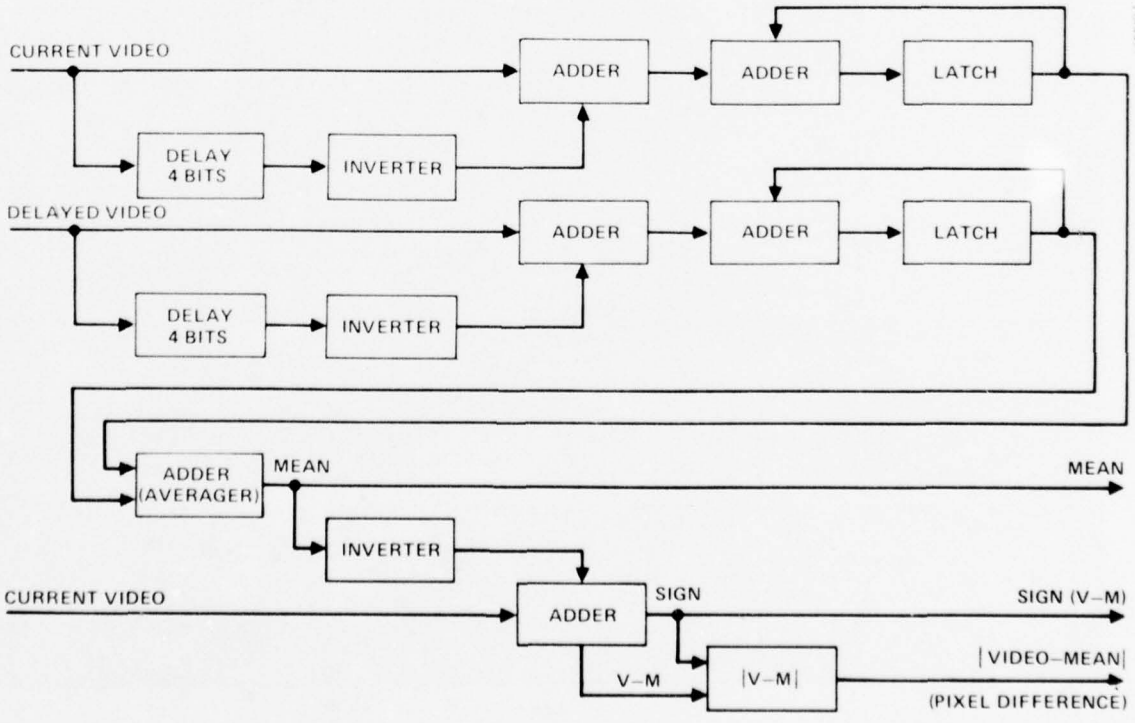


Figure 26. Local brightness measure (mean).

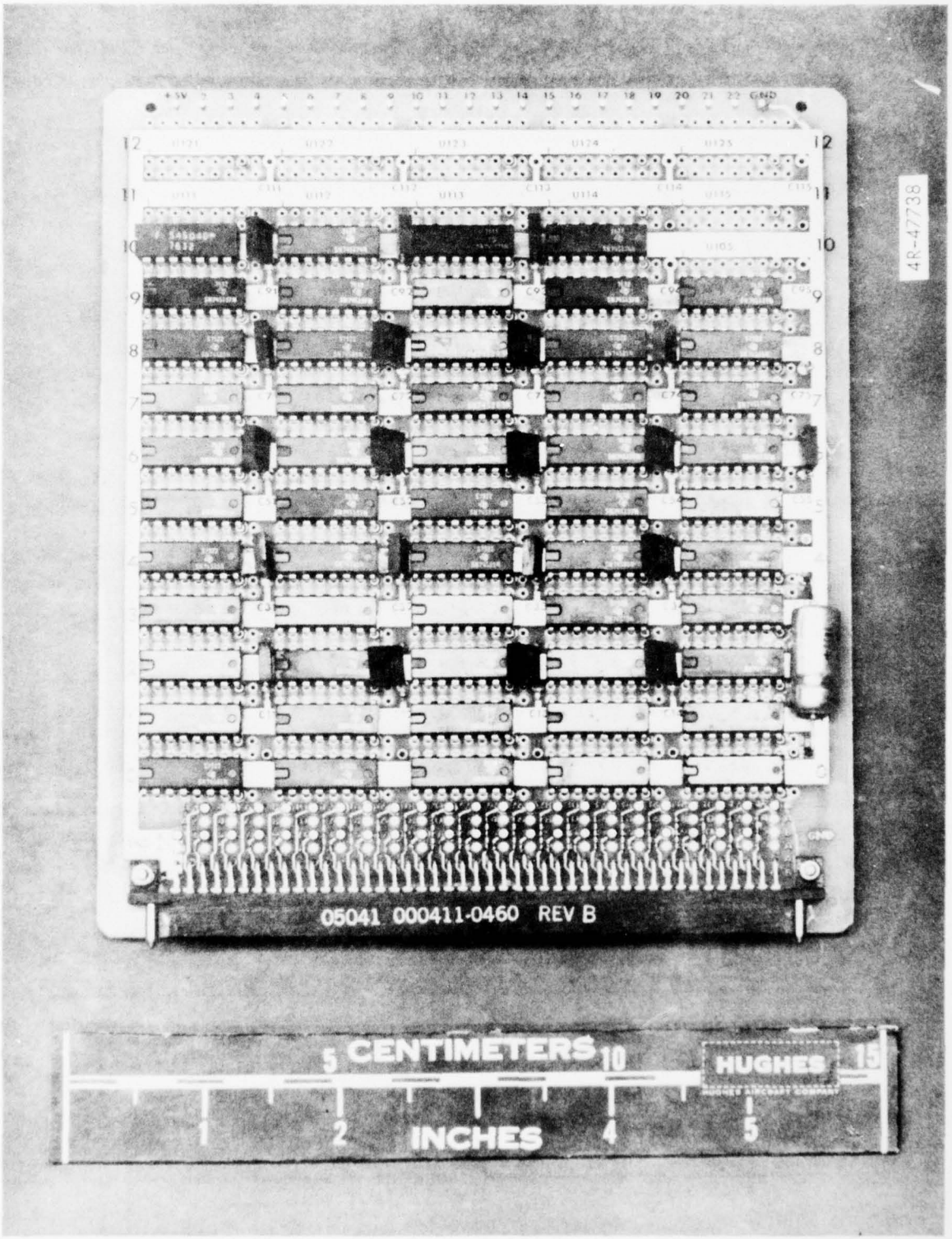


Figure 27, Mean board (A8).

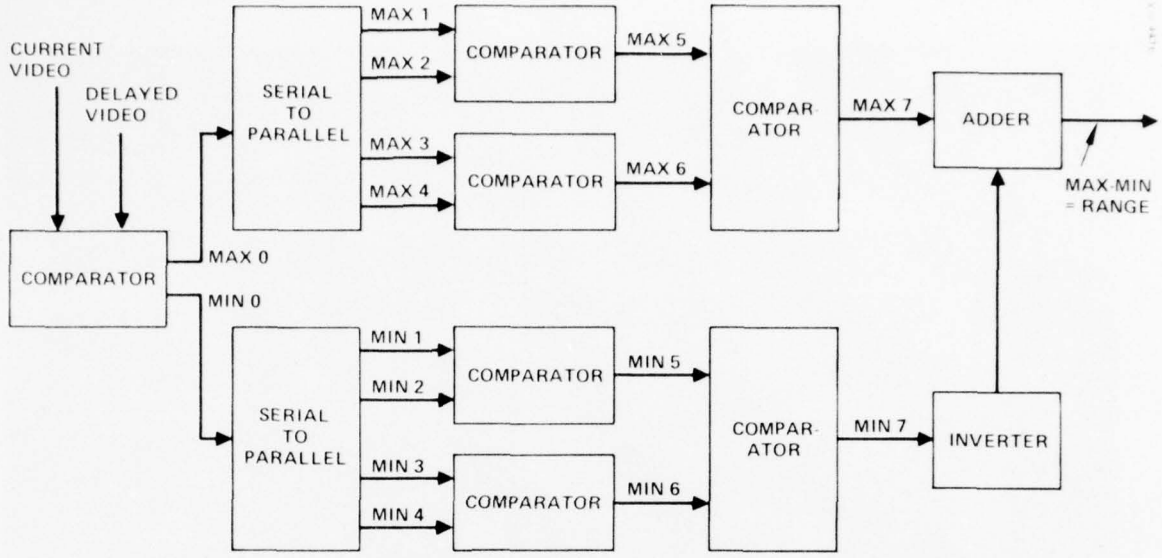


Figure 28. Local contrast measure (range).

are compared and the peak or minimum value is selected and multiplexed to the inputs of a subtractor. The difference is computed and outputted to the output processor. The computation delay is compensated to synchronize the data to the output processor module.

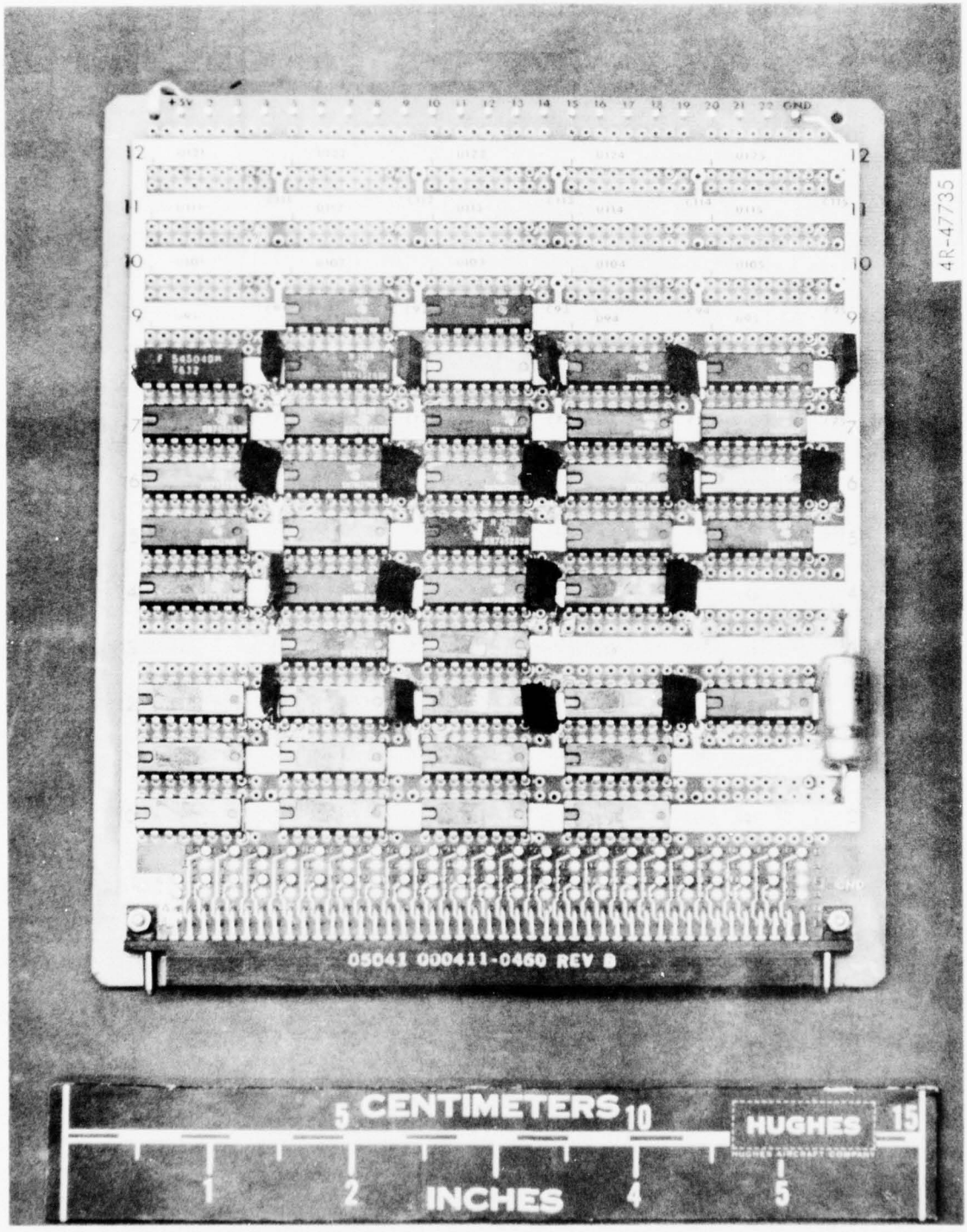


Figure 29. Range module (A9).

## Section 5.0
## UNIT DIAGNOSTICS TESTS

In the event that the Contrast Enhancement Unit should fail, the following diagnostic tests are supplied to help isolate the failure to a particular board within the system.

### ANALOG

With an appropriate input test source (such as a CCTV camera) connected to J3 (in video) turn the Mode switch to Bit 1. In this mode the input video is digitized through the A/D and then converted back to analog through the D/A. The picture on the monitor in Bit 1 should look very similar to the picture obtained with the Mode switch in BYPASS. In the bypass mode the video after sync stripping, and reinsertion is routed to the unit output. If the BYPASS mode does not work properly the trouble is on the Analog Board (XA5) or the timing control on the Input Processor Board (XA6). If BYPASS does work and Bit 1 fails the trouble is in the DDC A/D converter or in the D/A on the Analog Board (XA5). If Bit 1 works the trouble is now isolated to the digital boards within the system.

### DIGITAL

Run the acceptance test as outlined in the Acceptance Test document (Appendix C). If the acceptance test fails that is an indication that the trouble is in one of the digital boards. At this point remove the top cover and locate the Test PROM Data Selection Dip Switch on the Input Processor card (XA6). The switch package is located in the upper right-hand corner (U125) of the card. Looking at the switch observe that switch 5 is ON, 6 is ON, 7 is ON, and 8 is OFF. This selects the medium range of random numbers used for the acceptance test. If the switches are not in the above stated positions set them correctly and repeat the acceptance test. If the acceptance test passes the digital circuitry is operating correctly. No further testing is necessary. If the acceptance test fails, select the high range of random numbers by leaving switches 5 and 6 in their current positions and turning switch 7 OFF and switch 8 ON. (For more details on this refer to Table D-1 in the Test PROM Data Selection document, Appendix D.) The waveforms are recorded

for various points in the circuitry for this mode. Figure 19 is a block diagram of the Contrast Enhancement Unit. The waveforms found on each of the modules (XA6 - XA9) are shown on the following pages. These waveforms are shown for the PROM Select switch set at 2 and the Function Select switch set at 8 (front panel switches).

In the event that the waveforms are not stationary on the oscilloscope, it is suggested to go into the internal synchronization mode by using the crystal oscillator provided with the unit. The procedure to convert to internal mode is as follows:

1. Remove Analog card (XA5) and put aside.
2. Remove Input Processor card (XA6).
3. On the Input Processor card:
   a. Solder one wire of a twisted pair from U124-10 to U74-2 (signal).
   b. Solder the other wire from U124-8, 7 to U74-8 (ground).
4. Connect a wire from connector pin A8 to connector pin A13 (this is the HSYNC signal).
5. Connect a wire from connector pin B7 to connector pin A18 (this is the VSYNC signal).
6. Plug the oscillator in location U124. The Motorola trademark is directly above pin 1 of the oscillator.
7. Reinsert Input Processor card into chassis.
8. Turn unit on - the unit should now be operating in internal mode.

Input Processor

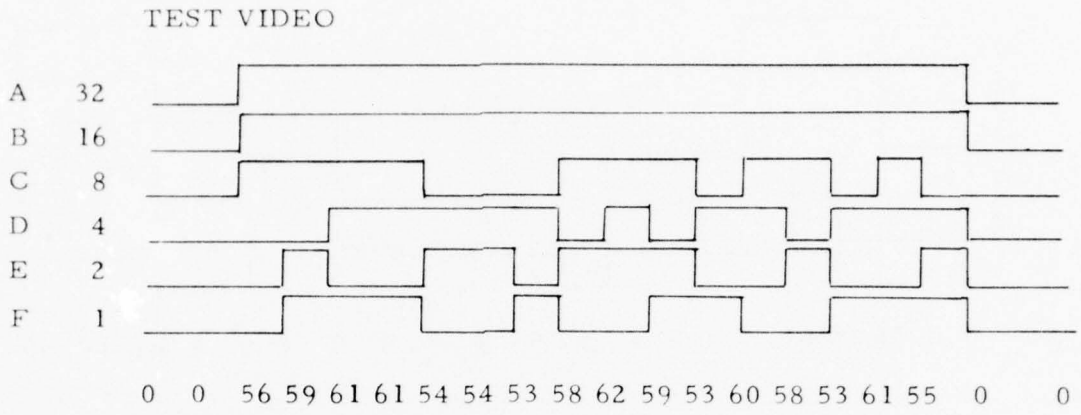


| Signal | Points Found |
|---|---|
| A | U85-4, U41-3, U33-2, U23-2, U121-2 |
| B | U85-7, U31-3, U33-5, U23-5, U121-5 |
| C | U85-12, U21-3, U33-7, U23-7, U121-7 |
| D | U85-9, U42-3, U33-10, U23-10, U121-10 |
| E | U84-4, U32-3, U33-12, U23-12, U121-12 |
| F | U84-7, U22-3, U33-15, U23-15, U121-15 |

NOTE: U33 is the latch for the current video line (CVID).
U23 is the latch for the delayed video line (DVID).
The waveforms at these two latches should be in phase with each other.

Range Board

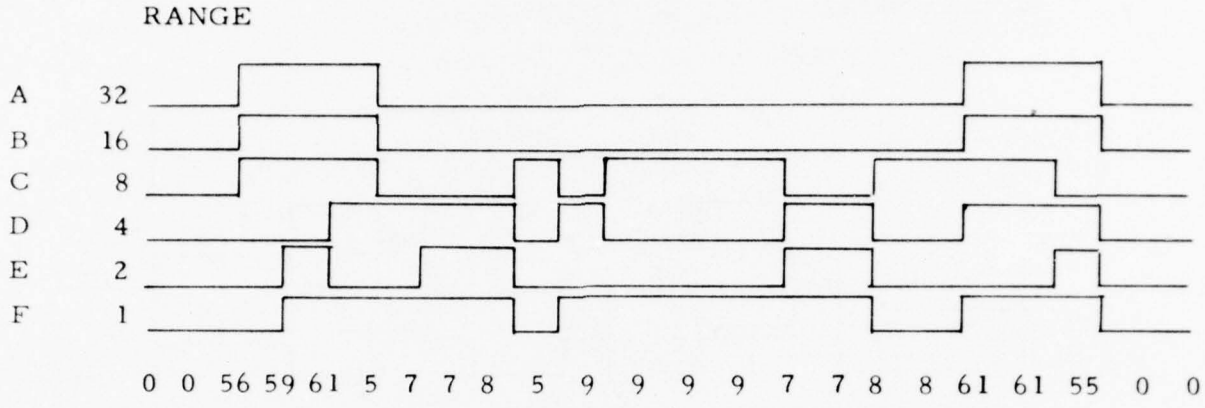


| Signal | Points Found |
|---|---|
| A | U63-2, TP16 |
| B | U63-5, TP17 |
| C | U63-7, TP18 |
| D | U63-10, TP19 |
| E | U63-12, TP20 |
| F | U63-15, TP21 |

Mean Board

ACCUMULATOR: LINE 1 or LINE 2

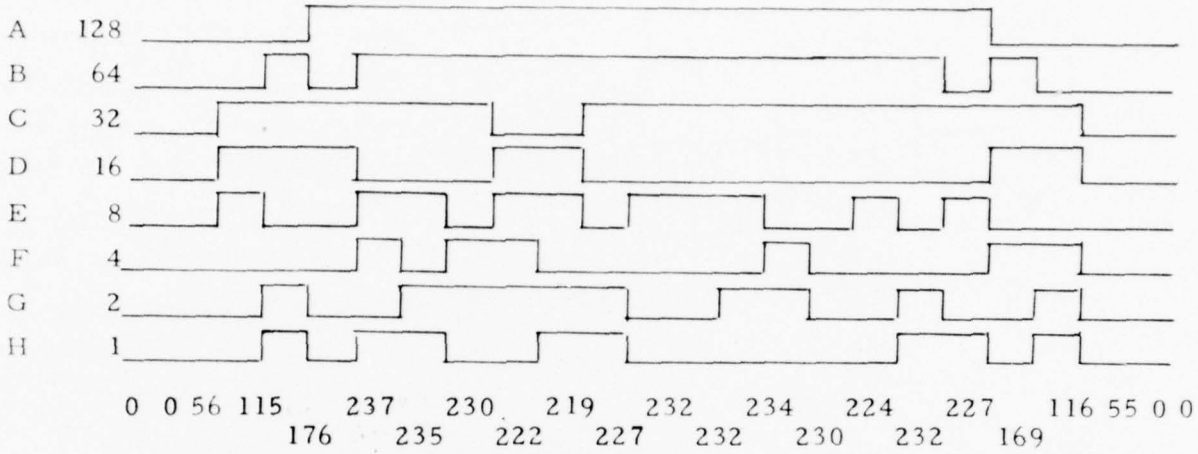


| Signal | Points Found |
|---|---|
| A | U51-2, U54-2 |
| B | U51-5, U54-5 |
| C | U51-7, U54-7 |
| D | U51-10, U54-10 |
| E | U62-2, U63-2 |
| F | U62-5, U63-5 |
| G | U62-7, U63-7 |
| H | U62-10, U63-10 |

NOTE: U51 and U62 is the accumulator latch for line 1.
U54 and U63 is the accumulator latch for line 2.
The waveforms at these two latches should be in phase with each other.

MEAN

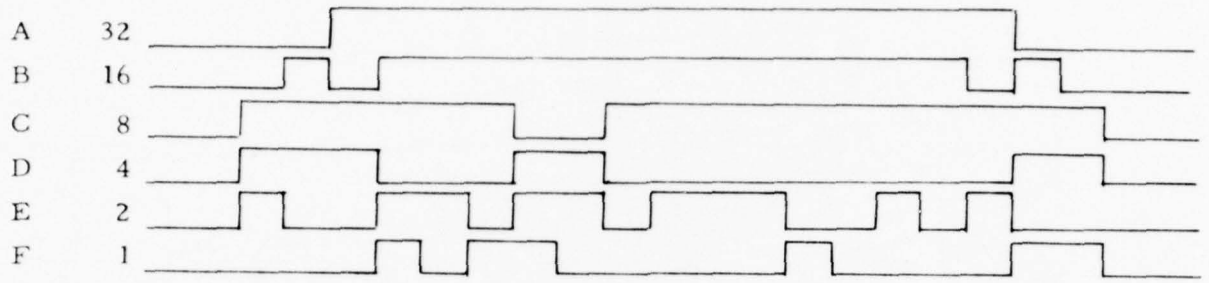


0 0 14 28 44 59 58 57 55 54 56 58 58 58 57 56 58 56 42 29 13 0 0

| Signal | Points Found |
|---|---|
| A | U93-2, TP10 |
| B | U93-5, TP11 |
| C | U93-7, TP12 |
| D | U93-10, TP13 |
| E | U93-12, TP14 |
| F | U93-15, TP15 |

SIGN BIT & ABS (VIDEO - MEAN)

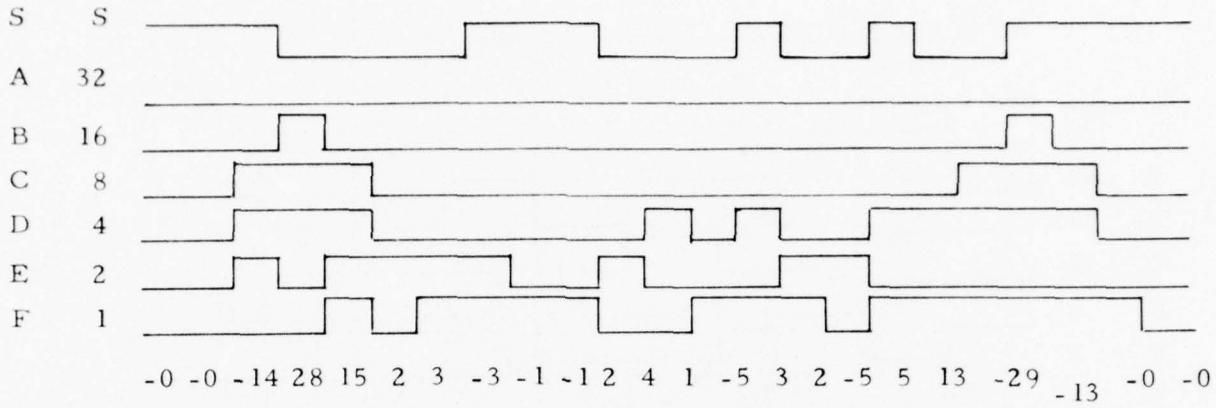


| Signal | Points Found |
|---|---|
| S | U84-5, TP16 |
| A | U55-2, TP17 |
| B | U55-5, TP18 |
| C | U55-7, TP19 |
| D | U55-10, TP20 |
| E | U55-12, TP21 |
| F | U55-15, TP22 |

## Output Processor

SIGN BIT & (VIDEO - MEAN) * GAIN + MEAN

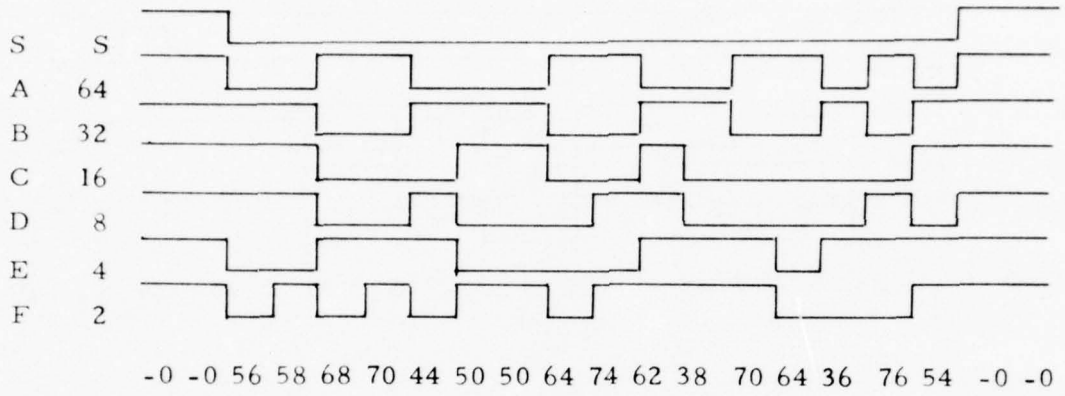


| Signal | Points Found |
|---|---|
| S | U75-15 |
| A | U45-2 |
| B | U45-5 |
| C | U45-7 |
| D | U45-10 |
| E | U45-12 |
| F | U45-15 |

## Section 6.0

## DISCUSSION OF PERFORMANCE STUDIES AND EVALUATIONS

### INTRODUCTION

Cockpit sensor displays provide pilots and sensor operators with radar, infrared and/or television information which can be used for performance of several mission tasks including navigation, intelligence gathering, target detection, recognition, identification and designation. The operational usefulness of such information is, however, dependent not only upon sensor parameters such as sensor dynamic range, resolution and field of view (FOV), but also upon the characteristics of the device on which the sensor information is displayed to the operator.

Due to the limited dynamic range of cathode ray tubes, typical devices for presenting sensor information, potentially available scene information may not be optimally displayed for use by an operator. For example, brightness differences between targets and their background, or brightness modulations within targets, may be too small to aid an observer in assessing the scene content. On conventional displays, where brightness and gain are constant over the entire image, operators may attempt to enhance small modulations by manually adjusting brightness and gain values. However, stretching the gray scale in one area, simultaneously causes compression in another. Thus, while an increase in video gain will improve contrast in the darker portions of the image, detail in light portions is likely to be lost due to saturation.

Local Area Brightness and Gain Control (LABGC) is an image processing algorithm designed to increase contrast in local areas of the display without causing saturation in other areas, thereby providing greater displayed detail. It is a contrast enhancement technique that automatically adjusts display brightness and gain in an effort to retain the maximum sensor video dynamic range while operating within the constraints of a limited dynamic range display device. Continuous adjustment of gain and brightness on a local basis throughout the picture is achieved by sliding a small window through the image and adjusting the gain and brightness of the center element based on the local image content within the window. As originally conceived

the gain applied to the center element in the sliding window was inversely proportional to the standard deviation of the brightness values in the window, so that minimum gain was applied in those areas where the video dynamic range was already high and maximum gain was applied in areas of low modulation. A brightness bias was also applied to the center element to prevent a processed pixel from exceeding the bounds of minimum black or maximum white.

Initial evaluations of the utility of LABGC processing were conducted using a computer simulation. Both subjective (Ketcham, Lowe, and Weber)[1] and quantitative evaluations were made and the methods, results, and conclusions are summarized in a subsequent section of the present paper. These evaluations, and a consideration of hardware complexity and cost (Ketcham, Lowe, and Weber)[1], led to a hardware design of a real-time LABGC processor. The present paper reports the results of an evaluation of processed imagery using this real-time hardware.

## PRELIMINARY RESEARCH

Three evaluations of the LABGC processing technique were conducted using computer simulated processing. The first involved a subjective evaluation of processed noisefree images, the second a subjective evaluation of processed noisy images, and the third a quantitative investigation of target detection performance.

In all three previous evaluations the stimulus images were converted to digital form for processing by a general purpose computer. The processed images were then scanned onto film in a 256-line by 256-element format (Ketcham, Lowe, and Weber)[1]. Digitized unprocessed images served as comparison stimuli. For the two subjective evaluations the sliding window was 9 pixels wide and 9 lines high. The statistical gain function was one in which the maximum equaled 4.0 and the gain dropped linearly to 1.0 at the point where the standard deviation was approximately 50 percent of the theoretical maximum and remained 1.0 thereafter. This function accentuated small original scene modulations by applying maximum gain to the center element when the standard deviation of the brightness values in the window was small. Unity gain was applied where contrast was already high. After the center element was multiplied by the appropriate gain value the brightness

of the center window element was adjusted, where necessary, to keep it from exceeding minimum black or maximum white (Ketcham, Lowe, and Weber)[1].

## Evaluation of Noisefree Images

The LABGC process increases local contrast within a scene. The objective of this first evaluation was to determine in what situations, and with what sensors such local contrast enhancement might prove operationally useful. Small samples of imagery were obtained representing the three major sensor types: Television (TV), Forward Looking Infrared (FLIR) and Synthetic Aperture Radar (SAR), and several operational tasks were considered.

### Method

Ten subjects with experience in the development, display, and interpretation of sensor imagery, subjectively rated 11 tactical scenes in terms of expected performance for several typical operational tasks. The rating was made on a seven point scale, with the original image serving as a reference point with a rank of 4, and the processed images being judged as better (5, 6, or 7) or worse (3, 2, or 1) than the original image.

The imagery was rated as to its potential use in the following seven operational tasks: vehicle control, sensor control, orientation, target detection, target recognition, target identification, and target designation. For each task the original sensor image was defined as being of rank 4. The ranks were associated with verbal labels as follows:

7 excellent
6 very good
5 good
4 acceptable
3 fair
2 poor
1 not usable.

Results

The mean ratings for the three sensor types are presented in Table 12. As can be seen from the table, the highest rating was obtained with TV imagery and the lowest with Synthetic Array Radar imagery.

TABLE 12. MEAN RATINGS BY SENSOR TYPE

| TV | FLIR | Radar |
|---|---|---|
| 4.9 | 4.4 | 3.7 |

The mean ratings for the seven operational tasks are presented in Table 13. The highest ratings were obtained with target identification and designation.

TABLE 13. MEAN RATINGS BY TASK

| Operational Task | Mean Rating |
|---|---|
| Vehicle Control | 4.1 |
| Sensor Control | 4.2 |
| Orientation | 4.1 |
| Target Detection | 4.2 |
| Target Recognition | 4.1 |
| Target Identification | 4.6 |
| Target Designation | 4.3 |

Discussion and Conclusion

The results from the first study were useful in identifying areas of interest for further research. The obtained rank orders for both sensor type and task served to indicate areas where LABGC would be most likely to improve performance. Thus, the investigators concluded that LABGC offered potential for performance improvement when applied to electro-optical sensor imagery, and hypothesized that processed imagery might prove most useful in detailed interpretation tasks (Ketcham, Lowe, and Weber)[1].

Although a definite trend was evident in these data, the magnitude of the expected performance improvement may not be unusually large. For example, the largest difference in rating, obtained with the simulated TV sensor, was 0.9 on a scale which ranged from 1 to 7. While it was not possible to assess the statistical significance of this obtained difference, the results do seem to indicate that the expected performance improvement may be relatively small. The same interpretation can be applied to the even smaller differences found for target identification and target designation tasks.

Every attempt was made in developing the LABGC computer simulation to approximate as nearly as possible the operation of a real-time processor. As with any simulation, however, certain limitations exist which limit the fidelity of the simulation. Because the simulated processed scenes were scanned onto film, any video noise which was present became fixed or frozen in the scene and there was no opportunity for an operator to "see through" the noise by visually integrating the stable signal. It may be that the gray shade rendition possible with the computer simulation did not duplicate that of a real-time hardware system where the outside world serves as the original stimulus upon which the LABGC algorithm operates. The computer simulation operated upon photographs of the world and was undoubtedly influenced by the gamma of the original film. Finally, the contrast of the computer processed imagery was subject to the modulation transfer function (MTF) of the film onto which the scenes were scanned, while contrast in real-time processed scenes would be influenced by display transfer functions. The performance impact of the differences between computer-simulated and real-time LABGC processing could not be analytically determined, necessitating the evaluation of a dynamic real-time system.

## Noise Sensitivity Study

Video noise increases the number of local brightness fluxuations within a displayed scene. Because LABGC was designed to enhance such small local modulations, it was hypothesized that this process might prove to be noise sensitive. Therefore, a preliminary examination of the effects of both analog and digital random noise on the utility of LABGC processed imagery was conducted.

### Method

Varying levels of noise were injected into noiseless images and the LABGC algorithm was applied to these images. Subjective ratings of the LABGC processed images were made, based on a consideration of two factors: (1) appearance of the imagery "beneath" the noise and (2) obscuration of the image by the noise.

Two random noise models were employed: a digital uniform bit serial noise model, with error rates of 0.01, 0.05, and 0.1 error per bit, and a gaussian analog noise model with signal-to-noise (S/N) ratios of 30, 16, and 5 db.

### Result

The primary result of the noise sensitivity study was that when images containing noise were processed, the apparent or perceived noise was also increased. However, it may be that noise in real-time dynamic images will not be as apparent because of the visual integration of the relatively constant scene content.

## Target Detection Study

In the past electro-optical sensors have been used to locate small mobile targets-of-opportunity at ranges up to approximately five kilometers (km). It was anticipated that the local contrast enhancement provided by LABGC processing might improve target search and detection performance by increasing target-to-background contrast. A quantitative laboratory study was conducted to examine operator target detection performance with LABGC processing.

The two previous subjective evaluations had indicated performance improvement would be most likely with noisefree television sensor data. Thus, processed and unprocessed photographs of realistic scenes served as the experimental stimuli for the target detection study. In addition to image processing, two other independent variables were manipulated in the study: scene complexity and original target-to-background contrast.

Scanlan[5] examined the effect of scene complexity on tactical target detection performance and found that under conditions of high scene complexity the time required to detect a target was twice as long as under conditions of low scene complexity. In this study, a low complexity scene was characterized by large areas of more or less uniform density, such as open fields, and a few objects of similar size and luminance to the target. A high complexity scene was one with considerable vegetation and many objects with features similar to the target.

In the case of a low complexity scene the contrast between the target and the background was a significant detection cue. Because LABGC increases small local contrasts, it may provide improved target detection performance. With complex scenes, the increased contrast between the target and the background will still result. However, any improvement in the visibility of the target may be offset by a similar increase in the contrast of clutter objects. Because the presence of clutter objects makes detection of the target difficult LABGC processing may not improve performance when the scene is complex.

Target-to-background contrast was also manipulated in the search/detection study. It was anticipated that since the primary advantage provided by LABGC processing was an increase in local contrast, the potential for performance improvement would be greatest for low contrast targets and minimal where original scene contrast was already high.

Method

The experiment examined two levels of target-to-background contrast, two levels of background complexity, and two replications as within subject variables. Because of limitations in available imagery, image processing was examined as a between subjects variable, with half of the subjects viewing unprocessed images and half viewing LABGC processed images.

---

5. Scanlan, L.A., Target acquisition model development: effect of realistic terrain, Tech. Rep. NVL P76-484. Ft. Belvoir, Virginia: Night Vision Laboratory, December 1976.

Stimuli

The image scenes used were low altitude oblique photographs of rural New York State with target vehicles optically embedded. The characteristics of the scenes were reasonably representative of the terrain found in Central Europe. The original films, from which the background scenes were selected, were 44.44 by 44.44 grads (40x40 degree) forward view aerial reconnaissance photographs taken from approximately 910 meters (3000 feet) altitude with a camera depression angle of 22.22 grads (20 degrees).

Targets were embedded into the background scene by superimposing a transparency of the target on a transparency of the background and optically processing the composite. The target transparencies were obtained by photographing scale models on a featureless background. Using a large print of the target an artist added a shadow, appropriate for the sun angle, in the background scene into which the target was to be embedded. The internal contrast of the target was also artificially enhanced so that the final composite image would more nearly approximate the internal modulation characteristics of real targets. Without the artificial contrast the embedded target generally appeared as a dark shape, devoid of internal brightness differences.

Eight test and seven training images were prepared, each containing a single tactical target and representing an 8.89 and 8.89 grad (8 by 8 degree) field-of-view. Experimental manipulation of scene complexity, target type, and target-to-background contrast was accomplished in the construction of these images as described below.

Scene Complexity. Initial quantification of scene complexity was accomplished by having six judges rank 75 candidate photographs according to their subjective interpretation of complexity. Some of the backgrounds depicted open fields generally lacking in natural or man-made features. Others contained features such as roads, buildings, low shrubbery and trees. Four complex and four simple backgrounds were selected based on mean rank and maximum agreement among judges (minimum standard deviation). In addition, four simple and three complex scenes were selected for use as training materials.

Targets. The targets used in this study were two M-60 tanks, three 2-1/2 ton trucks, and three armored personnel carriers (APCs). The image height of all targets was held constant at two percent of the 8.89 grad (8 degree) field of view. This height corresponds to a range of approximately 1.2 kilometers (0.75 mile) and was selected based on results from a previous study (Scanlan)[5] which indicated this target height was necessary to maintain acceptable levels of performance in all experimental conditions without LABGC processing.

Targets were positioned in the background scene so that their size and location was appropriate to other terrain features. To avoid having targets always appear at the vertical center of the display, the apparent depression angle of the sensor was varied to allow the target to appear anywhere in the center two-thirds of the image. Targets appeared as direct side views or quartering front views with an aspect angle consistent with the apparent depression angle.

Target-to-Background Contrast. The contrast between the target and its immediate surroundings was varied by changing the density of the superimposed target image while holding the background film density constant. Target-to-background contrast was calculated using the formula $(B_{max}-B_{min})/(B_{min})$ or, because the targets were darker than the surroundings, $(B_{background}-B_{target})/(B_{target})$. The high and low contrast conditions represented ranges of contrast with averages of 2.0 and 0.7, respectively.

LABGC Algorithm. The algorithm used to produce the stimuli was identical to the one selected for implementation in the real-time processor hardware. The window size was four pixels by two lines per television field, or four pixels by four lines per frame. The standard deviation of the pixels within the window was approximated by calculating the range of pixel values and multiplying by 0.402. This approximation and its derivation are treated in greater detail later, in the discussion of the real-time processor evaluation. The gain function used was the same as for the previously presented subjective evaluations.

Apparatus. A flying spot scanner was used to digitize the original photographic transparencies. This device consists of a cathode ray tube that generates a bright spot whose position is under computer control. The

spot is focused onto the image transparency by a lens. The amount of light passing through the transparency at that point is collected by another lens and focused onto a photomultiplier tube (PMT). The PMT output is converted from analog to digital form to produce a digital brightness value. This process is repeated until the spot has scanned the entire transparency. The digital numbers collected for each spot on the transparency then make up the digital image. The digitized processed and unprocessed scenes were scanned onto film from a CRT. Figure 30 diagrams the steps taken in preparing the test imagery.

A gray 11" x 14" board mounted on an easel, with a 2-1/4" x 2-1/2" rectangle cut in the middle, provided masking and background to display the photographs. Subject-to-display viewing distance was maintained at a constant value by means of a subject head restraint. A viewing distance of 9 inches was used to obtain target subtenses of 19.2 arc minutes.

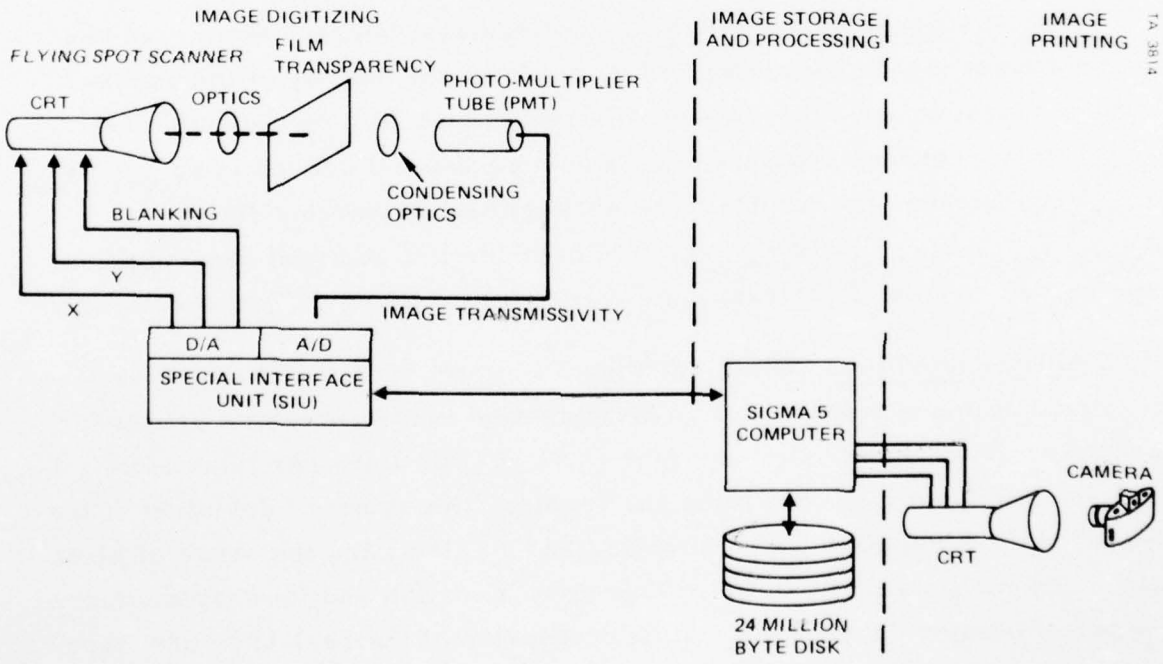


Figure 30. Equipment diagram of LABGC processing.

The subject indicated the position of a detected target using a wooden pointer and the experimenter verified the correctness of the designation visually. The time required to make a designation was recorded by the experimenter using a stop watch. Between trials the display could be blanked by placing a piece of cardboard between the subject and the scene. As an aid in identifying the targets, models of the three target types were positioned in front of the subject.

Research Design

A mixed-factors factorial design with four variables at two levels was used to examine target detection performance. Two levels of target-to-background contrast and scene complexity, and two replications of each condition, were within subjects variables. Each subject experienced all eight combinations of these variables. Image processing was examined as a between subjects variable with half the subjects viewing digitized but unprocessed images and half viewing the processed images of the same scenes.

Order of presentation of experimental conditions was counterbalanced to minimize order effects. The research design and the variable levels are summarized in Table 14.

TABLE 14. RESEARCH DESIGN

| | |
|---|---|
| Within Subjects | |
| Target-to-Background contrast | 0.7 and 2.0 |
| Scene complexity | High and Low |
| Replications | Trial 1 and Trial 2 |
| Between Subjects | |
| Image Processing | None and LABGC |

Subjects. All sixteen volunteer subjects were members of the technical staff at Hughes Aircraft Company. All subjects used in the experiment had tested visual acuity of 20/20 or better and were randomly assigned to one of the two groups of eight.

Procedures. Each subject attempted to detect and identify a target located in the eight realistic terrain backgrounds. Each trial began when the experimenter uncovered the photograph and simultaneously started a stop watch for recording detection time. Subjects searched the scene for the target vehicle and when found, pointed to it and said "there" to indicate a detection. The experimenter noted the time and correctness of the response. If one minute and 50 seconds elapsed without a response from the subject, the experimenter requested a "best guess" as to the target location. If the subject was correct at this point, a detection time of 120 seconds was recorded. In all cases, if the response was incorrect a miss was recorded.

Prior to the start of experimental trials, the subject was given a standardized set of written instructions which described the general purpose of the experiment, the nature of the task, and the characteristics of the target images. The experimenter verbally reiterated the major points in the instructions and answered questions posed by the subjects. Several minutes were provided to allow the subject to study the vehicle models and become familiar with their features. During this time subjects were encouraged to examine the models from several orientations. Following the target familiarization, seven training trials were given to clarify the procedures to be used.

The instructions to the subject were carefully worded in an attempt to minimize the response criterion problem discussed by Swets, Tanner, and Birdsall[6]. Probability of detection and time to detect are closely related to one another in that a short time can be obtained by sacrificing probability of detection. Obversely, a high probability can be obtained at the cost of time. Subjects were instructed to respond if they were 70 percent certain that the object was a target. The intent was for the probability of detection to have minimum variability so time could be the primary dependent measure.

This method of controlling response criterion is much less desirable and effective than, for example, using a forced-choice procedure. The principal difficulty lies in the subject's interpretation of the 70 percent instruction,

---

6. Swets, J.A., Tanner, W.P., and Birdsall, T.G., Decision processes in perception. Psychological Review, 1961, 68, 301-340.

which can vary widely. As a result some subjects will still be more willing to guess and thus have shorter time to detect. Although not an optimum solution, the inclusion of a criterion level in the instructions was the best technique available in the present experiment.

Results and Discussion

Time required for target detection was the primary performance measure. In those cases where an incorrect detection was made, an arbitrary detection time of 150 seconds was assigned so that the time scores would reflect the influence of incorrect detections.

An analysis of variance was conducted on the detection time data and a summary is given in Table 15. The main effects of target-to-background contrast, background complexity and replications were found to be significant. Although the main effect of LABGC processing was not significant, a significant two-way interaction was obtained between processing and background complexity, and a significant three-way interaction between processing, complexity and replications. Also reported in Table 15 is $Eta^2$, the proportion of variance accounted for by each effect, calculated as the sum-of-squares for the effect divided by the total sum-of-squares.

The main effect of background scene complexity is shown in Figure 31. As was expected, based on previous findings (Scanlan)[5] this parameter appeared to be a potent determinant of performance. Average detection time with low complexity backgrounds was 54.5 seconds while with high complexity backgrounds the average time increased by a factor of 1.8 to 97.1 seconds. This effect was reliable beyond the 0.01 level of significance which means that a difference this large would be expected to occur by chance less than once in a hundred replications of the experiment. It also accounted for 9.00 percent of the variance in the experiment.

With the particular LABGC algorithm examined, no reliable main effect of LABGC processing was found as is shown in Figure 32. Detection time increased from 72.8 seconds with the unprocessed to 78.8 seconds with the processed scenes.

One reason for this lack of a significant main effect is evident from the plot of the significant interaction between processing and background compexity shown in Figure 33. In the low complexity condition LABGC processing improved performance, reducing detection time by a factor of 1.5;

TABLE 15. SUMMARY OF ANALYSIS OF VARIANCE OF DETECTION TIME FOR TARGET DETECTION STUDY

| Source | SS | df | F | p | $Eta^2$ |
|---|---|---|---|---|---|
| LABGC Processing (P) | 1157.4 | 1 | 0.43 | NS | 0.001 |
| Subjects (S)/P | 37995.9 | 14 | | | |
| Background Complexity (B) | 58092.9 | 1 | 14.36 | 0.01 | 0.09 |
| BxP | 26298.4 | 1 | 6.50 | 0.05 | 0.04 |
| BxS/P | 56644.9 | 14 | | | |
| Target-to-Background Contrast (C) | 22273.7 | 1 | 7.25 | 0.05 | 0.03 |
| CxP | 1898.0 | 1 | 0.62 | NS | 0.003 |
| CxS/P | 43017.8 | 14 | | | |
| Replications (R) | 43604.6 | 1 | 7.54 | 0.05 | 0.07 |
| RxP | 16013.9 | 1 | 2.77 | NS | 0.02 |
| RxS/P | 80945.5 | 14 | | | |
| BxC | 14035.1 | 1 | 3.14 | NS | 0.02 |
| BxCxP | 6653.7 | 1 | 1.49 | NS | 0.01 |
| BxCxS/P | 62521.9 | 14 | | | |
| BxR | 3704.2 | 1 | 1.42 | NS | 0.01 |
| BxRxP | 21748.3 | 1 | 8.31 | 0.05 | 0.03 |
| BxRxS/P | 36643.1 | 14 | | | |
| CxR | 2405.7 | 1 | 0.79 | NS | 0.003 |
| CxRxP | 1103.6 | 1 | 0.36 | NS | 0.001 |
| CxRxS/P | 42453.5 | 14 | | | |
| BxCxR | 1203.92 | 1 | 0.64 | NS | 0.001 |
| BxCxRxP | 1959.2 | 1 | 1.05 | NS | 0.003 |
| BxCxRxS/P | 26247.5 | 14 | | | |

however, in the high complexity condition, LABGC processing degraded performance to approximately the same extent. In the computation of the main effect of processing, detection times are averaged across background conditions and processing overall has a negligible effect.

It is likely that the performance improvement observed with LABGC in the low complexity situation was a result of the increase in target-to-background contrast produced by the processing. In the high complexity

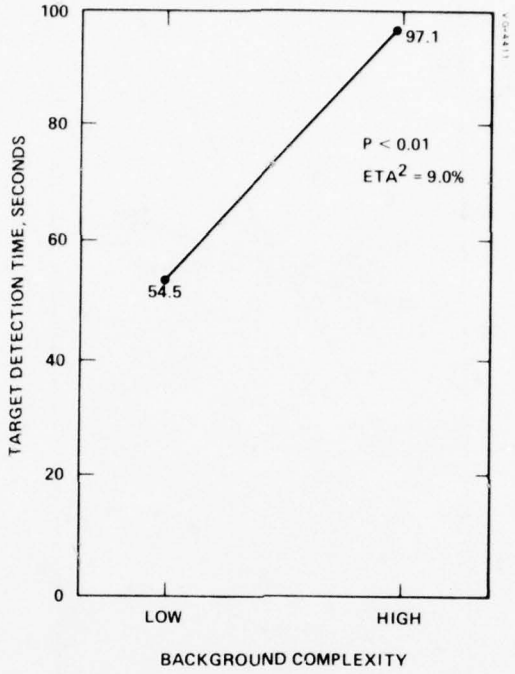


Figure 31. Effect of Background complexity on detection time.

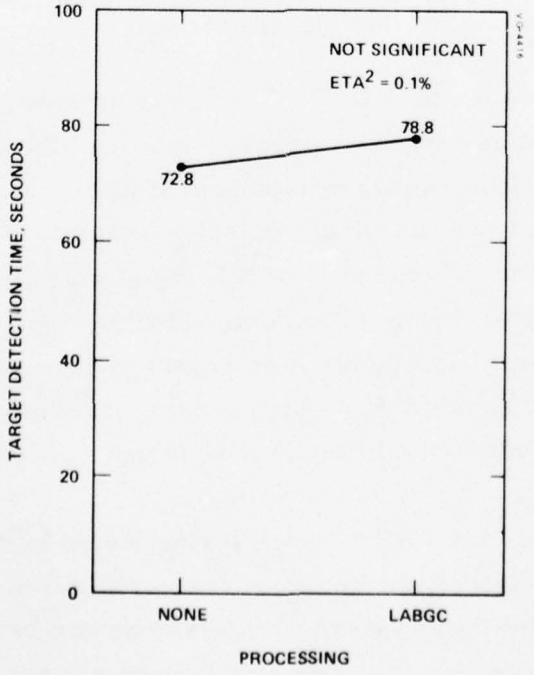


Figure 32. Effect of processing on detection time.

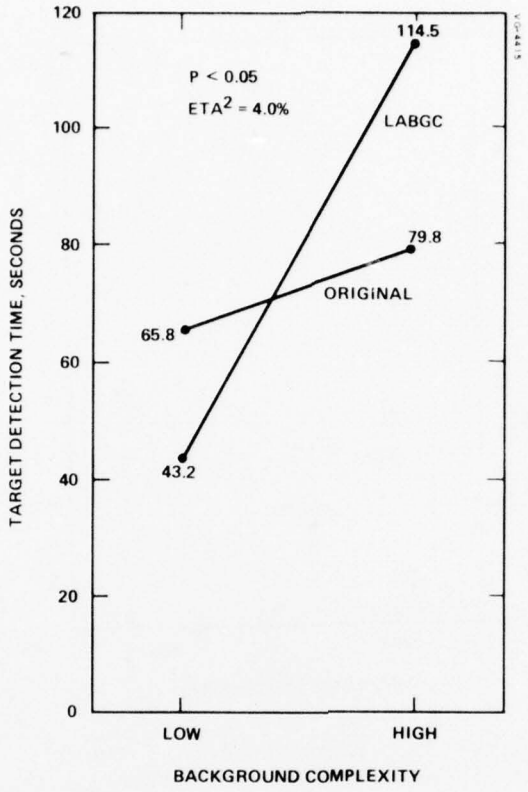


Figure 33. Effects of processing and complexity on detection time.

situation, however, it appears that LABGC processing enhanced background non-target objects as well as targets, thereby creating additional clutter objects which complicated the search component of the task.

The main effect of contrast on target detection time is shown in Figure 34. This effect was reliable beyond the 0.05 level of significance and accounted for 3.00 percent of the total experimental variance. Detection time decreased by a factor of 1.4 under high contrast conditions. This result is not unreasonable as luminance difference between a target and its immediate background is undoubtedly a cue to a target located in realistic terrain.

It had been anticipated that LABGC processing would increase performance to a greater extent with original low contrast than original high contrast targets, thereby giving rise to an interaction between contrast and processing as shown in Figure 35. The fact that this interaction did not attain statistical significance indicates that, in this situation, LABGC processing continued

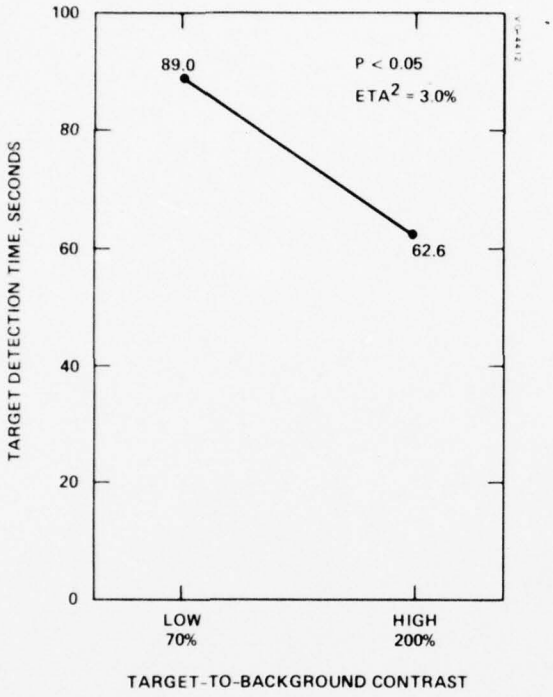


Figure 34. Effect on contrast on detection time.

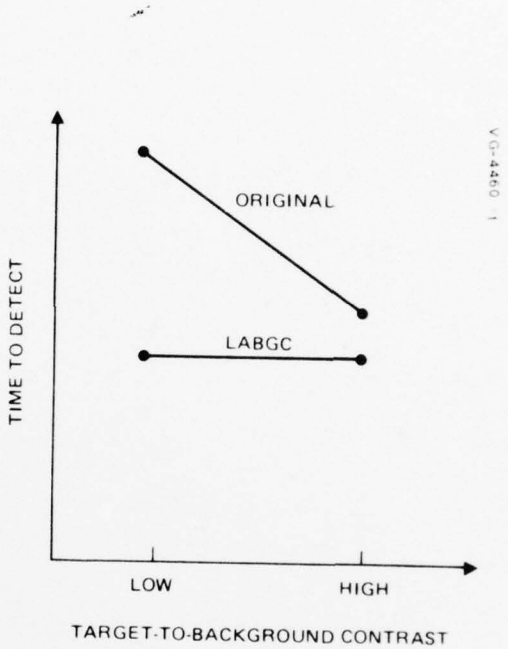


Figure 35. Expected contrast enhancement result.

to aid performance even under those conditions where the original target-to-background contrast was relatively high.

## REAL-TIME LABGC EVALUATION

Results from the previously described subjective evaluations and target detection study provided some indication that LABGC processing might improve operator task performance under specific conditions. For example, the first subjective evaluation indicated a potential for performance improvement in recognition and identification tasks with TV sensor data, while the quantitive target detection study indicated search and detection times decreased with LABGC processing for tactical targets in low complexity background. These results appeared sufficiently promising to justify the construction of a real-time hardware processor. Figure 36 is representative of a number of scenes LABGC processed in real-time and presented on a CRT monitor.

ORIGINAL

ENHANCED

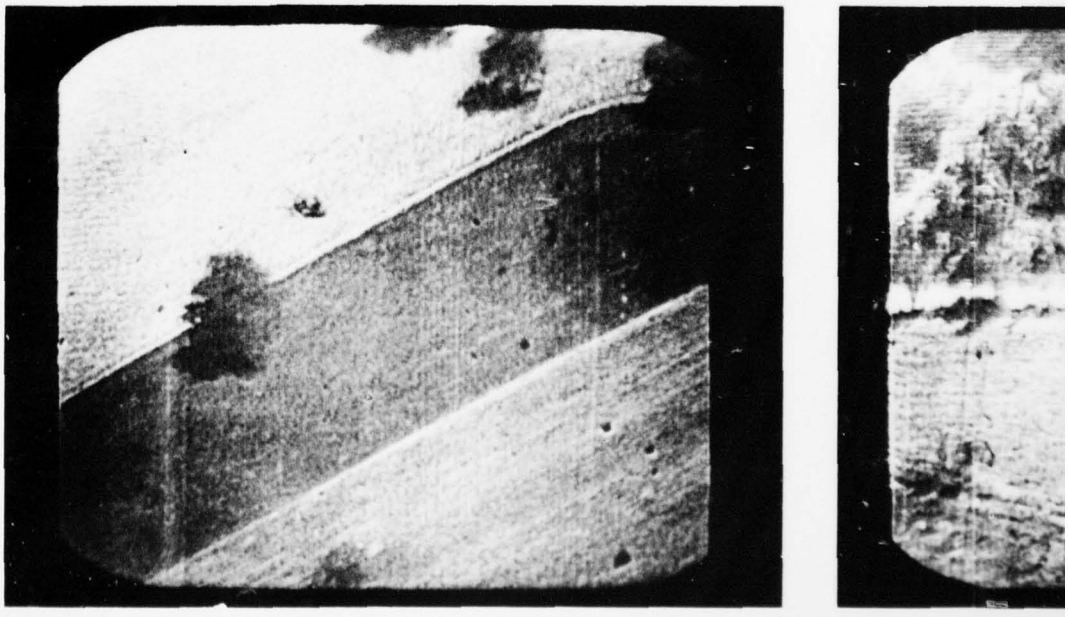

AD-A044 735 HUGHES AIRCRAFT CO CULVER CITY CALIF DISPLAY SYSTEMS LAB F/G 17/2
CONTRAST ENHANCEMENT TECHNIQUES STUDY. PHASE III.(U)
JUL 77 E W OPITTEK N00014-76-C-0563
UNCLASSIFIED HAC-P77-210R ONR-CR213-124-3F NL

2 OF 2
AD A044735

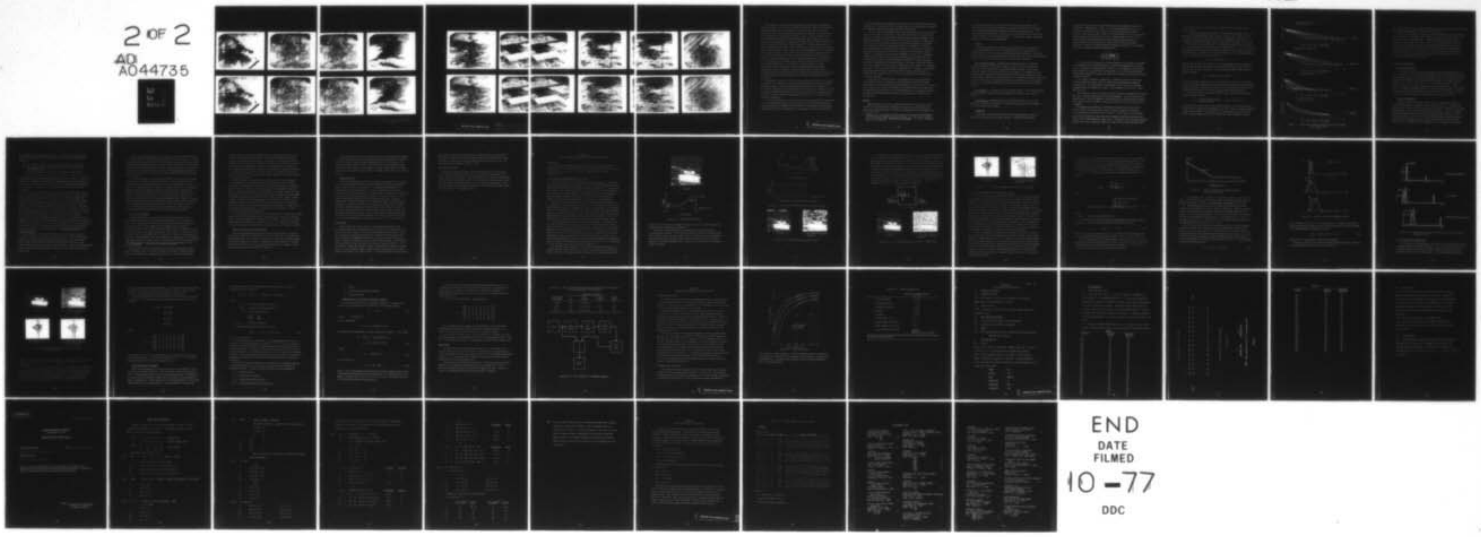

END
DATE FILMED
10-77
DDC

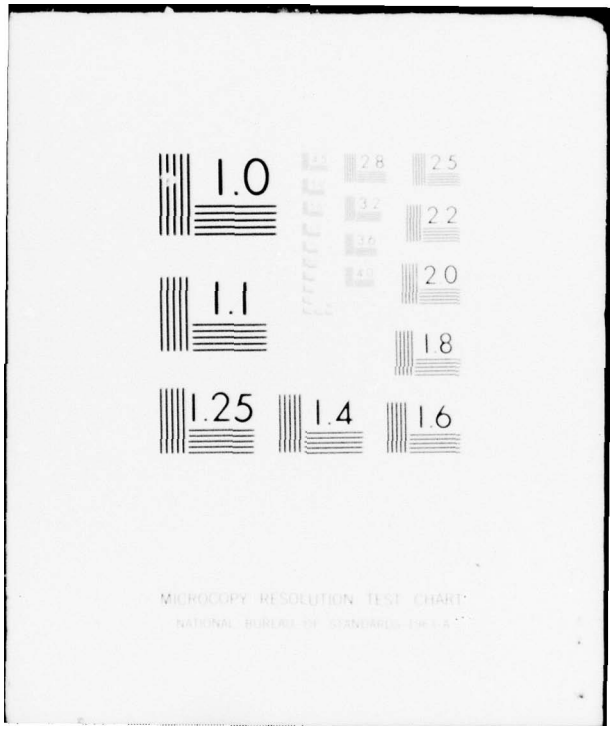
1.0
1.1
1.25
1.4
1.6
2.8
2.5
3.2
2.2
3.6
2.0
4.5
1.8
MICROCOPY RESOLUTION TEST CHART
NATIONAL BUREAU OF STANDARDS 1963-A

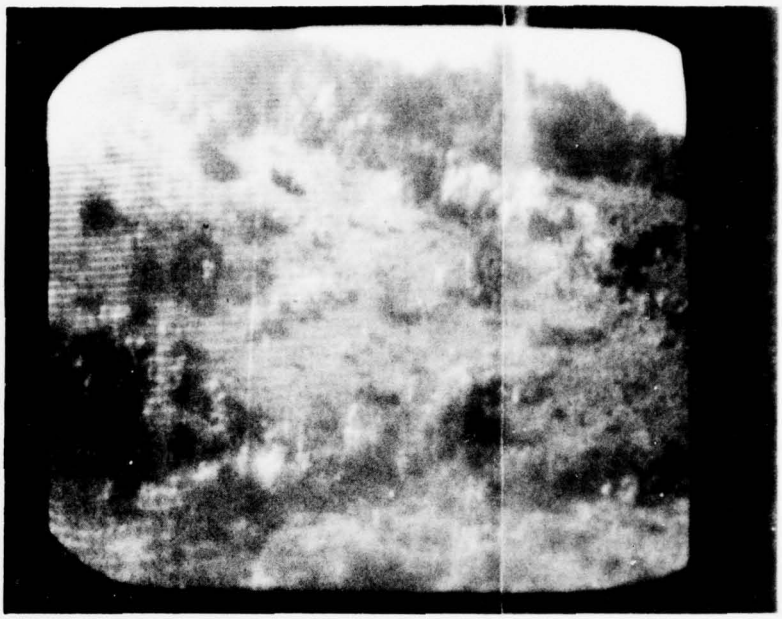

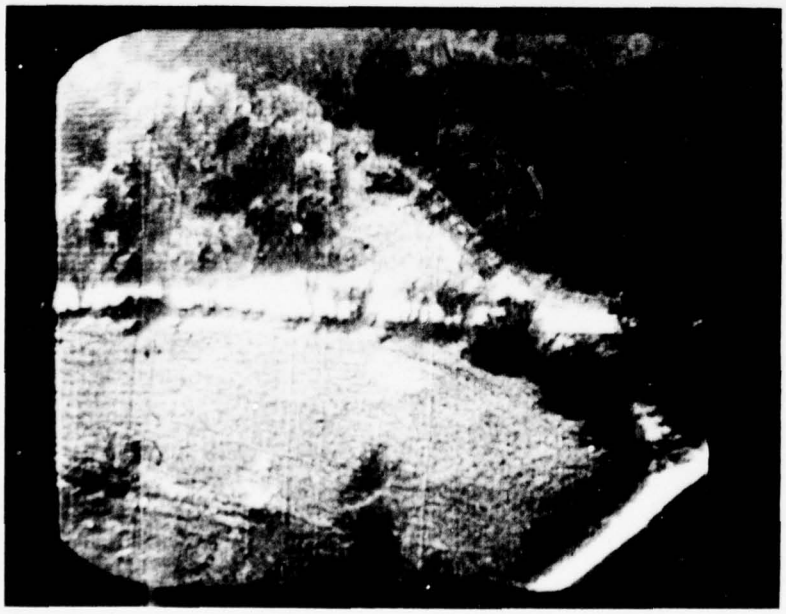

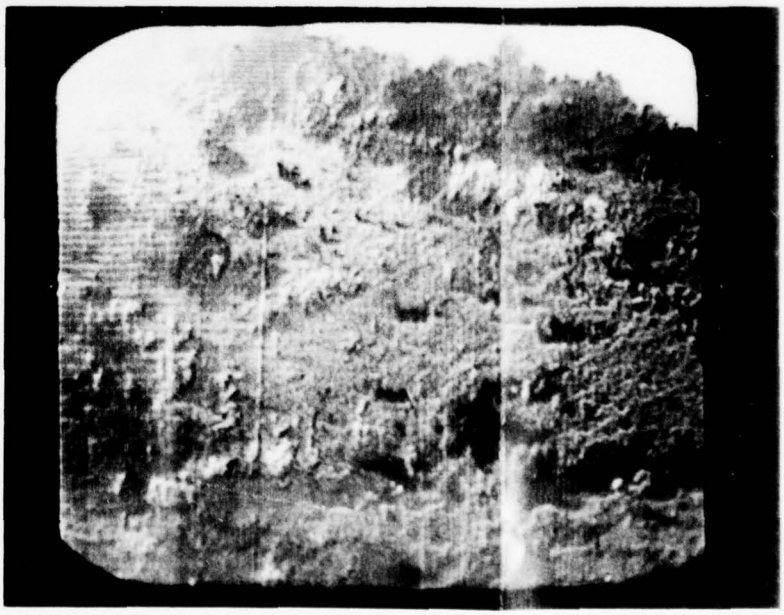

c.

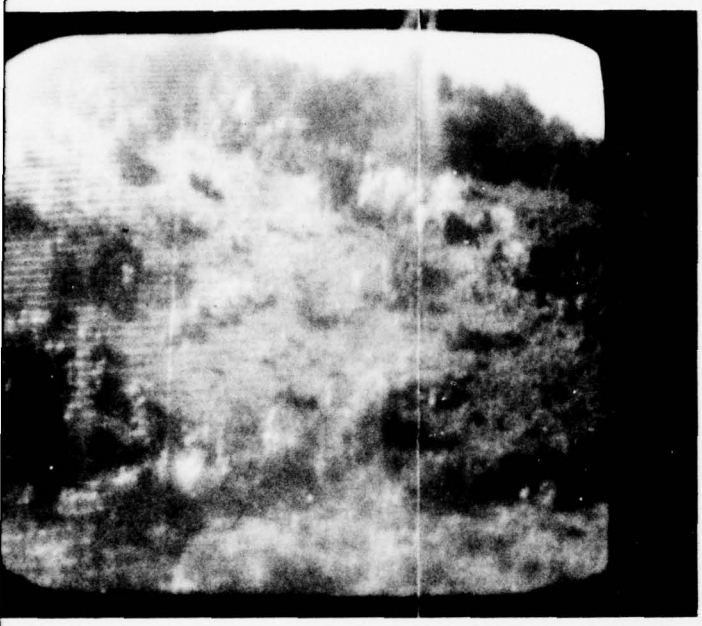

d.

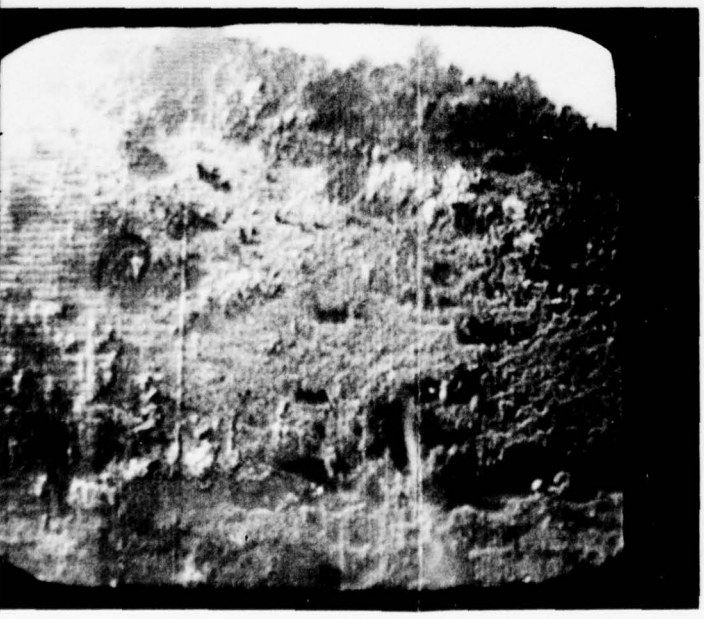

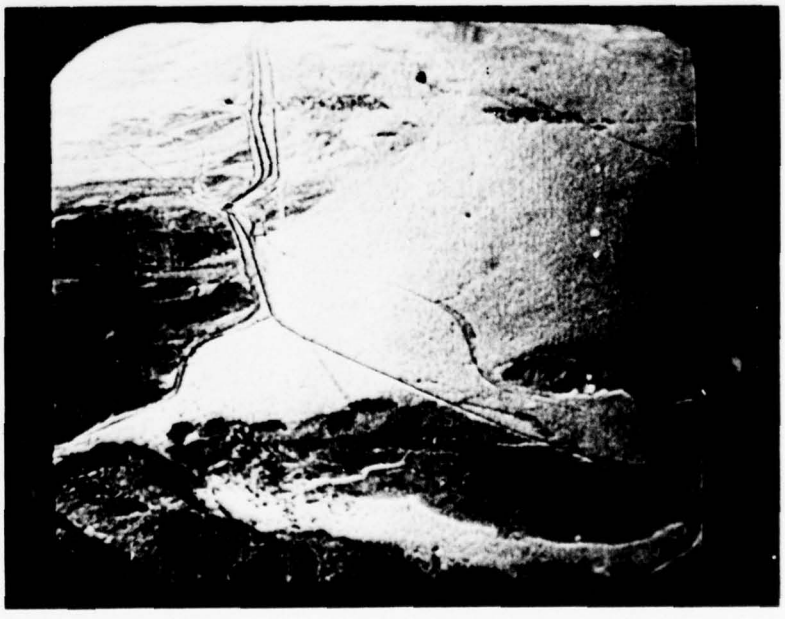

Figure 36. Sample photographs of real-time LABGC processing. (Sheet 1 of 2)

ORIGINAL

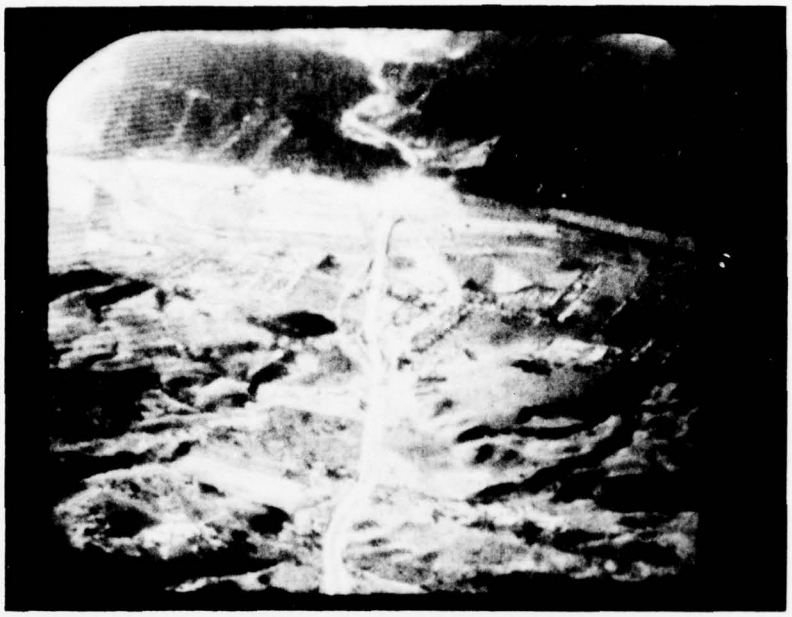

ENHANCED

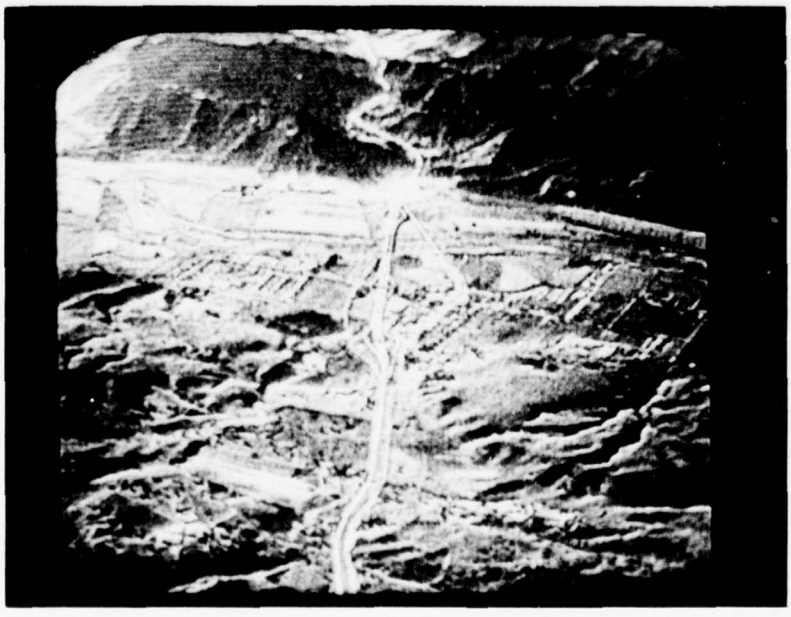

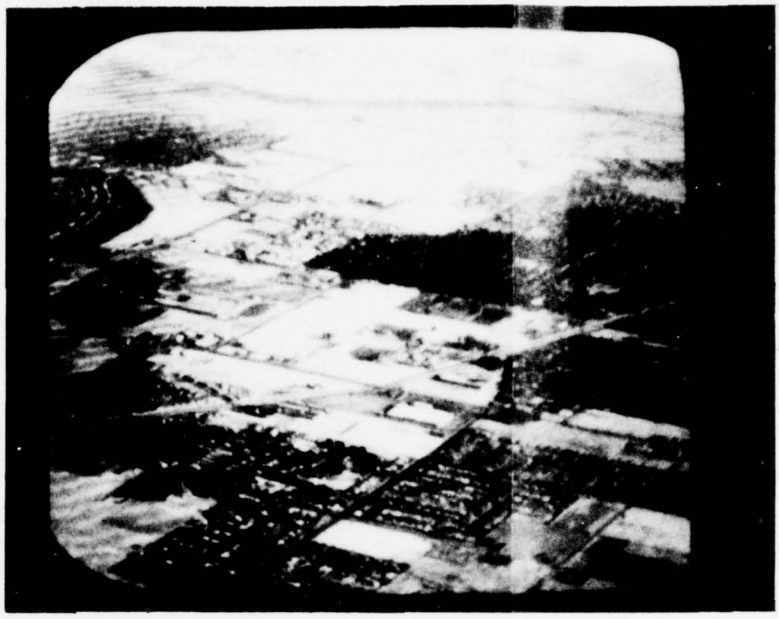

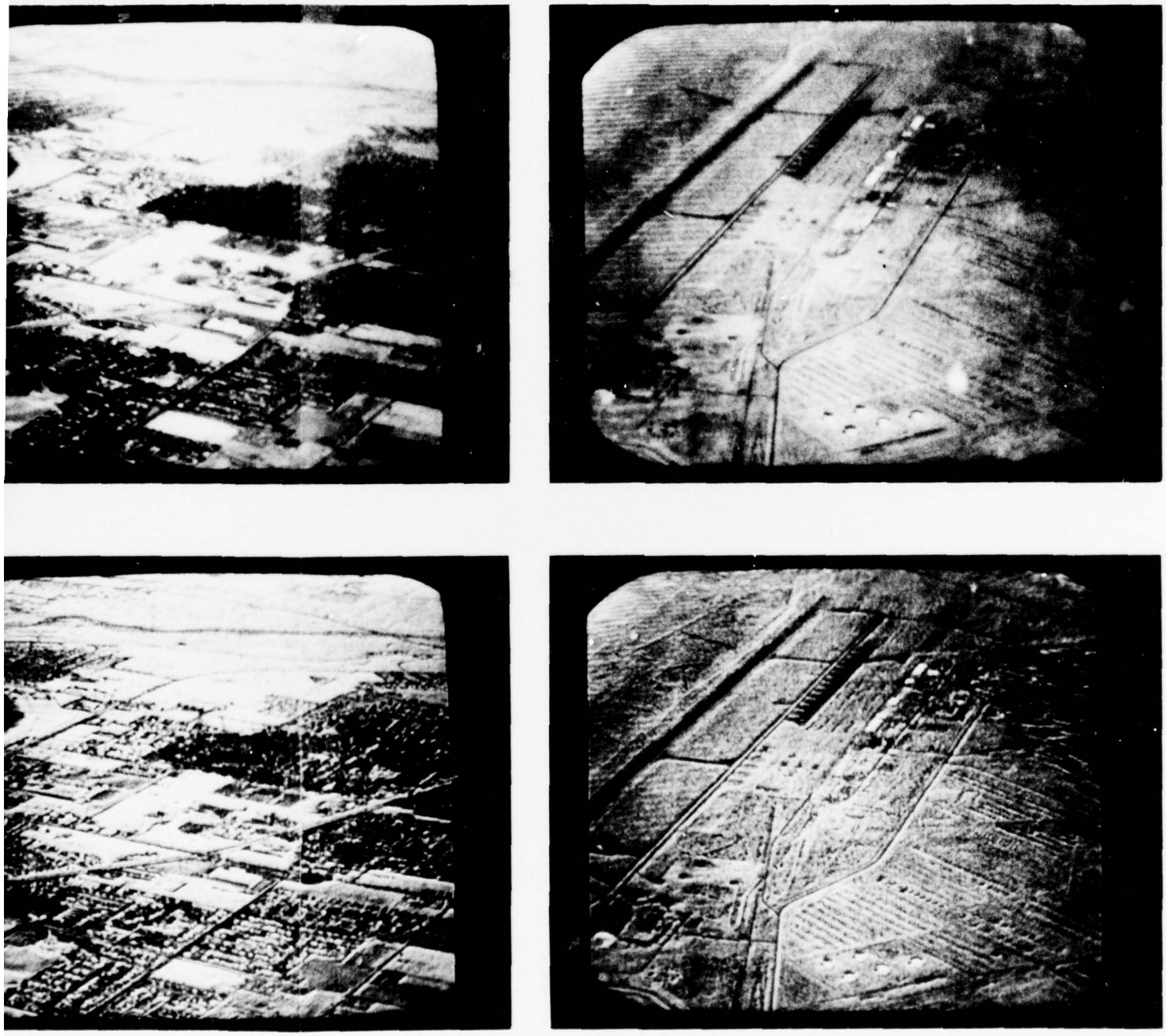

Figure 36. Sample photographs of real-time LABGC processing. (Sheet 2 of 2)

An evaluation of the real-time hardware processor was conducted for several reasons. First, it was desired to assess the validity of the results obtained in the previous evaluations, all of which had utilized computer simulated LABGC processing with its inherent limitations, which prevent exact duplication of real-time processes. Some of these limitations have been mentioned previously and the possibility of their influences on performance are supported by a comparison of the results of the LABGC target detection study and a similar study (Scanlan).[5]. Both studies used the same image scenes; however, in the Scanlan study, the transparencies were rear-projected, while in the LABGC study, the transparencies were digitized and scanned onto film. The subject task and procedures employed in the two studies were identical. The overall average detection time obtained with the comparable (unprocessed) computer digitized and scanned images was on the order of four times greater than that obtained with the rear-projected transparencies. A difference of this magnitude cannot be reconciled solely on the basis of image quantization and some other explanation must be explored. One possibility is that characteristics of the image were somehow altered in the computer image generation process. Such possibilities can be eliminated by an evaluation using the real-time hardware.

Additional evaluation of LABGC processing was desirable from another standpoint. All of the previous evaluations had looked at extremely limited imagery samples. It was anticipated that potential areas of application for LABGC might have been missed due to this restriction. Because previous evaluation indicated performance improvement would be most likely with TV imagery, it was decided to investigate a wide variety of TV images on the real-time hardware.

For any given image, performance improvement with LABGC processing can be assessed with respect to a long list of potential briefing conditions and mission tasks, including search, detection, recognition, identification, intelligence extraction, designation, and navigation. However, taking into

account the behavioral components of the different mission tasks and briefing conditions, it is possible to define a small number of tasks which encompass the important behavioral components of the other tasks.

There are three identifiable behavioral components, one or all of which are common to the various tasks. The first involves the perception by the observer of relatively gross target characteristics such as contrast, size, and general shape. The second involves the detection of more subtle target features such as fine outline details and internal modulations. The third involves the perception of contextual information, whether it consists of man-made objects or natural terrain features. For example, a target-of-opportunity search task would involve primarily the perception of gross features, because the search process consists of a series of eye fixations which have been shown to be at least partially directed by the nature of peripherally processed visual information (Robson).[6] Target detection, recognition, identification, and intelligence extraction, on the other hand, all involve a higher level of decision making based on repeated eye fixations (Robson)[6] and are subsumed under component two. Finally, a pre-briefed target acquisition task or a navigation task would presumably be more dependent upon component three, because in such cases perception of the terrain is essential.

In the present evaluation three operationally defined mission tasks: search and detection, recognition, and identification; and two briefing conditions: pre-briefed and target-of-opportunity, were examined. Because these parameters, taken in combination, incorporate the three behavioral components discussed above, the results obtained are generalizable to other specific mission tasks which can also be defined in terms of these same components.

## Method

Approximately 60 real-time LABGC processed TV images were subjectively compared with their digitized but unprocessed counterparts to evaluate the potential impact of LABGC processing for the performance of

---

7. Robson, J. G., Receptive fields: neural representation of the spatial and intensive attributes of the visual image. In E. C. Carterette and M. P. Friedman (Eds.) Handbook of perception. New York: Academic Press, 1975, 81-116.

three operational tasks: target search and detection, recognition, and classification. It should be noted that no apparent difference in quality was observed between the digitized unprocessed and the analog images. The scenes depicted high and low contrast, small-mobile and large-fixed targets against high and low clutter backgrounds. Various target ranges and sensor fields-of-view were also represented.

Tasks

Operational definitions of the three operator tasks were specified. It was recognized that under some conditions detection, recognition, and identification may occur almost simultaneously; the definitions nevertheless proved useful for directing attention to specific target and scene characteristics which were likely to impact performance in the three situations.

Search and Detection. Although search and detection are typically considered together as corollary processes, there are some important differences in the behavioral components of the two tasks. The search process consists of a series of more or less random eye fixations, driven by gross scene and target characteristics such as contrast, object size and general shape, which precede the localized eye fixations and decision processes involved in detection. Technically detection was defined as occurring when an observer correctly indicated that a target object existed in the field-of-view.

Recognition. Recognition occurred when an observer correctly indicated to which class the detected object belonged; for example, truck, tank or APC.

Identification. Identification occurred when an observer correctly indicated to which sub-class the recognized image belonged; for example, 2-1/2 ton truck or M-60 tank.

Apparatus

A Colorado Video camera and 525-line CRT simulated a relatively noisefree (25 db) television sensor system. LABGC processing was

accomplished with a real-time hardware processor designed to operate on standard 525 interlaced TV video. Local image brightness and local contrast were measured over a 4-pixel by 2-line sliding window: however, because of the interlace, the 2 lines of one field and the 2 lines of the second field combine to yield 4 lines per frame. Implementation of a true 4 x 4 window was decided against because of the large amount of memory which would be required to store an entire field of video information. The center element, to which brightness and gain adjustments were applied, was located within the window as shown below:

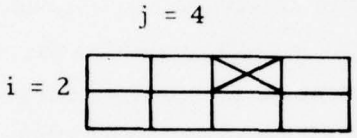


In order to provide maximum contrast enhancement in areas of originally low modulation, the LABGC algorithm required local application of gain in inverse proportion to original local contrast. Two methods for determining local contrast were implemented in the hardware, one involved calculation of the window brightness range, the other determination of the pixel difference within the window.

For relatively noisefree situations, an adequate measure of the local contrast within the window was determined by calculating the brightness range (B max - B min) and then multiplying the range value by a constant to approximate the standard deviation. This constant is 0.402 for a window size of 4 by 2.

If the range is used as a measure of local contrast in a high noise situation, however, contrast enhancement is usually negligible. Because noise pixels typically have extreme brightness values and because each noise pixel occurs as an element in four windows, large range values result and minimum gain is applied.

For high noise situations, calculation of the difference between the center element brightness and the mean window brightness constitutes a more appropriate measure of local contrast. The calculation of the window mean is less sensitive to the noise pixel brightness and the pixel difference value will be smaller than the range value, resulting in more gain being applied. Further, the value of the pixel difference will be the greatest when the noise

is the center element, thus avoiding the application of a high gain to the noise element.

Several gain functions which differed in shape and maximum value were programmed using PROMs, and are shown in Figure 37. A table look-up procedure was used to obtain a gain value corresponding to the pseudo-standard deviation based on the range or pixel difference input to the PROM.

To keep processed pixels from exceeding the bounds of minimum black and maximum white, a brightness bias was implemented. If the center element, after application of the gain, was within the dynamic range of the processor, the bias was zero. If the center element would have been less than minimum black, the following bias was calculated:

$$B_1 = \min (M, SD) * G - M.$$

That is, the smaller of the mean (M) or pseudo-standard deviation (SD) was multiplied by the gain (G), and the mean was subtracted from the result. If the center element would have exceeded maximum white a bias was calculated as follows:

$$B_2 = 63 - M - \min (63 - M, SD) * G$$

For the 6-bit video employed, zero was equivalent to minimum black and 63 to maximum white. Either the maximum white minus the mean or the pseudo-standard deviation, whichever was smaller, was multiplied by the gain value and the result subtracted from the maximum white minus the mean.

Mathematically the value of the center window element was determined by the following formula:

$$\hat{V} \quad \begin{matrix}\text{Value of center element} \\ \text{of enhanced video}\end{matrix} = (V - M) * G(SD) + M + B$$

That is, the new value of the center window element (V) was determined by subtracting the mean window brightness value (M) from the original brightness of the center element (V), multiplying the resulting value by a gain value G(SD), and then adding back the video mean (M) and a brightness bias (B)

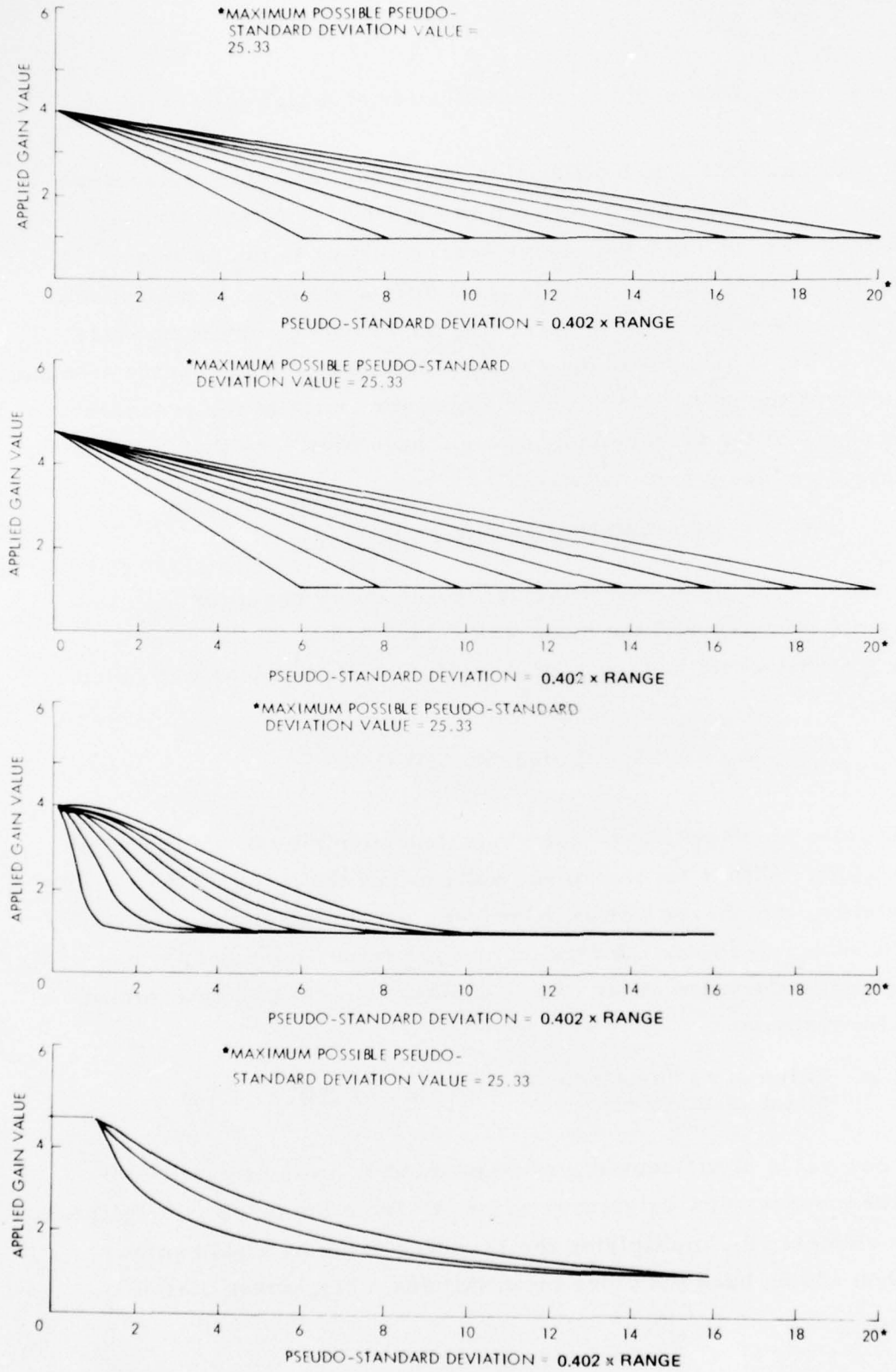


Figure 37. Linear gain functions programed in programmable read-only memory.

where applicable. As previously described, the value of the gain was determined by the gain function and the pseudo-standard deviation.

Based on a preliminary examination, a single LABGC processing function was selected as providing the best enhancement across all of the imagery and tasks of interest. This algorithm, employed during the subsequent task evaluation, utilized the range as a measure of local contrast and employed a 16/4.75 gain function, whereby the maximum gain applied was 4.75 and the gain value dropped to 1.0 when the calculated window pseudo-standard deviation reached 16.00 (see Figure 36). A single algorithm is desirable because it does not require the display operator to switch through several functions in an operational environment.

## Results and Discussion

### Search and Detection

Search can be defined as the observational process by which an observer comes to locate or detect an object of interest. The search strategy employed by an operator in any given situation is influenced to a great extent by the prior briefing information he has concerning both the nature of his target and its location. At one extreme he may receive few instructions other than to acquire all targets of tactical significance in a prescribed area. On the other, he may be supplied with high quality reconnaissance photographs. The implications of LABGC processing under these two extremes of briefing condition for a search and detection task will be discussed separately below.

### Target of Opportunity

Typically the objects of interest in a target of opportunity situation are small mobile targets. During the initial search process, eye fixations are influenced by such gross characteristics as object size, contrast, and perhaps global shape. In order for a detection decision to occur, however, targets must be distinguished not only from their backgrounds but also from other non-target clutter objects. To the extent that detection of a target requires discrimination to shape difference between the target and clutter objects, some level of recognition may be implied in the use of the term detection.

Presumably the decision that "this may be" or "this is" a target is based upon the observation of one or all of three object characteristics by the operator:

(1) the external outline features or shape-signature of the object.

(2) the density or textural differences between the object and its surroundings, and

(3) the internal shape cues (internal modulations) of the object.

LABCG processing affects each of these object characteristics, thus potentially affecting search and detection performance. However, the nature of this effect, and the usefulness of any additional information provided by LABGC processing, appears to depend on several factors, including target size and shape, original target-to-background contrast and background complexity.

The amount of useable information available with LABGC processed imagery was observed to vary with the size of the target. Images depicting target vehicles such as tanks, trucks and APCs, against both plain and realistic backgrounds, were viewed. By means of a manual zoom control, target size was manipulated through a wide range. In general, when the targets were small, and thus subtended only a few raster lines, little internal modulations was present in either the enhanced or unenhanced mode due to sensor sampling limitations. In such cases processing simply increased the luminance disparity between the target and its surroundings. Because the LABGC gain function applied is inversely proportional to the brightness range in the window, the higher the original target-to-background contrast, the less the effect. The practical impact of this increased target-to-background contrast on operator target search and detection performance appears to depend on two additional factors: target shape signature and background clutter.

For a target located in a low clutter area, its luminance alone was sometimes sufficient to identify it as an object of interest and LABGC processing increased the target-to-background contrast. For targets with unique shape characteristics, such as protruding guns and cranes, the contrast enhancement often brought out these features which remained invisible in the unenhanced image, thereby providing an aid to target detection (see Figure 36a).

Where background clutter was high, LABGC processing also enhanced non-target objects creating additional clutter (see Figure 36 b and c). Based on the present observations and results of the previous target detection study, it appears that search performance in high clutter situations will be degraded with LABGC processing because of the increase in the number of high contrast, similar size, non-target objects. However, the detection decision process may be improved in such a situation by LABGC enhancement of local target shape features.

For larger targets, where internal modulation information was present in the sensor video, the advantage provided by contrast enhancement was dependent to some extent upon the nature of the modulations themselves. Thus where local contrasts were the result of sunlight reflections or cast shadows which did not convey additional target shape information, enhancement tended to "break up" the target shape by emphasizing this irrelevant information. In other situations the local contrasts reflected actual target structural characteristics such as treads and wheel wells. However, by the time the targets were large enough that the internal modulations proved helpful in recognizing the target in the enhanced mode, the targets were also obvious in the unenhanced mode and thus the potential for performance improvement due to enhanced internal modulation appears minimal.

Pre-Briefed Targets

Briefing information may provide operators with various levels of knowledge about the nature and locations of the targets to be detected. In some cases only the general area of the target will be known so that once an operator arrives in the appropriate geographical area he again must rely on the features of the target (its shape, density, modulations, etc.) to aid him in the search and detection task. When, however, the exact target location is known, contextual features may become useful for aiding task performance. The particular class of contextual cues which become operationally important depends, to a large extent, upon the nature of the briefing material. Both map briefing and similar-sensor imagery briefing situations will be considered below.

Location-known target positions can be located on topographic maps by their coordinates; however, only terrain and road feature contextual information is available from such briefing material. To the extent that such

terrain features are visible and identifiable on the display they may prove useful in aiding target detection and acquisition by pinpointing the target location even when the target itself is not visible. The LABGC technique appears to be very useful for bringing out roadways (see Figure 36 d and e), and defining field shapes (see Figure 36 f) especially under conditions of low contrast which might occur because of atmospheric conditions like haze. It is likely this characteristic will prove useful in enabling the detection of map-briefed location-known targets at farther ranges than would be possible with unprocessed video.

Detailed target area information can be provided by reconnaissance briefing photos made with the same type of sensor to be used for target acquisition, especially when field-of-view, depression angle, and approach (aspect) angle are matched. For targets located in unpopulated regions, however, the contextual information available from similar sensor briefing materials is likely to be of the same limited nature as that from topographic maps; that is, primarily terrain and road features will be visible. In this situation LABGC processing again appears potentially beneficial because with the processed video it is likely an operator could more easily match the terrain features on the photos with those on the display. Further improvement might be realized if the reconnaissance briefing photos were also processed using the LABGC algorithm.

For targets located in industrial or residential areas, LABGC processing appeared to be detrimental because it enhanced all the individual man-made features thereby tending to de-emphasize large shape or pattern cues which might aid in the identification of the target area. The enhanced non-target information appeared very distracting in this situation (see Figure 36 g and h).

Target Recognition and Identification

Many of the implications of LABGC processing discussed in relation to the target search and detection task are also relevant to the recognition and identification task. For example, in the case of a pre-briefed target location with a known target type, target recognition and classification are complete upon detection. However, in a pre-briefed location only, situation, recognition and identification may still be necessary

For small target sizes, as previously noted, LABGC processing brought out unique target outline features which presumably would provide a significant aid in target recognition and identification as well as detection. For moderately large targets, LABGC brought out internal modulations which helped to further define the target shape but did not appear likely to impact performance because the large targets were highly visible in the unprocessed images.

Roof-house Test

It was hypothesized that LABGC processing might improve the visibility of long range targets under low contrast conditions caused by atmospheric factors such as smog, fog and haze. To investigate this hypothesis the enhancement unit was installed in a roof-house laboratory from which terrain and culteral features were examined using a commercial TV monitor. Two fields of view were provided by using a 1-1/2 and 6 inch lens. While LABGC enhancement did provide some improvement under conditions of atmospheric contrast attenuation, by "sharpening" edges of structures and bringing out roadways, terrain features and power lines it was concluded that the magnitude of the expected performance improvement is likely to be small. It should however be noted that the commercial TV camera used possessed relatively low dynamic range. In theory the LABGC processing should be most effective when used with a wide dynamic range sensor such as FLIR, where the display dynamic range limits the overall performance.

Conclusions

Based on the above observations, it was hypothesized that LABGC processing may improve operator task performance in two situations. For targets with unique shape cues such as protruding guns and cranes, LABGC processing may permit target detection, recognition, and identification to occur with smaller displayed target sizes because it brings out the unique features which are difficult to perceive in the original image. Operationally this means that for a given sensor field-of-view, targets could be detected (recognized, identified) at farther ranges with LABGC processing. Alternatively, for a given target range, LABGC processed targets may be visible with a wider field-of-view (FOV) sensor. For targets located in undeveloped

areas where terrain and road features are likely to be the significant contextual cues, and for map-briefed targets where terrain and road cues predominate, LABGC processing, by significantly enhancing such cues, may allow detection of targets at farther ranges.

## RECOMMENDATIONS

The major of the evaluations conducted using LABGC have been subjective and little data exist which allow a quantitative assessment of the improvement to be expected. Carefully designed and conducted experiments are needed to test the hypothesized results based on subjective observations. Because LABGC provides a means of accommodating wide dynamic range video, a second recommendation would be to examine the processing results when the input is TV compatible FLIR.

Appendix A

# REAL-TIME IMAGE ENHANCEMENT TECHNIQUES

ABSTRACT

Most image enhancement techniques are not suitable for real-time applications. The following discussion presents three contrast enhancement techniques that can work at TV rates with fairly simple hardware mechanizations.

## Local Area Histogram Equalization (LAHE)

LAHE is a unique image contrast enhancement technique. Historically, histogram equalization has been applied only to an entire picture frame and has been called full frame histogram equalization (FFHE).[1,2] A procedure is described here for applying histogram equalization to a smaller portion or local area of a picture frame. The advantage of the LAHE technique is that it eliminates contrast attenuation in image areas that represent a statistically small but important portion of the gray scale histogram.

An image histogram is formed by tabulating the number of times that each intensity occurs throughout the image. For the example in Figure A-1a the intensities range over 64 quantized levels. The histogram for the entire image is characterized in Figure A-1b. This distribution indicates that the picture is generally light but has a few areas in the mid-gray range and some predominantly very dark areas. It shows that the distribution of gray scale information lies primarily at either end of the light/dark intensity scale.

It becomes apparent that if the amount of information is related to the level of occurrence of each gray scale then each intensity level in the displayed image does not carry the same amount of information. If the picture intensities are distributed as in Figure A-1b, it might be better to use more display gray scale levels where there are more occurrences of gray scale information in the image and fewer levels where there is less data. This nonuniform distribution of gray scale levels can be determined by finding the total area under the histogram and dividing this area into N or, for example, 16 slices having equal areas as shown in Figure A-2a.

The intensity level boundaries for each slice then define the range of original intensity levels that will be assigned a new gray scale level for the displayed image. When this is done a histogram of the resulting displayed

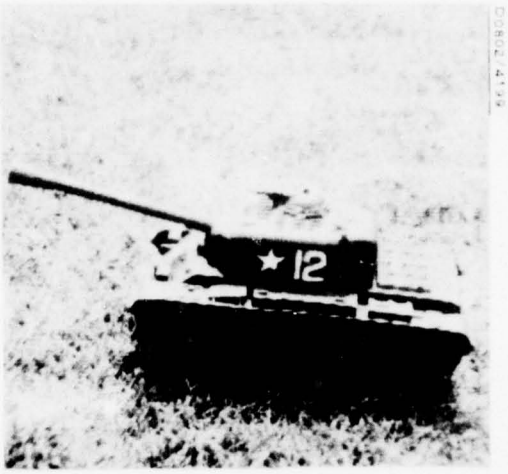


a. Original

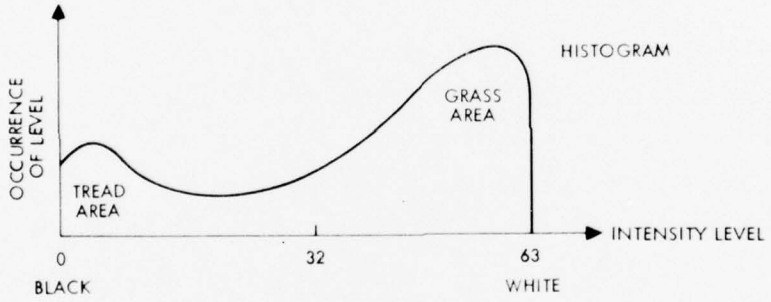


b. Histogram

Figure A-1. Histogram formation.

image has a flat or equal distribution of gray scale levels as in Figure A-2b. Hence the name "Histogram Equalization."

Figure A-3 shows the result of performing histogram equalization across the entire image. The contrast and hence the detail in the light areas of the image, such as the grass and the top of the tank, have been enchanced. The dark areas of the image, mainly around the tread area, have not been enhnaced since these brightness levels do not show a high level of occurrence in the histogram.

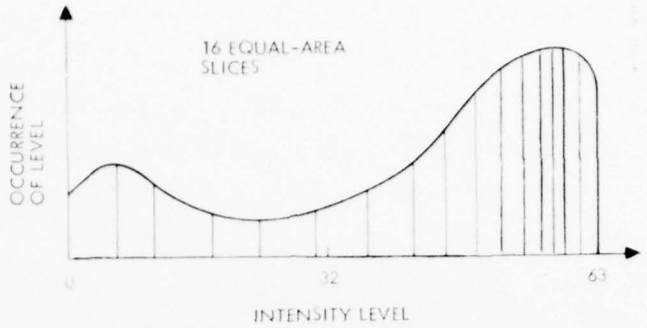


a. Equal area slicing

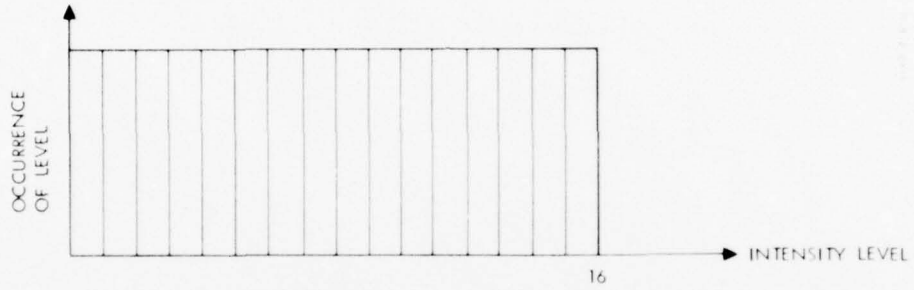


b. Histogram of histogram equalized image

Figure A-2. Method of generating histogram equalized image.


a. Original

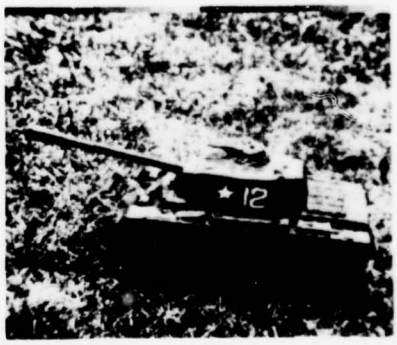


b. Full frame histogram equalized

Figure A-3. Full frame histogram equalization.

This difficulty can be resolved by using local area histogram equalization. That is, rather than redistributing the gray scale levels based on a histogram representing the entire image, the equalization can be carried out on a two-dimensional sliding window basis. Thus, the intensity of any particular point in the image is adjusted according to a histogram of the area contained within a window immediately surrounding the point as shown in Figure A-4a. In operation, this window moves across the image in two dimensions, horizontally and vertically. These reassigned center picture elements then make up the processed image. On images like the tank, detail is greatly enhanced in regions like the tread rollers as shown in Figure A-4c. Figure A-5 is another example of local area histogram equalization.

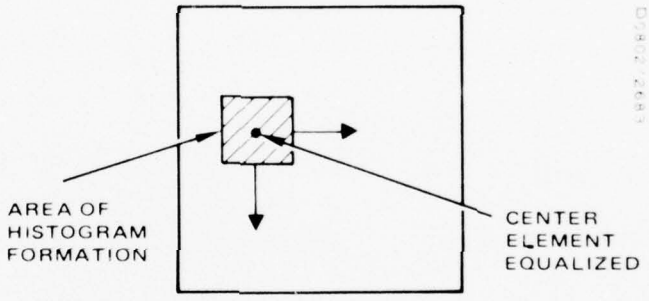


a. Local area

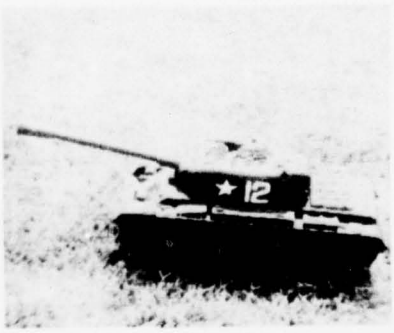


b. Original

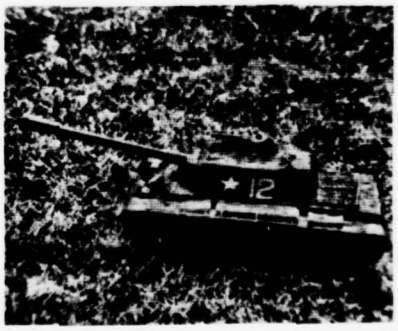


c. Local area histogram equalized

Figure A-4. Local area histogram equalization of tank image.

a. Original

b. Local area histogram equalized

Figure A-5. Local area histogram equalization of road image.

Local Area Brightness and Gain Control (LABGC)

The Local Area Brightness and Gain Control (LABGC) technique utilizes two prominent variables in a display system: brightness and gain. These variables help match the image video offset and dynamic range to the display in such a way that the operator can extract the greatest amount of useful visual information. However, in a display system these variables are constant over an entire picture frame. While for the most part this is acceptable, no significant enhancement can be achieved by manipulating these variables. Increasing video gain does increase overall image contrast, but detail in dark and light portions of the image saturate the system because the dynamic range of the display device (usually a CRT) is limited. What is needed is a way of increasing the contrast in small areas of an image without causing saturation in other areas. Continuous adjustment of gain and brightness in small areas throughout the picture would achieve this purpose.

LABGC is performed by sliding a small window (as in the LAHE technique) through the image and adjusting the gain and brightness of the center element. Earlier attempts at LABGC consisted of first adjusting the brightness of the center element of the window and then applying a constant gain factor. This provided some enhancement but produced a picture that tended to be washed out, lacking the absolute gray scale rendition of the original scene. In some cases when a high uniform gain factor was applied, the resulting image became binary in nature, being either black or white with little shading between.

The LABGC enhancement technique was improved by making brightness and gain to vary as a function of the local statistics within the image. The gain was made to be a function of the standard deviation of pixel (picture element) values within the sliding window. The brightness adjustment was made to be a function of the mean pixel value within the sliding window.

Within a 9x9 sliding window the mean and standard deviations are computed as

$$\text{mean} = M = \frac{\sum_{i=1}^{9}\sum_{j=1}^{9} I(i,j)}{81} \qquad \text{(A1)}$$

and

$$\text{standard deviation} = S = \sqrt{\frac{\sum_{i=1}^{9}\sum_{j=1}^{9} I^2(i,j)}{81} - \text{mean}^2} \qquad \text{(A2)}$$

where

$I(i,j)$ = a pixel within sliding window.

The best function relating video gain and standard deviation is shown in Figure A-6. The gain function inside the limits is then given by

$$\text{gain} = G = A - KS \qquad \text{(A3)}$$

where A is the upper limit of the gain, K is the slope of the function, and S is the standard deviation within the window. If $G < 1$, then G is set to 1.

The multiplication of the center window element by the video gain factor provides the contrast enhancement we desire. However, in many cases, this multiplication factor causes bright and dark saturation to occur. This is overcome by the application of a brightness bias term.

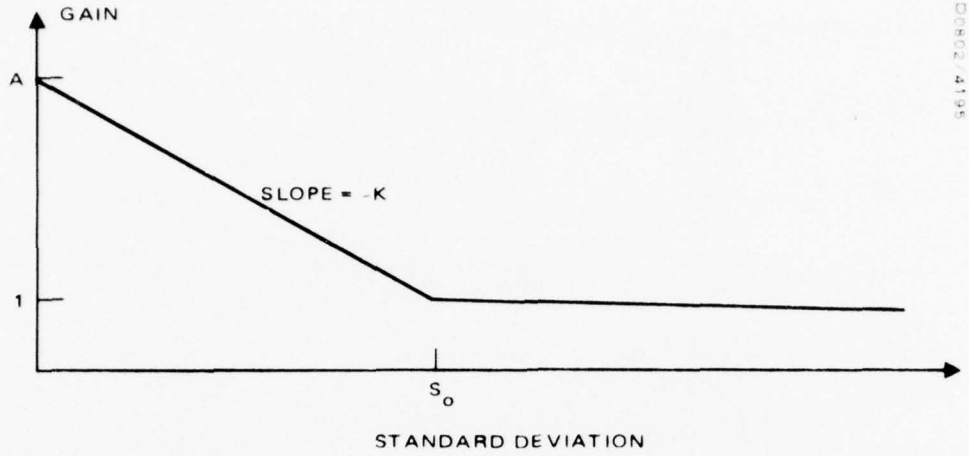


Figure A-6. Gain as a function of standard deviation within sliding window.

The computation of the brightness control value is based on the following logic. Most of the pixels in the sliding window lie within the standard deviation about the mean. Hence, most intensities are bounded by M - S and M + S. This information can be used to learn whether the gain adjusted video will exceed the black or white intensity boundaries. Figure A-7 depicts a situation where the black intensity boundary is exceeded after the gain is applied. The value of the brightness bias control for this case is the distance that the video distribution extends beyond 0 or maximum black. Thus, the brightness bias is GS - M. Similarly, for the maximum white boundary (63) the brightness bias is given by 63 - (M + GS).

However, this logic sometimes breaks down as shown in the histogram example of Figure A-8. When the gain and brightness bias controls are applied, the resulting distribution is biased more than necessary to prevent the enhanced pixels from exceeding maximum black as in Figure A-8c. This problem is solved by limiting the value of brightness under such conditions. A better brightness bias value for Figure A-8b is MG - M. For the maximum white limit, the bias value is

$$B = 63 - [M + G(63 - M)] \qquad (A4)$$

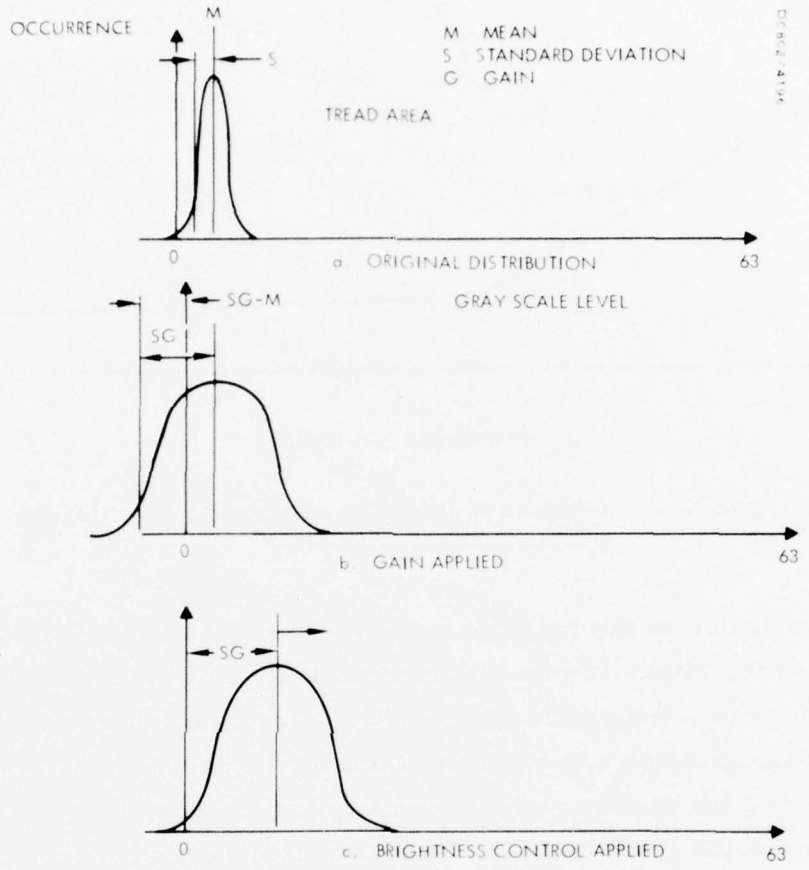


Figure A-7. Statistical gain and brightness control.

If the brightness bias value B is computed from a combination of both the mean and standard deviation logic discussed above, then the center element of the sliding window is enhanced as follows:

$$\hat{I}(5,5) = [I(5,5) - M]\,G + B + M \qquad (A5)$$

where $\hat{I}(5,5)$ is the enhanced center window element.

Images processed by the LABGC techniques utilizing the above logic for gain and brightness control are shown in Figure A-9.

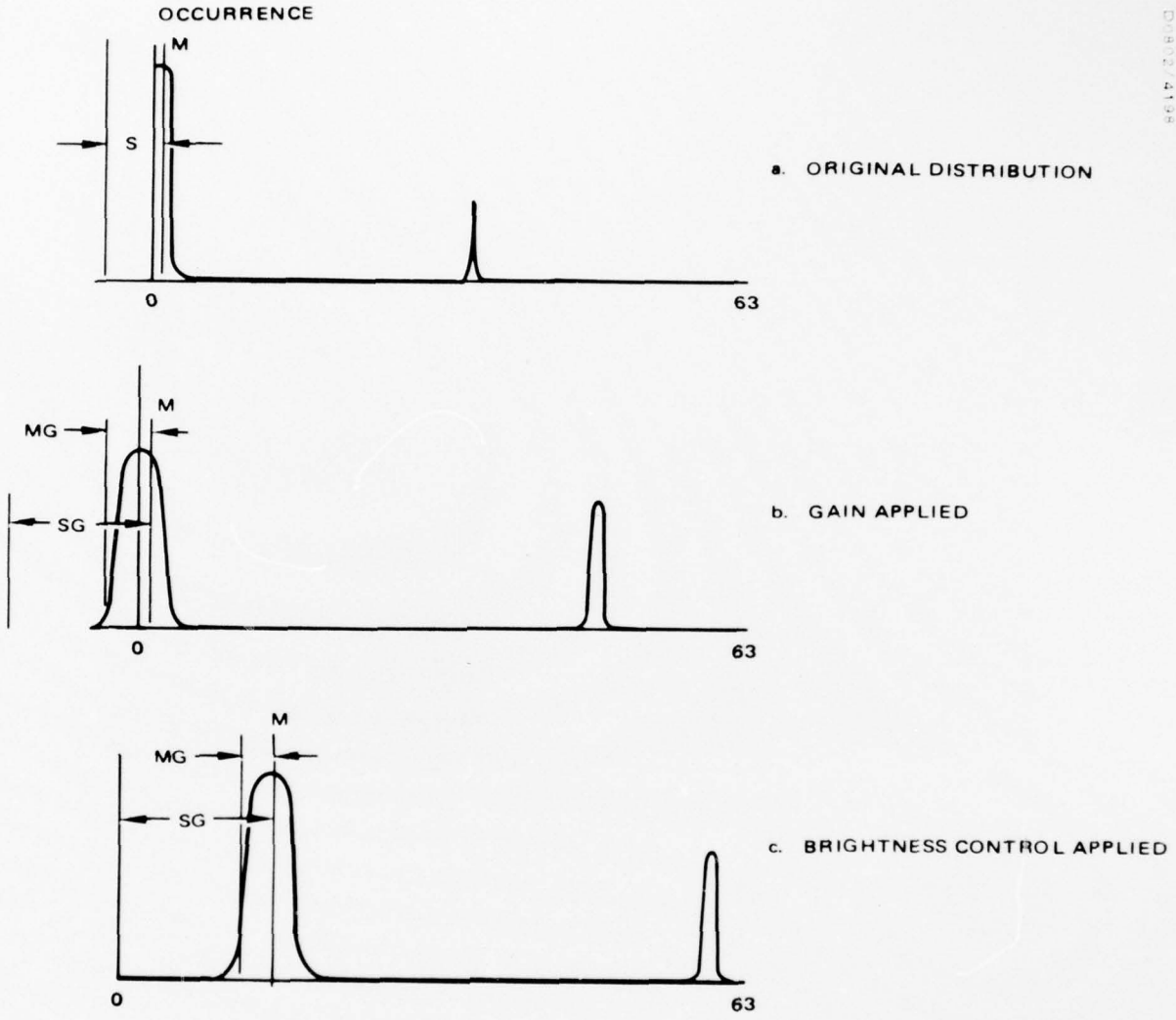


Figure A-8. Distributions causing bordering (halos) due to improper brightness control.

Haar Transform Filtering (HTC)

Much analysis and experimental work has been done in the general area of spatial frequency filtering of images. What is discussed here is a way of achieving results similar to the Fourier Transform techniques without requiring an actual Fourier Transform. The Haar transform is utilized

a. Original

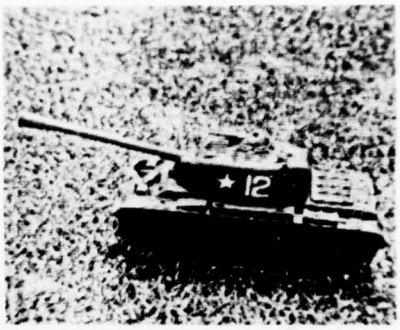

b. Local area brightness and gain control

c. Original

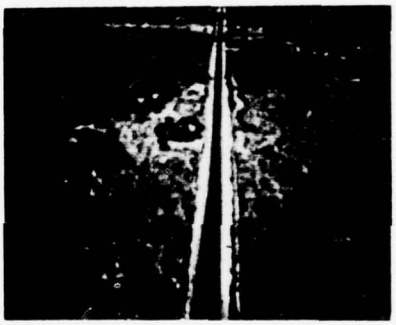

d. Local area brightness and gain control

Figure A-9. Examples of local area brightness and gain control enhancement.

since it is much faster and easier to compute. It requires far fewer computations than other transforms such as Fourier, FFT, Hadamard/Walsh or convolutions.

The Haar decomposition is characterized by a differential-like breakdown that suggests its use for crispening. The rational Haar waveforms contain many zero areas that result in fewer computations. The Fourier transform is composed of both a sine and cosine function. The magnitudes of the Fourier waveform are generally less than 1. This necessitates complex

multiplication rather than simple addition. The Hadamard and rational Haar waveforms on the other hand have magnitudes of only 1, -1 and 0. This results in only addition and subtraction for their computation.

The forward and inverse Haar transform of Image I can be shown to be as follows: (The complete derivation is presented in Ketcham, Lowe and Weber[1].)

$$H^T H(I) = (F\hat{H})^T F\hat{H}I$$

$$= \hat{H}^T F^T F\hat{H}I$$

$$= \hat{H}^T F F\hat{H}I$$

$$= \hat{H}^T F^2 \hat{H}I$$

where

$$F^2 = 1/8 \begin{bmatrix} 1 & 0 & 0 & 0 & 0 & 0 & 0 & 0 \\ 0 & 1 & 0 & 0 & 0 & 0 & 0 & 0 \\ 0 & 0 & 2 & 0 & 0 & 0 & 0 & 0 \\ 0 & 0 & 0 & 2 & 0 & 0 & 0 & 0 \\ 0 & 0 & 0 & 0 & 4 & 0 & 0 & 0 \\ 0 & 0 & 0 & 0 & 0 & 4 & 0 & 0 \\ 0 & 0 & 0 & 0 & 0 & 0 & 4 & 0 \\ 0 & 0 & 0 & 0 & 0 & 0 & 0 & 4 \end{bmatrix}$$

The transpose of H, $H^T$, is employed in the above equation as the inverse Haar transform since H is real and orthogonal, i.e., $H^{-1} = H^T$. In the following equations $H^{-1}$ will be used in place of $H^T$.

Haar Transform Crispening

High spatial frequencies of an image that have been attenuated can be restored via transform filtering. This is normally called "image restoration." "Image enhancement" results when further emphasis or amplification is placed on selected spatial frequencies of the image. Early attempts at image "crispening" or "edge enhancement" were implemented by using differential operators in the spatial domain. A generalized set of even order

partial derivatives with constant coefficients can be used to form the crispening function as follows:

$$\hat{p}(x, y) = A\, p(x, y) + B\, \nabla^2 p(x, y) + C\, \nabla^4 p(x, y) + \ldots$$

where:

$p(x, y)$ = a picture element at location x, y

$\hat{p}(x, y)$ = enhanced picture element at x, y

$\nabla^n$ = $n^{th}$ gradient operator

$$= \left( \frac{\delta^n}{\delta x^n} + \frac{\delta^n}{\delta y^n} \right)$$

A, B, C, ... = arbitrary constants

The simplest crispening operator is given by

$$\hat{p}(x, y) = p(x, y) - k\, \nabla^2 p(x, y) \qquad (A6)$$

where k is a constant.

As mentioned before, the operator $1 - kD_x^2$ when applied to a function p(x) acts as a crispening operator, where $D_x^2 = \delta^2/\delta x^2$. We have chosen to implement this one-dimensional crispening operator in the Haar domain for image enhancement. The reason for this is that most resolution loss from a sensor system is one-dimensional in nature. In a TV system, for example, horizontal resolution requires the greatest system bandwidth. All the Haar transform crispening done for this study has been done in the horizontal dimension.

The following equation defines the one-dimensional crispening function, G, that when applied in the Haar domain, achieves the equivalent of the crispening operator. Let the following variables hold in this equation:

H = Haar transform

$H^{-1}$ = inverse Haar transform

$\hat{H}$ = rationalized Haar transform

$\hat{H}^{-1}$ = inverse rationalized Haar transform

I = image

G = Haar domain crispening operator

$\hat{I}$ = enhanced image

Implementation of the Haar Crispening Operator

The Haar transform domain crispening operator G was previously derived such that an image I is enhanced by the following equation:

$$\hat{I} = H^{-1} GHI \tag{A7}$$

where $G = 1 - kF\hat{H}D_x^2 \hat{H}^{-1}F$.

Now by substitution

$$\hat{I} = H^{-1} (1 - kF\hat{H}D_x^2 \hat{H}^{-1}F) HI.$$

Reducing the Haar transform to rational transforms where $H = F\hat{H}$, yields

$$\hat{I} = (F\hat{H})^{-1} (1 - kF\hat{H}D_x^2 \hat{H}^{-1}F) FHI$$

$$= (1 - k\hat{H}^{-1} F^2\hat{H}D_x^2 \hat{H}^{-1}F^2\hat{H}) I \tag{A8}$$

Letting

$$A = F^2\hat{H}D_x^2 \hat{H}^{-1}F^2 \tag{A9}$$

we have from (A8)

$$\hat{I} = (1 - k\hat{H}^{-1} A\hat{H}) I \tag{A10}$$

where A now represents the Haar transform domain weighting function that when applied to the rationalized Haar transform of an image produces crispening. Note that (A9) contains $F^2$ matrices that are conveniently powers of two, simplifying hardware mechanization.

Since the forward and inverse rational Haar transforms are easy to compute, the complexity of the entire crispening process of equation (A10) relies upon the complexity of the matrix A. Note that the matrix A is independent of the input image and can, therefore, be computed before the processing occurs.

For the 8x8 case the matrix A approximation is

$$A = 4 \begin{bmatrix} 0 & 0 & 0 & 0 & 0 & 0 & 0 & 0 \\ 0 & -1 & 0 & 0 & 0 & 0 & 0 & 0 \\ 0 & 0 & -8 & 0 & 0 & 0 & 0 & 0 \\ 0 & 0 & 0 & -8 & 0 & 0 & 0 & 0 \\ 0 & 0 & 0 & 0 & -32 & 0 & 0 & 0 \\ 0 & 0 & 0 & 0 & 0 & -32 & 0 & 0 \\ 0 & 0 & 0 & 0 & 0 & 0 & -32 & 0 \\ 0 & 0 & 0 & 0 & 0 & 0 & 0 & -32 \end{bmatrix}$$

The crispening process using the Haar transform can now be totally implemented by using only addition, subtraction and binary shifts. Figure A-10 summarizes the Haar transform crispening technique.

Now that the derivation of the crispening operator is complete, only one variable remains to be determined: the value of k from equation (A10). Note that k determines the amount of crispening to be added to the original image.

## Conclusions

The application of histogram equalization in local image areas is an effective image enhancement technique. A similar local area application of simple brightness and video gain factors is also a viable contrast enhancement approach. The Haar transform crispening technique showed little overall improvement in operator performance.

All three of these techniques work directly in the pixel domain and lend themselves to hardware mechanizations that can operate at TV rates. A functional hardware design for the three techniques was done. Table A-1 shows the corresponding real-time mechanization complexity.

TABLE A-I. REAL-TIME HARDWARE MECHANIZATION COMPLEXITY OF ENHANCEMENT TECHNIQUES

| Enhancement Technique | Hardware Complexity | | | |
|---|---|---|---|---|
| | ICs | Size, Inches | Weight, Pounds | Power, Watts |
| LABGC | 330 | 6 x 8 x 8.6 | 5 | 66 |
| LAHE | 770 | 6 x 8 x 17.4 | 11.5 | 154 |
| HTC | 384 | 6 x 8 x 9.7 | 5.8 | 77 |

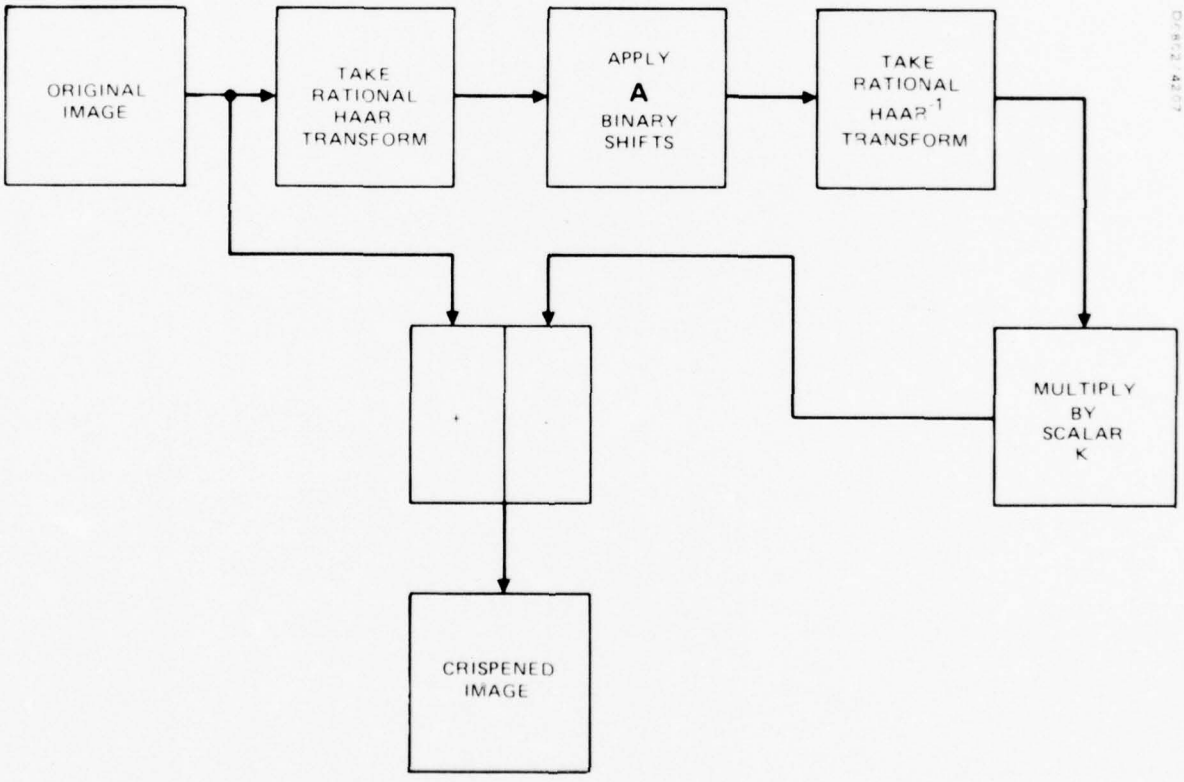


Figure A-10. Block diagram of crispening operator.

Appendix B

# THERMAL AND RELIABILITY ANALYSIS

## THERMAL ANALYSIS

An analysis was performed to investigate the thermal capability of the contrast enhancement unit. The unit is cooled by a single rear mounted axial fan. The fan draws air through two 3.5 inch diameter orifices on both sides of the unit exiting in the rear of the unit.

Power dissipation in the +5V cards totals 72 watts with a maximum average of 390/mw/DIP on the mean board. Thus cooling of these ICs determines the thermal performance requirements for the unit. Maximum allowable junction temperature is assumed to be 70°C. Results of the analysis are shown in Figure B-1 as curves of maximum inlet air temperature as a function of airflow over the +5V PC boards for three altitudes. This is the inlet air condition necessary to limit the maximum IC chip temperature to 70°C.

Two fans were selected for interchangeable use on the ground and in the aircraft. The Panmotor Model 4500 operates from 60 Hz line power and provides an airflow to the PC boards of 32 cubic feet per minute. The second, a Spartan Model 139545 operates from 400 Hz line power (for aircraft applications) and provides an airflow of 53 cubic feet per minute. To maintain the recommended junction temperature (70°C) the inlet air temperature should not exceed 30°C using the 60 Hz fan nor 40°C when using the 400 Hz fan at sea level. For airborne operation, using the 400 Hz fan, the inlet air should not exceed 30°C at 10,000 feet nor 20°C at 20,000 feet. Operation at air inlet temperatures above these limits will result in reduced unit reliability.

## RELIABILITY ANALYSIS

The MTBF (mean time between failure) of the LABGC unit is approximately 7000 hours as indicated by Table B-1 (at 70°C $T_j$). The estimate is based on the use of military temperature (-55 to 125°C) range integrated circuits and commercial (0 to 70°C) temperature range subassemblies

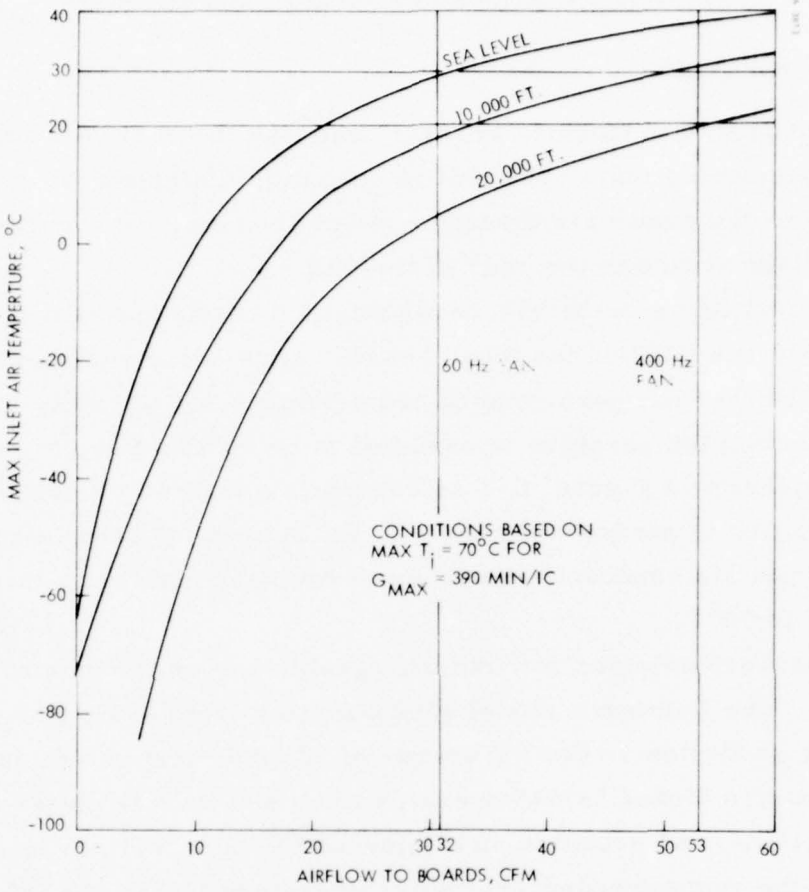


Figure B-1. Thermal analysis.

(A/D converter, power supplies). The switches and connector reliability is assumed to be negligible for the purpose of this estimate. Failure rates of the individual components were obtained from Mil Standard Handbook 217B or manufacture data.

TABLE B-1. UNIT RELIABILITY

| | Failures per Million Hours at 70°C |
|---|---|
| A5 Sync Stripper | 4.248 |
| A6 Input Processor | 7.032 |
| A7 Output Processor | 7.681 |
| A8 Mean | 6.279 |
| A9 Range | 6.279 |
| A1-A4 VADC - 8/17 | < 20.0 |
| Power Supply LCS-A5-0V | 33.3* |
| Power Supply LJS11-5-0V | 33.3* |
| Power Supply LXD-A152R | 25.0* |
| | 143.119 = 6987 hr MTBF |

*Reliability does not change with temperature since maximum rated current decreases with temperature.

# Appendix C

# ACCEPTANCE TEST PLAN

1. GENERAL INFORMATION

1.1 ASSEMBLIES TESTED

1.1.1 This document describes the procedure for testing the Hughes LABGC Contrast Enhancement System.

1.2 Purpose of Test

1.2.1 The purpose of this test is to verify proper operation of the LABGC system.

2. TEST EQUIPMENT REQUIRED

2.1 TV Camera Shibedan Model V550 or equivalent

2.2 TV Monitor Conrac SNA 9 or equivalent.

3. POWER

3.1 The following power forms are required for system operation.

105-132 VAC; 47-440 Hz

4. TEST PREPARATION

4.1 General

4.1.1 Connect output of TV camera to LABGC video input. Provide 75 ohm ±5%, .25 watt termination on the LABGC video output.

4.1.2 Connect enhanced output of the LABGC to the TV monitor input. The monitor requires a 75 ohm ±5%, .25 watt termination.

4.1.3 All front panel switches shall be in the following positions at the start of any test.

| | | |
|---|---|---|
| POWER | - | ON |
| 875/525 | - | 525 |
| MODE | - | BYPASS |
| INPUT BITS | - | 6 |
| X POSITION | - | 000 |
| Y POSITION | - | 100 |

5. TEST PROCEDURE

5.1 Range/Pixel Difference

5.1.1 Switch the mode control to the BIT 2 position, set INPUT BIT to 6, PROM SELECT to 2 and FUNCTION SELECT to 3. In this mode a known pre-programmed test pattern is internally inserted at the input and the range processing algorithm is performed. The digital display shall read the following values for the X position values listed (see Table I). The pre-programmed test pattern is as indicated in Figure 1. A sample calculation is provided in Appendix C of the final report to verify the resultant test values.

5.1.2 Change the FUNCTION SELECT switch to 8. The digital display shall read the following values for the following X position values (see Table II).

TABLE I.

| X (Octal) | Display (Octal) | Reference (Decimal) |
|---|---|---|
| 333 | 77 | 63 |
| 334 | 77 | 63 |
| 335 | 77 | 63 |
| 336 | 34 | 28 |
| 337 | 34 | 28 |
| 340 | 20 | 16 |
| 341 | 46 | 38 |
| 342 | 52 | 42 |
| 343 | 40 | 32 |
| 344 | 50 | 40 |
| 345 | 42 | 34 |
| 346 | 22 | 18 |
| 347 | 50 | 40 |
| 350 | 32 | 26 |
| 351 | 26 | 22 |
| 352 | 50 | 40 |
| 353 | 46 | 38 |
| 354 | 40 | 32 |
| 355 | 34 | 28 |
| 356 | 77 | 63 |
| 357 | 77 | 63 |

Data continues to top of display

| | | | | | | | | | | | | | | | |
|---|---|---|---|---|---|---|---|---|---|---|---|---|---|---|---|
| | 28 | 32 | 33 | 33 | 29 | 30 | 32 | 27 | 31 | 33 | 32 | 35 | 34 | 27 | 29 | |
| BLANK | 28 | 32 | 33 | 33 | 29 | 30 | 32 | 27 | 31 | 33 | 32 | 35 | 34 | 27 | 29 | BLANK |
| | . | . | . | . | . | . | . | . | . | . | . | . | . | . | . | |
| | . | . | . | . | . | . | . | . | . | . | . | . | . | . | . | |
| | . | . | . | . | . | . | . | . | . | . | . | . | . | . | . | |
| | 28 | 32 | 33 | 33 | 29 | 30 | 32 | 27 | 31 | 33 | 32 | 35 | 34 | 27 | 29 | |

127

Data continues to bottom of display

Test Input Data

0 maximum black

63 maximum white

NOTE: Blank spaces are at the "0" brightness level.

FIGURE 1

TABLE II.

| X OCTAL | DISPLAY (OCTAL) | REFERENCE (DECIMAL) |
|---|---|---|
| 333 | 77 | 63 |
| 334 | 75 | 61 |
| 335 | 73 | 59 |
| 336 | 60 | 48 |
| 337 | 34 | 28 |
| 340 | 16 | 14 |
| 341 | 50 | 40 |
| 342 | 52 | 42 |
| 343 | 40 | 32 |
| 344 | 52 | 42 |
| 345 | 42 | 34 |
| 346 | 20 | 16 |
| 347 | 52 | 42 |
| 350 | 32 | 26 |
| 351 | 26 | 22 |
| 352 | 50 | 40 |
| 353 | 50 | 40 |
| 354 | 62 | 50 |
| 355 | 70 | 56 |
| 356 | 73 | 59 |
| 357 | 77 | 63 |

5.2 Video Channel

5.2.1 Switch the mode control to the BIT 1 position. In this mode the digital processing circuitry is bypassed. Verify that the camera video is displayed on the monitor by visual inspection.

5.2.2 Switch the mode control to the RANGE mode. In this mode, the LABGC range processing is performed on the TV input video. Verify that camera video is displayed on the monitor by visual inspection.

5.2.3 Switch the mode control to the BYPASS mode.

5.2.4 Switch the mode control to the PIXEL DIFFERENCE mode. Verify by visual inspection that the camera video is displayed on the monitor.

## 6. FLIGHT SAFETY

6.1 The LABGC Contrast Enhancement system has been fabricated and inspected to flight safety standards as prescribed by the program quality requirements. A certificate of compliance will be completed prior to the delivery of the unit. (A sample certificate is attached.)

HUGHES
HUGHES AIRCRAFT COMPANY

NO _____

HUGHES AIRCRAFT COMPANY
EL SEGUNDO DIVISION

# CERTIFICATE OF COMPLIANCE

PROCUREMENT DOCUMENT

_____

DATE _____

PACKING SHEET NO.

_____

THIS CERTIFIES THAT THE MATERIALS, PARTS, OR ASSEMBLIES, SUPPLIED UNDER THE ABOVE PROCUREMENT DOCUMENT, HAVE BEEN MANUFACTURED AND PROCESSED IN CONFORMANCE WITH THE REQUIREMENTS, SPECIFICATIONS, AND DRAWINGS AS SPECIFIED.

SIGNED _____

QUALITY CONTROL DEPARTMENT
HUGHES, EL SEGUNDO

## Sample LABGC Calculation

A sample calculation of the LABGC algorithm will be shown to provide a complete understanding of the process. The example shown will use the input data used for the test procedure.

DATA 0 0 0 28 32 33 33 CURRENT VIDEO

0 0 0 28 32 33 33 ONE LINE DELAYED VIDEO

WINDOW Ci Ci+1 Ci+2 Ci+3

Di Di+1 Di+2 Di+3 CENTER ELEMENT

VIDEO ENH = (ci+2 - M) G + M + B

Step 1 MEAN = $\overset{i+4}{Ci} + \overset{i+4}{Di}$ /8 = AVERAGE OF WINDOW

I 0 + 0 + 0 + 28 + 0 + 0 + 0 + 28/8 = 7

II 0 + 0 + 28 + 32 + 0 + 0 + 28 + 32/8 = 15

III 0 + 28 + 32 + 33 + 0 + 28 + 32 + 33/8 = 23

IV 28 + 32 + 33 + 33 + 28 + 32 + 33 + 33/8 = 31

Step 2 RANGE = Vmax - Vmin = MAXIMUM - MINIMUM VIDEO ELEMENT IN THE WINDOW

I 28 - 0 = 28

II 32 - 0 = 32

III 33 - 0 = 33

IV 33 - 28 = 5

Step 3 V - M = VALUE OF CENTER VIDEO ELEMENT - MEAN

= Ci+2 - MEAN

I 0 - 7 = -7

II 28 - 15 = 13

III 32 - 23 = 9

IV 33 - 31 = 2

Step 4 GAIN = RANGE * CONSTANT * FUNCTION

The LABGC algorithm is computed for two Gain functions.

G (2,8) = G1

G (2,3) = G2

| | G1 | G2 |
|---|---|---|
| I | 2.75 | 1 |
| II | 2.25 | 1 |
| III | 2.25 | 1 |
| IV | 4.25 | 4 |

The Gain functions are listed as a function of the Range value in Appendix D.

Step 5 (V - M)G

| | G1 |
|---|---|
| I | -7 * 1.75 = -19 |
| II | 13 * 1.25 = 29 |
| III | 9 * 1.25 = 20 |
| IV | 2 * 3.00 = 9 |

| | G2 |
|---|---|
| I | -7 * 1 = -9 |
| II | 13 * 1 = 13 |
| III | 9 * 1 = 9 |
| IV | 2 * 4 = 8 |

Step 6 (V - M)G + M

| | | |
|---|---|---|
| I | -19 + 7 = -12 | -7 + 7 = 0 |
| II | 29 + 15 = 44 | 13 + 15 = 28 |
| III | 20 + 23 = 43 | 9 + 23 = 32 |
| IV | 9 + 31 = 40 | 8 + 31 = 39 |

The B1 and B2 terms calculated below are computed without including any truncation. The actual values generated via the PROM lookup table are listed next to the calculated values.

Step 7 B1 = MIN(SD,M)G - M (for B170)

B2 = 63-M-MIN(SD, 63-M) x G (of B260)

SD = STANDARD DEVIATION = RANGE x .402

R * .402 =

I 28 * .402 = 11.3

II 32 * .402 = 12.9

III 33 * .402 = 13.3

IV 5 * .402 = 2.0

G1

| B1 = | MIN (SD,M)G - M | Calculated | Truncated |
|---|---|---|---|
| I = | MIN (11.3, 7) 2.75 - 7 = | 12 | 12 |
| II = | MIN (12.9, 15) 2.25 - 15 = | 14 | 16 |
| III = | MIN (13.3, 23) 2.25 - 23 = | 7 | 8 |
| IV = | MIN (2, 31) 4.25 - 31 = | -22; 0 | 0 |

G1

| B2 = | 63-M-MIN (SD, 63 - M) x G | Calculated | Truncated |
|---|---|---|---|
| I = | 63 - 7 - (13.3, 63 - 7) 2.75 = | 25; 0 | 0 |
| II = | 63 - 15 - (12.9, 63 - 15) 2.25 = | 19; 0 | 0 |
| III = | 63 - 23 - (13.3, 63 - 23) 2.25 = | 10; 0 | 0 |
| IV = | 63 - 31 - (2, 63 - 31) 4.25 = | 24; 0 | 0 |

G2

| | | | Calculated | Actual |
|---|---|---|---|---|
| B1 | = | MIN (SD, M) G - M | | |
| I | = | MIN (11.3, 7) 1 - 7 = | 0 | 0 |
| II | = | MIN (12.9, 15) 1 - 15 = | - 2; 0 | 0 |
| III | = | MIN (13.3, 23) 1 - 23 = | -10; 0 | 0 |
| IV | = | MIN (2, 31) 4 - 31 = | -23; 0 | 0 |

G2

| | | | Calculated | Actual |
|---|---|---|---|---|
| B2 | = | 63 - M - MIN (SD, 63 - M)G | | |
| I | = | 63 - 7 - MIN (11.3, 63 - 7)1 = | 45; 0 | 0 |
| II | = | 63 - 15 - MIN (12.9, 63 - 15)1 = | 35; 0 | 0 |
| III | = | 63 - 23 - MIN (13.3, 63 - 23)1 = | 27; 0 | 0 |
| IV | = | 63 - 31 - MIN (2, 63 - 31)4 = | 24; 0 | 0 |

Step 8 $(V - M)G + M + B$

$(V - M)G + M + B$

G1

| | | |
|---|---|---|
| I | -12 + 12 = 0 | 0 + 0 = 0 |
| II | 44 + 16 = 60 | 28 + 0 = 28 |
| III | 43 + 8 = 52 | 32 + 0 = 32 |
| IV | 40 + 0 = 40 | 39 + 0 = 39 |

Comparison of Calculated to Actual outputs

$(V - M)G + M + B$

| | G1 | | G2 | |
|---|---|---|---|---|
| | Calculated | Actual | Calculated | Actual |
| I | 0 | 59; -4 | 0 | 63; 0 |
| II | 60 | 56 | 28 | 28 |
| III | 52 | 50 | 32 | 32 |
| IV | 40 | 40 | 39 | 38 |

NOTE: The test display output does not discriminate between small negative numbers and large positive numbers. The processing carries one additional bit of data for this discrimination. The caret is placed above the negative number representation and the actual negative number is shown. All negative numbers are forced to zero and all numbers above 63 are forced to 63 by the actual algorithm after the test display.

## Appendix D
## TEST PROM DATA SELECTION

The Input Processor board has two signetics 82S131 512 x 4 Proms which contain test pattern data. These Proms are labeled TPRRA and TPRRB. TPRRA contains the 4 MSB's and TPRRB contains the 2 LSB's of the data. Specifically the Test Proms contain four 64 word (6-bit) groups of random numbers. The four groups of random numbers were generated using the BASIC RND function. The range of the four groups is defined as follows:

LO - INT (10*RND (0))

MED - 27 + INT (10*RND (0))

HI - 53 + INT (10*RND (0))

FULL- INT (64*RND)

The RND function generates a number between 0 and 1; hence the range of each group is:

LO - 0 to 9

MED - 27 to 36

HI - 53 to 62

FULL - 0 to 63

A dip switch has been provided on the Input Processor board at location U125 to select the desired range of random numbers. In addition to the range select it is possible to select 1 of 4 groups of 16 numbers within each 64 number range. The first four switches in the dip switch are not wired at this time. Switches 5 and 6 select the group of 16 numbers within a specific range. Switches 7 and 8 select the range. Table D-1 lists the possible switch positions and the random numbers obtained for each position.

TABLE D-1. TEST PROM DATA SELECTION

| Switch Number 5 | 6 | 7 | 8 | Group | Range | Random Numbers |
|---|---|---|---|---|---|---|
| 0 | 0 | 0 | 0 | 0 | LO | 2 6 7 8 3 1 3 6 9 3 8 9 9 9 1 5 |
| * 0 | 0 | 0 | 1 | 0 | MED | 28 32 33 33 29 30 32 27 31 33 32 35 34 27 29 29 |
| † 0 | 0 | 1 | 0 | 0 | HI | 56 59 61 61 54 54 53 58 62 59 53 60 58 53 61 55 |
| 0 | 0 | 1 | 1 | 0 | FUL | 50 31 10 57 13 8 6 1 18 46 38 42 7 39 16 27 |
| 0 | 1 | 0 | 0 | 1 | LO | 3 4 9 9 5 9 4 8 6 7 7 7 9 7 2 6 |
| 0 | 1 | 0 | 1 | 1 | MED | 32 35 33 34 32 34 27 32 36 29 31 29 28 35 35 34 |
| 0 | 1 | 1 | 0 | 1 | HI | 53 56 54 59 59 54 55 58 56 62 53 55 59 53 58 62 |
| 0 | 1 | 1 | 1 | 1 | FUL | 46 4 36 40 7 20 1 28 15 37 3 45 2 1 5 39 |
| 1 | 0 | 0 | 0 | 2 | LO | 4 9 6 8 4 1 9 4 5 0 2 6 9 5 9 6 |
| 1 | 0 | 0 | 1 | 2 | MED | 32 27 30 28 35 32 35 35 28 32 28 31 28 27 28 33 |
| 1 | 0 | 1 | 0 | 2 | HI | 57 62 61 55 58 57 61 61 53 56 56 54 59 58 60 59 |
| 1 | 0 | 1 | 1 | 2 | FUL | 24 47 28 11 6 53 29 33 63 21 27 42 53 14 37 5 |
| 1 | 1 | 0 | 0 | 3 | LO | 0 3 3 7 4 6 0 3 6 6 9 3 5 1 6 6 |
| 1 | 1 | 0 | 1 | 3 | MED | 35 35 36 36 33 29 27 35 29 28 35 29 29 33 29 30 |
| 1 | 1 | 1 | 0 | 3 | HI | 57 54 55 60 60 60 56 62 62 54 55 59 58 62 60 54 |
| 1 | 1 | 1 | 1 | 3 | FUL | 21 32 6 11 11 3 11 25 0 49 58 4 26 31 24 4 |

NOTES

# 0 - Switch On; 1 - Switch Off

* Used for Acceptance Test

† Used for Waveform Diagnostics

## Distribution List

Chief of Naval Research
Department of the Navy
Arlington, Virginia 22217
ATTN: Codes 221 4
437 1
455 1

Defense Documentation Center
Cameron Station
Alexandria, Virginia 22314 12

Director
Naval Research Laboratory
Washington, D. C. 20375
ATTN: Tech Info Division 1
Library, Code 2620 1

Director, ONR Branch Office
536 S. Clark Street
Chicago, Illinois 60505 1

Director
Office of Naval Research
Branch Office
1030 East Green Street
Pasadena, California 91106 1

Director
Office of Naval Research
Branch Office
495 Summer Street
Boston, Massachusetts 02210 1

Office of Naval Research
Branch Office
New York Area Office
715 Broadway (5th Floor)
New York, New York 10003 1

Office of the Chief of Naval
Operations
Department of the Navy
Washington, D.C. 20350
ATTN: OP-098T 1
OP-506 1

Office of the Secretary of Defense
Deputy Director, Tactical Warfare Program
Washington, D. C. 20360
ATTN: Dr. Robert Fisher 1

Headquarters
Department of the Navy
Naval Material Command
Washington, D. C. 20360
ATTN: MAT 03 1

Commander
Naval Air Systems Command
Washington, D. C. 20360
ATTN: AIR 5337 1
5313 1
340D 1
340F 1
360F 1
03P 1
41043 1
310B 1

Commander Naval Sea Systems Command
Code 034
Washington, D. C. 20360 1

Commander
Naval Electronic Systems Command
Washington, D. C. 20360
ATTN: ELEX 310 1
320 1

Officer in Charge
Naval Aerospace Medical Research Laboratory
Pensacola, FL 32512
ATTN CDR J. Goodson 1

Commanding Officer
U.S. Naval Air Development Center
Warminster, PA 13974
ATTN: Code 402 1
505 1

Institute for Defense Analysis
400 Army-Navy Drive
Arlington, Virginia 22204
ATTN: L. Biberman 1

Commander
Naval Electronics Laboratory Center
271 Catalina Boulevard
San Diego, California 92152 1

Commander
Naval Missile Center
Pt. Mugu, California 93051
ATTN: T. Perry 1

Commander
Naval Weapons Center
China Lake, CA 93555
ATTN: Code 4011 1

Commander
Naval Avionics Facility
Indianapolis, Indiana 46218
ATTN: R. Katz 1

Dean of Research Administration
Naval Postgraduate School
Monterey, California 93940 4

Commandant, U.S. Marine Corps
Headquarters, U.S. Marine Corps
Washington, D.C. 20380
ATTN: RD-1 1

Commandant
U.S. Coast Guard Headquarters
400 7th Street, NW
Washington, D. C. 20591 1

Director, U.S. Army Research
Institute
1300 Wilson Boulevard
Arlington, Virginia 22209 1

Commanding General
U.S. Army Material Command
Washington, D. C. 20315
ATTN: AMCRD-HA 1

Commanding General
U.S. Army Electronics Command
Fort Monmouth, New Jersey
ATTN: AMSEL-VL-E 1
AMSEL-TL-BO 1
AMSEL-VL-I 1

Director Human Engineering Labs
Aberdeen Proving Ground, MD
ATTN: AMXRD-HEL 1

Aero Medical Research Laboratory
Air Force Systems Command
Wright-Patterson AFB, Ohio 45433 1

Headquarters AFSC-XRLA
Andrews AFB
Washington, D. C. 20334 1

Air Force Avionics Laboratory
Air Force Systems Command
Wright-Patterson AFB, Ohio 45433
ATTN: AFAL/AA (Mr. Steve Young) 30

Headquarters Rome Air Development
Center
Air Force Systems Command
Griffiss Air Force Base, N.Y. 13441
ATTN: RBRAC 1

Federal Aviation Agency
NAFEC Bldg. 10
Atlantic City, N.J. 03405 1

Air Force Office of Scientific Research
1400 Wilson Boulevard
Arlington, Virginia 22209 1

Honeywell, Inc.
Systems and Research Division
2700 Ridgeway Parkway
Minneapolis, Minnesota 55413
ATTN: Dr. L. Williams 1

RCA Laboratories
David Sarnoff Research Center
Princeton, N. J. 08540
ATTN: Dr. Cohen 1

Defense Advanced Research Projects
Agency
1400 Wilson Blvd.
Arlington, Virginia 22209
ATTN: K. Kresa 1
K. Perko 1